THE ROLE OF C-KIT MUTATIONS IN TUMORIGENESIS IN HUMANS AND DOGS

By

Tuddow Thaiwong

A DISSERTATION

Submitted to
Michigan State University
in partial fulfillment of the requirements
for the degree of

DOCTOR OF PHILSOPHY

Comparative Medicine and Integrative Biology

2012

ABSTRACT

THE ROLE OF C-KIT MUTATIONS IN TUMORIGENESIS IN HUMANS AND DOGS

By

Tuddow Thaiwong

The proto-oncogene c-KIT is a tyrosine kinase receptor that plays important roles in many pathways. Mutations of the *c-KIT* gene have been reported in many types of tumors, but it is not clear if the mutant c-KIT isoforms observed can drive tumorigenesis. The mutational spectrum observed in c-KIT in dogs is slightly different than in humans and ranges from deletion mutations to a varying set of tandem repeat mutations in the juxtamembrane domain. In dogs, c-KIT mutations correlate with tumor grade and poor survival. To study the molecular and cellular changes resulting directly from mutations in c-KIT, expression vectors containing normal and mutant canine KIT genes were constructed in the plasmid vector, pACGFP1N1, and transfected into canine primary fibroblasts with the resultant cells and progeny selected for stable expression of the plasmid. The mutations included three deletion mutations and three internal tandem duplications, all within exon 11. As fibroblasts do not constitutively express c-KIT, any effect on phenotype can be attributed to the experimentally induced expression. In the canine primary fibroblast context, ectopic expression of c-KIT mutant isoforms caused the immotalization, malignant transformation, chromosomal instability, and soft tissue sarcoma formation in immunodeficient mice. In the human fibroblast context, the retroviral vectors carrying c-KIT mutations observed in human GISTs, canine GISTs, and canine mast cell tumors were transduced into human primary fibroblasts. Functional consequences derived from ectopic expression showed that mutations identified in GISTs can lead to extended lifespan and immortalization, whereas cells transduced with duplication mutations reported uniquely in

canine mast cell tumors resulted in premature senescence. Unlike the results obtained from canine primary fibroblasts, the introduction of a single hit of mutant c-KIT into human primary fibroblasts was demonstrated to have immortalization capacity but not transformation activity, which suggests that additional genetic alteration(s) may be required for c-KIT driven tumorigenesis in the human context. In conclusion, our findings have shown the impact of different c-KIT mutation isoforms in tumorigenesis within the context of primary fibroblasts. Preclinical study models of cells carrying specific genetic alterations that are responsible for diseases are needed to improve the processes of clinical study. As dogs and humans share close similarity in their genome contents and living environments, comparative medicine using canine cells as study models will provide much needed information on tumorigenesis and new cancer therapies in humans.

ACKNOWLEDGMENTS

First and foremost, I would like to thank my family for giving me strength, encouragement, and all of their love. Their unconditional support and understanding have meant everything for me. I would like to gratefully and sincerely thank all of my PhD Guidance committee. I am thankful to Dr. Matti Kiupel for providing me with the opportunity to come to the U.S. and pursue my doctorate at Michigan State University. He has helped me so much in my education as well as in my professional life. Without him I could never have come so far. I must give my deep, respectful gratitude to Dr. Vilma Yuzbasiyan-Gurkan, who is my co-mentor and so many things to me, for giving me precious advice in order to improve myself to become a better person. She is not only a mentor who has molded me to become a scientist of substance, but a mother who has guided me to become a person of worth. My endless thanks to Dr. Mary Rheuben who fundamentally matured the university into me, instructed me in the fine art of teaching, and helped me throughout my PhD. I would like to express my appreciation towards Dr. Elizabeth McNiel for her advice, ideas, inspiration, and problem solving, which have been invaluable throughout these last five years.

I thank my labmates, Drs. Manish Neupane, Nicholaos Dervisis, Elizabeth Bartlett, Emmalena Gregory-Bryson, Ya-Ting Yang, and Maciej Parys, for their help and friendship. They all make me enjoy working in the lab and make my days bright. I would like to thank Dr. Patrick Venta who always answers for whatever kind of questions I have, for his invaluable discussions and comments.

I would like to acknowledge the support from the College of Veterinary Medicine and the Graduate School, Michigan State University for funding and scholarship.

My thanks are extended to Dr. Suat Gurkan and Jonathan Gurkan, who are my second family and home away from home, for their love and support. Finally, a big thank you goes to Russell Nebelung for keeping me focused and happy, and for his never ending motivation throughout this time.

TABLE OF CONTENTS

LIST OF TABLES

LIST OF FIGURES

SYMBOLS

β	Beta
μ	Micro (10^{-6})
α	Alpha
°	Degree
n	Nano (10^{-9})
Δ	Delta
k	Kilo (10^{3})

ABBREVIATIONS

AgNORs	Argyrophilic nucleolar organizer region-associated proteins
CAFs	Canine primary fibroblasts
CD	Cluster differentiation
CIN	Chromosomal instability
CMV	Cytomegalovirus
Ct	Threshold cycle
Da	Daltons
DMEM	Dulbecco's Modified Eagle Medium
DMSO	Dimethyl sulfoxide
DPBS	Dulbecco's Phosphate-Buffered Saline
EDTA	Ethylenediaminetetraacetic acid
EGFR	Epidermal growth factor receptor
FACs	Fluorescence activated cell sort
FBS	Fetal bovine serum
GFP	Green fluorescence protein
GISTs	Gastrointestinal stromal tumors
HBSS	Hank's Balanced Salt Solution
IL	Interleukin
ITD	Internal tandem duplication
JAK/STAT	Janus kinase/signal transducers and activators of transcription
JMD	Juxtamembrane domain

MCs	Mast cells
MCTs	Mast cell tumors
OIS	Oncogen-induced senescence
PCR	Polymerase chain reaction
PD	Population doubling
PDGF	Platelet derive growth factor
PET	Polyethylene terephthalate
RQ	Relative quantification
RT-PCR	Reverse transcription Polymerase chain reaction
SCF	Stem cell factor
SCID	Severe combined immunodeficiency
TGF	Transforming growth factor
TKI	Tyrosine kinase inhibitor
YFP	Yellow fluorescence protein

CHAPTER 1

INTRODUCTION

A) Mast cell, Mast cell proliferation, and canine mast cell tumors (MCTs)

Mast cells derive their name from the term "mastzellen," meaning well-fed cells, given by Paul Ehrlich in the late 1800s to a cell type replete with numerous granules in its cytoplasm (Knol and Olszewski, 2011). Mast cells (MCs) are derived from CD34+ multipotent hematopoietic progenitor cells. These MC progenitor cells are present in the bone marrow and in the peripheral blood, and can migrate through the endothelium before undergoing differentiation and maturation into MCs in tissues. A number of different factors including the microenvironment, stroma cell-derived factors, and cytokines control the development of MC from their CD34+/CD117+ progenitor cells (Valent et al., 2010). MCs especially differentiate under the influence of stem cell factor, which is the ligand for the receptor kinase, KIT (also called CD117, stem cell factor receptor or mast cell growth factor receptor). Stem cell factor (SCF, mast cell growth factor, c-kit ligand) is a critical factor for the development, survival, proliferation, and functional activation of mast cells (Galli et al., 1994). During SCF-induced differentiation, MC progenitors acquire cell-specific differentiation antigens via FceRI receptor (Linnekin, 1999). The mast cell development in tissue is fine-tuned by additional cytokines, such as TGF-β, IL-4, IL-9 and matrix proteins, resulting in different phenotypes of mucosal tissue mast cells compared to connective tissue mast cells (Knol and Olszewski, 2011). SCF can induce mast cells in their migration, adhesion to extracellular matrix components, as well as secretion of mediators of immune responses such as allergy, inflammation, and also immune tolerance (Kalesnikoff and Galli, 2008).

Mast cells are key effector cells in immunoglobulin E (IgE)-associated immune responses, including allergic disorders and certain protective immune responses to parasites (Bischoff, 2007). Mast cells can be recognized in tissues microscopically by their mononuclear

morphology with cytoplasmic granules. These granules store mediators of inflammation, including histamine, proteases, chemotactic factors, cytokines and vasoactive amines. IgE-dependent activation of mast cells leads to the secretion of mediators in the cytoplasmic granules (Dobson and Scase, 2007). In addition, mast cells are directly involved in innate immunity and IgE independent activation, through direct germicidal activity by phagocytosis or bactericidal peptide release. Thus, they are implicated in the pathogenesis of several autoimmune diseases such as asthma and arthritis (Benoist and Mathis, 2002). Moreover, mast cell activators can lead to the cascade of either pro- or anti-inflammatory responses (Galli et al., 2008). The diverse biological characteristics of mast cells and, their wide distribution near blood vessels, nerves, inflamed tissues and neoplastic foci allow them to play a central role in many physiologic, immunologic and pathological processes (Gurish and Austen, 2001). Recent studies also show that mast cells play an important role in remodeling tumor microenvironment (Liu et al., 2011). Tumor-infiltrating MCs are derived both from sentinel and recruited progenitor cells. MC can directly influence tumor cell proliferation and invasion but also help tumors indirectly by reorganizing their microenvironment and modulating immune responses to tumor cells (Khazaie et al., 2011). Mediators secreted from mast cells can facilitate tumor development through neovascularization, by disruption of surrounding matrix promoting metastasis, by providing various growth factors for tumor cell proliferation, and by exacerbating immunosuppression and thereby decreasing immune system destruction of tumor cells (Liu et al., 2011).

In humans the term Mast Cell Activating Diseases (MCADs) is used to indicate a collection of disorders characterized by (a) accumulation of pathological mast cells in potentially any or all organs and tissues and/or (b) aberrant release of variable subsets of mast cell mediators (Molderings et al., 2011). MCADs include systemic mastocytosis (SM), mast cell activation

syndrome (MCAS), and mast cell leukemia (MCL). SM is characterized by distinct clinical features, certain immunohistochemistry profiles, and alteration in specific gene (Valent et al., 2003). MCAS gives rise to a complex clinical feature of multiple mast cell mediator-induced symptoms involving the dermis, gastrointestinal track, and cardiovascular system, and its frequently accompanied by neurologic complaints (Akin et al., 2010). MCL is an aggressive mast cell neoplasm characterized by increased numbers of mast cells in bone marrow smears (≥20%) and by circulating mast cells (Molderings et al., 2011).

Canine cutaneous mast cell tumors (MCTs) are one of the most common neoplasms in dogs, and the most common skin neoplasm in dogs. The tumor prevalence has been reported to be 17% (Bostock, 1986) to 25% (O'Keefe, 1990) of canine skin neoplasm. They are found in any region of the skin with equal frequency in both genders. Notably, they occur with greater frequency in some breeds such as the Boxer, Boston terrier, Bull terrier, Staffordshire terrier, Fox terrier and Shar-Peis (Patnaik et al., 1984).

MCTs have biologically variable clinical behavior, ranging from benign to aggressive. Canine MCTs may present as locally solitary or multiple cutaneous masses, as well as visceral or systemic mastocytosis. Complications related to the MC degranulation occur locally and consist of pain, swelling, ulceration, and local bleeding. In some cases, especially in the presence of systemic mast cell disease, the paraneoplastic syndrome may be remarkably more severe, characterized by gastric ulcerations, coagulopathies, and glomerular disease (Misdorp, 2004). MCTs are often detected in the skin, but can also develop in and metastasize into other organs. MCTs usually metastasize to local lymph nodes first with prospect of metastasis increasing with histologic grade (Sfiligoi et al., 2005). Metastasis typically occurs to the regional lymph node

first and then can involve the liver, spleen, and bone marrow. Mast cell tumors rarely metastasize to the lung.

The MCT treatment options include surgery, chemotherapy, radiation, or combinations of these modalities. Surgery is the first choice of treatment. The recommended surgical procedure is to remove the tumor completely and to eliminate possible microscopic neoplastic mast cells with substantial margins that extend 2 or 3 centimeters laterally and 1 tissue plane deeper than the tumor. Radiation therapy is an effective way to treat mast cell tumors that cannot be completely removed. Chemotherapy is recommended for disseminated tumors or in cases where excision is incomplete. Some novel targeted therapies including tyrosine kinase inhibitors targeting c-KIT are being studied. Blocking the KIT-induced phosphorylation of the tyrosine residues from either receptor or ligand overexpression and mutation of the receptor is the main idea of this treatment. The result of these drugs is a potential inhibition of cellular proliferation, promotion of apoptosis, and inhibition of angiogenesis. The tyrosine kinase inhibitors (TKI) including Imatinib, Nilotinib, Dasatinib, and Midostaurin can block proliferation, induce apoptosis, and inhibit c-KIT activation in both primary canine neoplastic mast cells and canine MC lines that contained c-KIT mutations *in vitro*, with potent synergistic effect in combination treatment (Gleixner et al, 2007). Other small molecules, histone deacetylase inhibitors (HDACis), such as heat shock protein 90 (HSP90) inhibitors have demonstrated the *in vitro, ex vivo*, and *in vivo* biologic activity against malignant mast cells expressing either wild type or mutant c-KIT (Lin et al, 2008; Lin et al., 2010). Recently, a two-tier histological grading system for canine MCTs has been developed to more accurately predict biological behavior (Kiupel et al, 2011), along with the previously well developed MCTs prognostication panel. The panel includes c-KIT immunostaining pattern, AgNORs, and Ki-67 staining that shows that a MCT with higher

proliferation marker, and a higher KIT staining pattern will have poorer prognosis (Webster et al., 2007).

In dogs, mutation of c-kit exon 11, which induces constitutive phosphorylation of KIT, is thought to be one of the mechanisms for the development or progression of MCTs. Our previous studies (Zemke et al., 2002, Webster et al., 2006) reported a significant association between mutation and higher grade of tumor. The results showed that canine MCTs with c-KIT mutations were significantly associated with an increased incidence of recurrent disease and death. Also, c-KIT mutations were significantly associated with aberrant protein localization (Webster et al., 2006). In addition, 85% of the dogs without this mutation revealed the survival time to be longer than 3 years, whereas only 15% of the dogs with the mutation were yet alive.

B) *c-KIT* gene, c-KIT protein, and c-KIT signaling pathway

KIT, the product of the c-*KIT* gene, was initially identified as the cellular homologue of the transforming gene of the Hardy-Zuckerman 4-feline sarcoma virus that captured an activated and truncated form of the receptor (Besmer et al., 1986). The *c-KIT* gene is classified as a receptor tyrosine kinase (TK) subclass III (Chabot et al., 1988), which also includes the PDGF-receptor-α, and β, CSF-1 receptor, and the FLT-3 receptor (Blume-Jensen and Hunter, 2001). This subclass of receptor kinases has three major characteristics. One is an extracellular domain consisting of five immunoglobulin (Ig)-like motifs (encoded by exon 1-9), which are involved in ligand binding and ligand-induced dimerization. Another is a transmembrane domain (encoded by exon 10) followed by the juxtamembrane domain, which serves as a negative control domain that prevents the kinase activation in the absence of ligand (encoded by exon 11). Finally, the bipartite tyrosine kinase domain (encoded by exon 12-21) splits in two by a kinase insert region.

Activation of c-KIT occurs by the binding of the c-KIT ligand, stem cell factor (SCF). This growth factor is produced by fibroblasts and endothelial cells, and is widely distributed throughout the body, and can be detected at low levels in the blood. This cytokine is encoded by a gene located in chromosome 12 in humans, by the Sl locus in mouse chromosome 10 (Copeland et al., 1990), and in chromosome 15 in dogs. The SCF is also known as steel factor or mast cell growth factor, and exists in membrane-bound (lacking exon 6) and soluble (including exon 6) form (Huang et al., 1992) generated by alternative RNA splicing and by proteolytic processing (Yuzawa et al., 2007). SCF functions as a noncovalent homodimer. The two forms of SCF display distinct effects (Theou-Anton et al., 2006) in regard to the survival and proliferation of hematopoietic cell lines (Caruana et al., 1993; Miyazawa et al., 1995) and primary cells (Torsoz et al., 1992). SCF in the membrane-bound form can induce more persistent activation of c-KIT kinase and more prolonged lifespan of the c-KIT protein than soluble form. The soluble form of SCF appears to induce rapid downstream signaling of cell-surface c-kit expression and its protein degradation (Miyazawa et al., 1995). Mutations of SCF have been reported. Mutant Steel-17H (Sl^{17H}) leads to complete absence of coat pigmentation, sterility in males (Brannan et al., 1992), anemia, mast cell deficiencies (Tajima et al., 1998), and other developmental defects (Wehrle-Haller and Weston, 1999).

The *c-KIT* gene comprises a total of 21 exons and locates in chromosome 4q12 in human, in mouse chromosome 5, which corresponds with the white-spotting (W) locus, and in chromosome 13 in dogs. The *c-KIT* gene encodes c-KIT protein, which is composed of 976 amino acids, producing a 145 kilo-daltons, glycosilated protein. It is widely expressed by hematopietic progenitors, germ cells, a subset of cerebellar neurons, natural killer (NK) cells, epithelial cells in breast, and the intersitital cells of Cajal, melanocytes, and mast cells

(Miettinen and Lasota, 2005). Recently interesting is the c-KIT expression has been identified in many subpopulations of cells ranging from normal breast epithelium (Yared et al., 2004) to lung cancer stem cells in Non Small Cell Lung Cancer (NSCLC) (Levina et al, 2008).

Isoforms of c-KIT derived from alternative splicing patterns have been identified in human, mouse, and dog (shown in Figure 1). The two common isoforms of c-KIT protein, presence (+) and absence (-) of a tetrapeptide sequence, can be found in human and mouse (GNNK-isoform) and dog (GNSK-isoform) at the extracellular domain. Both isoforms are co-expressed in most tissues in varying ratios (Ashman, 1999). The GNNK (−) isoform reveals faster SCF-induced internalization than the GNNK+ isoform (Caruana et al., 1999). An additional splicing variant resulting in the presence or absence of a single serine residue in the interkinase region was also reported in human c-KIT (Ashman, 1999). Moreover, truncated form of c-KIT occurs from use of cryptic promoters in intron 15 and 16 and yields lacking the extracellular and transmembrane domains of 30 kDa c-KIT protein. This isoform of c-KIT was reported in mouse haploid germ cells (Sette et al., 2004), human spermatozoa (Muciaccia et al., 2010), murine hematopoietic stem cells and multipotent progenitors (Zayas et al., 2008), colon carcinoma (Toyota et al., 1994), human gastric carcinoma cell lines (Hassan et al., 1998), hematopoietic tumor cell lines (Takaoka et al., 1997), and human prostate cancer (Paronetto et al., 2004)

Figure 1: Schematic representation of c-KIT gene and its isoforms. Alternative splicing generates five c-KIT isoforms. At the Ig-like motif, there are two isoforms: with (+) and without (-) GNSK amino acid. Two isoforms, with (+) and without (-) serine (S), are reported. The truncated c-KIT isoform consists of 12 amino acids encoded by the 16th intron and the C-terminals of last 190 amino acids of the c-kit protein.

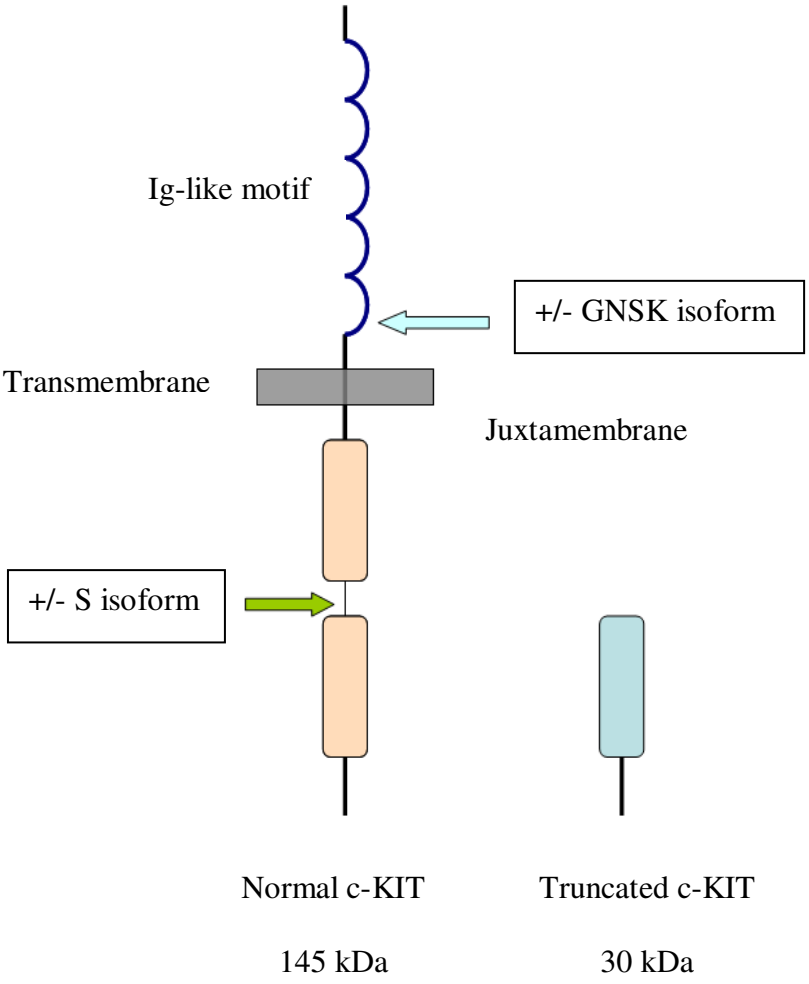

"For interpretation of the references to color in this and all other figures, the reader is refered to the electronic version of this dissertation."

Diverse cellular responses associated with c-KIT activation include differentiation, proliferation, growth, survival, adhesion, and chemotaxis. Binding of SCF to c-KIT results in receptor dimerization and change the conformation of the receptor, leading to the stabilization of the receptor-receptor interaction. After activation, the initial tyrosine residue in the juxtamembrane domain is autophosphorylated and functions as a docking site for signal transduction molecules. The phosphorylation of tyrosine residues mediates the specific binding of a class of cytoplasmic signaling proteins containing Src homology 2 (SH2) domains or phosphotyrosine binding (PTB) domains, which in turn controls various intracellular signaling pathways (Lennartsson and Rönnstrand, 2006). Recruitment of particular targets is mediated by the ability of their SH2 domains to recognize specific phosphotyrosine (pTyr)-containing motifs on the activated receptor. Numerous signaling molecules have been identified as binding partners for specific pTyr residues on the activated KIT of GNNK-absence isoform of murine c-KIT, including the p85 subunit of phosphatidylinositol 3′ kinase (by means of tyrosine (Y) 719; Y716 of GNSK-absence isoform of canine c-KIT), phospholipase Cγ (by means of Y728; Y725 of GNSK-absence isoform of canine c-KIT), and the Grb2 and Grb7 adapter proteins (by means of Y 702 and Y934; Y698 and Y931 of GNSK-absence isoform of canine c-KIT). Additionally, signaling molecules, including Src family kinases and the protein tyrosine phosphatases Shp-1 and Shp-2, have been shown to associate with a dual tyrosine motif in the juxtamembrane (Jx) region of Kit (Y 567 and Y569; Y563 and Y565 of GNSK-absence isoform of canine c-KIT) (Kimura et al., 2004).

The recruitment of these signaling molecules is leading to the activation of multiple signal transduction pathways (Linnekin, 1999). These include Src family kinases (Krystal et al., 1998), JAK/STAT pathway (Caruana et al., 1999), phosphatidyl-inositol 3 kinase (PI3K) (Chian

et al., 2001), the Ras/Raf/Map kinase cascade, and phospholipid C (Jacob-Helber et al., 1997). Because many of these proteins are the products of proto-oncogenes, alterations in regulation of these pathways could result in cellular transformation.

C) c-KIT mutations and role of c-KIT mutations in tumors

c-KIT signaling is important in erythropoiesis, lymphopoiesis, mast cell development and function, megakaryopoiesis, gametogenesis, and melanogenesis. Abnormal expression or function of c-KIT has been reported in several human and animal diseases. Various types of loss-of-function and gain-of-function mutation of c-KIT have been reported.

Mutations resulting in reduced expression or loss-of-function of c-KIT result in a wide spectrum of disorders including autosomal-dominant piebaldism (Giebel and Spritz, 1991) characterized by a white forelock and large, nonpigmented patches on the forehead, eyebrows, chin, chest, abdomen, and extremities and other aberrations of pigmentation, macrocytic anemia, decreased fertility, mast cell deficiency, reduction in gastrointerstinal motility, and impairment of learning function (Ashman, 1999). Mutations at the mouse W locus lead to pleiotropic developmental defects, including sterility, coat color abnormalities, severe macrocytic anaemia and mast cell deficiency (Bernstein et al., 1990). Interestingly, loss of expression of c-KIT has also been associated with some tumors (Ronnstrand, 2004), including thyroid cancer (Natali et al., 1995), melanoma (Kurosawa et al., 1996), and breast cancer in humans (Natali et al., 1992).

A wide range in gain of function mutations in c-*KIT* results in activation of the receptor. These include deletion, duplication, and point mutation in various species, including human, mouse, dog, and cat. The activating mutations of c-KIT cause the constitutional tyrosine phosphorylation and downstream activation independent of ligand binding. Several gain-of-

function c-KIT mutations, resulting in constitutive activation of KIT, have been identified in various mast cell leukemia cell lines from human mast-cell leukemia cell line (HMC-I) (Furitsu, et al., 1993), murine mastocytoma cell line (P-815) (Tsujimura et al. 1994), rat mast cell leukemia cell line (RBL-2H3) (Tsujimura et al., 1995), and canine mast cell line (C2) (London et al., 1999). The c-KIT gene in these cell lines or tumor cells was found to carry constitutively activating mutations clustered exclusively in two distinct regions: the juxtamembrane domain of the receptor and the phosphotransferase domain.

Activating mutations causing constitutive activation of c-KIT have been implicated in the tumorigenesis through positively regulating mitogenesis and inducing neoplastic transformation. Cancers in which c-KIT mutations have been identified in all domains of c-KIT have been formed in a variety types of tumors including systemic mastocytosis in human (Buttner at el., 1998; Nagata et al., 1995), mast cell leukemia in human (Ning et al., 2001), mast cell tumor in dog (Zemke et al., 2002) and cat (Isotani et al, 2006), gastrointestinal stromal tumors (GISTs) in human (Hirota et al, 1998; Heinrich et al., 2003) and dog (Gregory-Bryson et al, 2011), sinonasal T-cell lymphomas in human (Hongyo et al., 2000), small cell lung cancer in human (Boldrini et al., 2004), seminomas/dysgerminomas in human (Tian et al, 1999; Rapley et al., 2004), melanoma in human (Willmore-Payne et al., 2005) , and acute myeloid leukemia in human (Ashman et al., 2000) as shown in the Figure 2.

Figure 2: Mutation of c-KIT in malignancies. Schematic diagram of c-KIT illustrating domains and mutations found in many tumors ranging from human to animal is depicted. Mutation codon locations and amino acid substitutions caused by mutations are shown. Abbreviations for amino acid residues: A, alanine; D, aspartic acid; E, glutamic acid; F, phenylalanine; H, histidine; I, isoleucine; K, lysine; L, leucine; M, methionine; N, asparagine; P, proline; W, tryptophan; V, valine; Y, tyrosine. Abbreviations used: ITD, Internal tandem duplication; AML, Acute myeloid leukemia; GISTs, Gastrointestinal stromal tumors; MCTs, Mast cell tumors; NK, Natural killer; Δ, deletion mutation.

Extracellular domain	
Disease	**Mutation**
AML	Δ418, Δ419, Δ418-419
GISTs	Δ419
Mastocytosis	Δ419
Canine MCTs	ITD
Feline MCTs	ITD

Transmembrane domain	
Disease	**Mutation**
AML	V530I
GISTs	K509I
Desmoid tumor	V530I

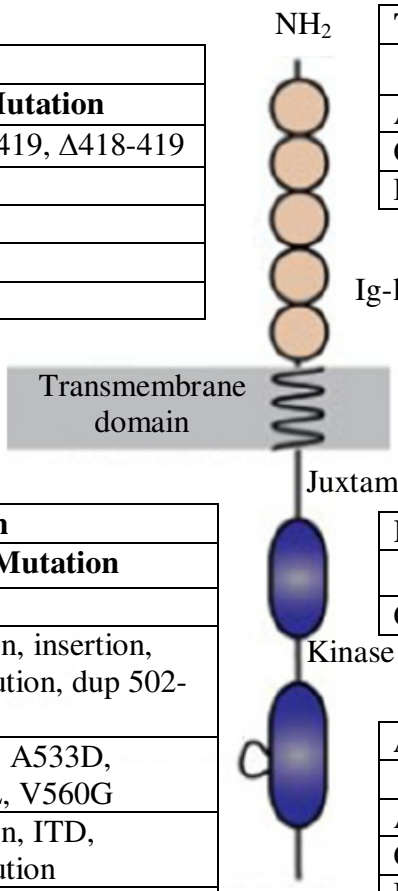

Juxtamembrane domain	
Disease	**Mutation**
AML	ITD
GIST	Deletion, insertion, substitution, dup 502-503
Mastocytosis	F522C, A533D, M541L, V560G
Canine MCTs	Deletion, ITD, substitution
Canine GISTs	deletion
Sinosital NK/T cell lymphoma	V559I, E561K
Melanoma	L576P
Germ cell tumor	W557R, L576P

Kinase domain	
Disease	**Mutation**
GISTs	K642E

Activation loop	
Disease	**Mutation**
AML	D816V, D816Y
GISTs	D820Y
Mastocytosis	D816V, D816Y
Sinosital NK/T cell lymphoma	V825A, D816N
Germ cell tumor	D816H, D816Y, D816V, Y823N, D816E, D820H

Different mutations are leading to different molecular mechanism responsible for the receptor activation. Residues 553-663 of exon 11, encoded intracellular juxtamembrane region of c-KIT, form an alpha helix that suppresses phosphorylation and kinase activity in ligand unoccupied c-KIT (Longley et al., 2001). Without SCF, the juxtamembrane domain inserts into the active site of the kinase and inhibits the activation of kinase activity. Mutations in the juxtamembrane domain have been proposed to release an inhibitory alpha-helix, disrupt the negative regulation of the kinase domain, and thereby result in uncontrolled receptor activation (Ma et al., 1999). Unregulated c-KIT activity has also been proposed to contribute to malignancies through increased proliferation and suppression of apoptosis (Lennartsson et al., 2005). In addition, point mutation in the juxtamembrane domain can induce constitutive c-KIT dimerization. Another hot spot of the c-KIT activating mutation is in the activation loop. Mutations are associated with several human malignancies such as mast cell leukemia, acute myeloid leukemia, mastocytosis, germ cell tumor, Sinonasal NK/T cell lymphoma, and GISTs. At codon 816, the aspartic acid residue (D) have been found mutated into either a tyrosine (D816Y), histidine (D816H), asparagine (D816N), or valine (D816V) residue, and cause similar consequences in ligand-independent activation (Lennartsson and Rönnstrand, 2006).

Mutations in the juxtamembrane domain including point mutation, substitution, deletion, internal tandem duplication or combination are commonly seen in human patients suffering from gastrointestinal stromal tumors (GISTs). Among GIST patients, 57-71% are reported to have mutations in exon11. The presence of these mutations is associated with poor prognosis. A recent study by Heinrich et al showed that 35% of GISTs had mutations in platelet derived growth factor receptor alpha (PDGFRα) but did not carry cKIT mutations (Heinrich et al., 2003).

In dog, mutations in the juxtamembrane domain have been reported by our group in canine mast cell tumors (Zemke et al., 2002; Webster et al., 2006), and canine GISTs (Gregory-Bryson et al., 2010) up to 33% of canine cutaneous MCTs. Both deletion and ITDs in canine MCTs have been identified, and others (Ma et al., 1999; London et al, 1999) have also reported ITDs in canine MCTs . However, functional consequences of these mutatations have not been studied except in the case of one mast cell line carrying a juxtamembrane ITD mutation (Ma et al., 1999). Both *c-KIT* ITD mutations and aberrant c-KIT protein localization (cytoplasmic) in canine MCTs are associated with worse prognoses, as compared with MCTs that lack such mutations or have normal perimembrane protein localization, respectively (Kiupel, 2004; Webster et al., 2007).

Our previous research also suggests that a downstream consequence of *c-KIT* mutations and aberrant c-KIT protein localization in canine MCTs may be an increase in cellular proliferation, by both increasing the rate at which the cells enter the cell cycle and by increasing the rate at which the neoplastic cells progress through the cell cycle (Webster et al., 2006). However, the biologic significance and biochemical consequence of the range of mutations observed in canine MCTs have yet to be determined. In addition, to date, no effective chemotherapeutic agent has been identified for their treatment. Recent studies suggest that tumors expressing activating mutations in KIT may be amenable to treatment with KIT inhibitors such as ST1571 (Gleixner et al., 2007, Tuveson et al., 2001). Interestingly, JMD mutants are more sensitive to ST1571 (Gleevec, Novartis) than the kinase domain mutants (Frost et al., 2002). As of now there are no drugs identified that can specifically target the kinase domain mutants. Thus, the functional consequences of the *c-KIT* mutations will elucidate their role of the

activating mutations of *c-KIT* proto-oncogene in tumorigenesis, and the cell lines generated might have therapeutic relevance in the assessment of new tyrosine kinase inhibitor therapies.

D) Tumorigenesis, Tumorigenic transformation, and chromosomal instability

Cancer is a distinct type of genetic disease in which not one, but several, mutations are required. Each mutation drives a wave of cellular multiplication associated with gradual increases in tumor size, disorganization and malignancy (Vogelstein and Kinzler, 1993). Tumorigenesis is a multi-step process in which a normal cell acquires inherited changes in a number of critical cancer-related genes (Zhang, 2007)

The hallmarks of cancer on distinctive and complementary capabilities that enable tumor growth and metastatic dissemination, as proposed in 2000 and updated in 2011 by Hanahan and Weinberg, are composed of 1) sustaining proliferative signaling, 2) evading growth suppressors, 3) activating invasion and metastasis, 4) enabling replicative immortally, 5) inducing angiogenesis, 6) resisting cell death, 7) avoiding immune destruction, 8) tumor-promoting inflammation, 9) genomic instability and mutation, and 10) deregulating cellular energies.

The concept of cellular senescence was first described by Hayflick in 1965 when he observed that human embryonic fibroblast undergo a replicative senescence in culture after dividing a finite number of passages. Other mechanisms that can contribute to premature forms of cellular senescence are oncogene-induced senescence (OIS) and PTEN loss-induced cellular senescence (Nardella et al., 2011). An important step in tumorigenic transformation and tumorigenesis is immortalization, a process in which cells must escape senescence and acquire an infinite lifespan. In the absence of immortalization although a cell might undergo malignant transformation it could not proliferate indefinitely (Fridman and Tainsky, 2008). In addition,

cells require the ability to overcome senescence checkpoint that imposes a limited number of divisions in culture and grow indefinitely (Sun H. and Taneja R, 2007).

The activation of a telomere maintenance mechanism either through telomerase activation or through an alternative mechanism to elongate telomerase (ALT) mechanism as well as disruption of the pRB and p53 pathways are integral parts in the induction of cellular immortalization, which is itself a prerequisite of malignant transformation in human cells (Heeg et al., 2006). The simian virus 40 (SV40) large T antigen or the human papillomavirus (HPV) E6 and E7 protein, combined SV40 large T with the hTERT gene, the cyclin D1 overexpression combined with p53 inactivation can allow presenescent cells to bypass senescence (Bond et al., 1999, Shay et al., 1993).

The process of malignant transformation is mediated by the disruption of only a few molecular circuits. Biochemical and molecular studies of the regulatory pathways involved in most types of human cancer have shown that. Introduction of immortalized cells without oncogene (ras) has failed to produce tumor formation in immunocompromised mice. In the human primary fibroblast, inactivation of RB and p53 by the early region of SV40 is the key component for tumorigenic transformation (Hahn et al, 2002). The expression of specific genetic alteration including the human Telomerase reverse transcriptase subunit (hTERT) and oncogenic HRasV12 is capable of immortalizing and transforming human primary fibroblasts into neoplastic cells (Hahn et al., 1999). In epidermal keratinocytes, the coexpression of cdk4 and oncogenic ras led to malignant transformation and enabled cells to grow in immunocompromised mice (Brookes et al., 2002). Interestingly, dysregulation of mitogenic signaling pathways have also been successfully used to transform human cells. The overexpression of EGFR acting through PI3K-AKT pathway and the overexpression of c-myc as a new downstream target of

PP2A can induce malignant transformation (Boehm et al., 2005; Yeh et al., 2004). A recent study by Lenos et al (2011) also confirmed that inactivation of p53 by hMDMX overexpression contributes to the oncogenic phenotype of transformed human cells.

Aneuploidy is a common feature of cancer cells, and is believed to play a critical role in tumorigenesis and cancer progression. Most cancer cells also exhibit high rates of mitotic chromosome mis-segregation, a phenomenon known as chromosomal instability, which leads to high variability of the karyotype (Nicholson and Cimini, 2011). In 1914 Theodor Boveri proposed the aneuploidy theory that aneuploidy is a cause of a cancerous transformation. Today, it is clear that aneuploidy is a common genetic feature of solid human tumours (Weaver and Cleveland, 2006). It is generally considered that the magnitude of aneuploidy is greater in malignant than in non-malignant cells, and increase in aneuploidy correlates with increasing malignancy, development of multidrug resistance and poor prognosis (Ried et al., 1999). The degree of malignancy is proportional to the degree of aneuploidy (Duesberg et al., 1998). However, whether aneuploidy is a cause or a consequence of malignant transformation remains debated. One possibility is that aneuploidy, per se, creates protein imbalances that facilitate the development of tumours by promoting additional genomic instability. In rare instances, this increased instability might allow the acquisition of transforming mutations that promote cancer. A second possibility is that aneuploidy allows for the duplication of a chromosome that contains an oncogenic allele or allows for the loss of a chromosome that possesses the remaining wild-type copy of a tumour suppressor gene (Holland and Cleveland, 2009).

E) Critical question

The c-KIT proto-oncogene encodes a transmembrane tyrosine kinase identified as the receptor for stem cell factor (SCF). The c-KIT dysfunction through mutation or through overexpression has been linked to abnormal cell growth in a variety of cell lines and is associated with high tumor grade and a poor prognosis in several human cancers. As canine cutaneous MCTs comprise the most common cutaneous tumors in the dog, varying from benign to metastatic cancers that result in death. Our laboratory has documented that some MCTs have mutations in the c-KIT gene which are associated with poor prognosis. The mutational spectrum observed in c-KIT in dogs is different than in humans and ranges from deletion mutations to varying set of tandem repeat mutations in the juxtamembrane domain. Indeed, NIH3/T3 cells stably transfected with murine wild-type c-KIT exhibit prolonged c-KIT phosphorylation and signal transduction following SCF stimulation and enhanced in vitro and in vivo tumorigenicity. While gain-of-function is predicted in production of a ligand-independent and tumorigenic phenotype, detailed studies of each mutation have not been carried out.

F) Significance

Introduction of c-KIT mutant isoforms into primary fibroblasts will reveal the effects of the mutations on ligand-independent activation of KIT, tumorigenic transformation, and metastasis property. The functional consequences of the c-KIT mutations observed in canine MCTs will elucidate their role in tumorigenesis, and these study models will have therapeutic relevance in the assessment of new tyrosine kinase inhibitor therapies.

REFERENCES

REFERENCES

1. Akin C, Valent P, Metcalfe DD. Mast cell activation syndrome: Proposed diagnostic criteria. J Allergy Clin Immunol. 2010 Dec;126(6):1099-104

2. Ashman LK, Ferrao P, Cole SR, Cambareri AC. Effects of mutant c-kit in early myeloid cells. Leuk Lymphoma. 2000 Mar;37(1-2):233-43.

3. Ashman LK. 1999. The biology of stem cell factor and its receptor C-kit. Int J Biochem Cell Biol. 31(10): 1037-51.

4. Benoist C, Mathis D. Mast cells in autoimmune disease. Nature. 2002 Dec 19-26;420(6917):875-8.

5. Bernstein A, Chabot B, Dubreuil P, Reith A, Nocka K, Majumder S, Ray P, Besmer P. The mouse W/c-kit locus. Ciba Found Symp. 1990;148:158-66

6. Besmer P, Lader E, George PC, Bergold PJ, Qiu FH, Zuckerman EE, Hardy WD. 1986.A new acute transforming feline retrovirus with fms homology specifies a C-terminally truncated version of the c-fms protein that is different from SM-feline sarcoma virus v-fms protein. J Virol. 60(1):194–203.

7. Bischoff SC. 2007. Role of mast cells in allergic and non-allergic immune responses:comparison of human and murine data . Nature Immunology. 7: 93-104.

8. Blume-Jensen P, Hunter T. 2001. Oncogenic kinase signalling. Nature. 411(6835): 355-65.

9. Boehm JS, Hession MT, Bulmer SE, Hahn WC. 2005. Transformation of human and murine fibroblasts without viral oncoproteins. Mol Cell Biol. 25:6464-74.

10. Boldrini L, Ursino S, Gisfredi S, Faviana P, Donati V, Camacci T, Lucchi M, Mussi A, Basolo F, Pingitore R, Fontanini G. Expression and mutational status of c-kit in small-cell lung cancer: prognostic relevance. Clin Cancer Res. 2004 Jun 15;10(12 Pt 1):4101-8.

11. Bond JA, Haughton MF, Rowson JM, Smith PJ, Gire V, Wynford-Thomas D, Wyllie FS. 1999. Control of replicative life span in human cells: barriers to clonal expansion intermediate between M1 senescence and M2 crisis. Mol Cell Biol. 19(4):3103-14.

12. Bostock DE. 1986. Neoplasms of the skin and subcutaneous tissues in dogs and cats. Br Vet J 142: 1-19.

13. Brannan CI, Bedell MA, Resnick JL, Eppig JJ, Handel MA, Williams DE, Lyman SD, Donovan PJ, Jenkins NA, Copeland NG. Developmental abnormalities in Steel17H mice result from a splicing defect in the steel factor cytoplasmic tail. Genes Dev. 1992 Oct;6(10):1832-42.

14. Brookes S, Rowe J, Ruas M, Llanos S, Clark PA, Lomax M, James MC, Vatcheva R, Bates S, Vousden KH, Parry D, Gruis N, Smit N, Bergman W, Peters G. 2002. INK4a-deficient human diploid fibroblasts are resistant to RAS-induced senescence. EMBO J. 21(12):2936-45.

15. Büttner C, Henz BM, Welker P, Sepp NT, Grabbe J. Identification of activating c-kit mutations in adult-, but not in childhood-onset indolent mastocytosis: a possible explanation for divergent clinical behavior. J Invest Dermatol. 1998 Dec;111(6):1227-31.

16. Caruana G, Ashman LK, Fujita J, Gonda TJ. Responses of the murine myeloid cell line FDC-P1 to soluble and membrane-bound forms of steel factor (SLF). Exp Hematol. 1993 Jun;21(6):761-8.

17. Caruana G, Cambareri AC and Ashman LK. 1999. Isoforms of c-KIT differ in activation of signalling pathways and transformation of NIH3T3 fibroblasts. Oncogene. 18: 5573-5581.

18. Chabot DA, Stephenson VM, Chapman P, Besmer P, Bernstein A. 1988. The proto-oncogene c-kit encoding a transmembrane tyrosine kinase receptor maps to the mouse W locus. Nature. 335: 88–89.

19. Chian R, Young S, Danilkovitch-Miagkova A, Rönnstrand L, Leonard E, Ferrao P, Ashman L, Linnekin D. 2001. Phosphatidylinositol 3 kinase contributes to the transformation of hematopoietic cells by the D816V c-Kit mutant. Blood. 98: 1365-1373.

20. Copeland NG, Gilbert DJ, Cho BC, Donovan PJ, Jenkins NA, Cosman D, Anderson D, Lyman SD, Williams DE. Mast cell growth factor maps near the steel locus on mouse chromosome 10 and is deleted in a number of steel alleles. Cell. 1990 Oct 5;63(1):175-83.

21. Dobson JM, Scase TJ. 2007. Advances in the diagnosis and management of cutaneous mast cell tumours in dogs. J Small Anim Pract. 48(8): 424-31.

22. Duesberg P, Rausch C, Rasnick D, Hehlmann R. 1998. Genetic instability of cancer cells is proportional to their degree of aneuploidy. Proc Natl Acad Sci USA. 95(23):13692–7.

23. Fridman AL, Tainsky MA. Critical pathways in cellular senescence and immortalization revealed by gene expression profiling. Oncogene. 2008 Oct 9;27(46):5975-87.

24. Frost MJ, Ferrao PT, Hughes TP, Ashman LK. Juxtamembrane mutant V560GKit is more sensitive to Imatinib (STI571) compared with wild-type c-kit whereas the kinase domain mutant D816VKit is resistant. Mol Cancer Ther. 2002 Oct;1(12):1115-24.

25. Furitsu T, Tsujimura T, Tono T, Ikeda H, Kitayama H, Koshimizu U, Sugahara H, Butterfield JH, Ashman LK, Kanayama Y, Matsuzawa Y, Kitamura Y, Kanakura Y. 1993. Identification of mutations in the coding sequence of the proto-oncogene c-kit in a human mast cell leukemia cell line causing ligand-independent activation of *c-kit* product. J Clin Invest. 92:1736-1744.

26. Galli SJ, Grimbaldeston M, Tsai M. Immunomodulatory mast cells: negative, as well as positive, regulators of immunity. Nat Rev Immunol 2008;8(6):478–86.

27. Galli SJ, Zsebo KM, Geissler EN. The kit ligand, stem cell factor. Adv Immunol. 1994;55:1-96.

28. Giebel LB, Spritz RA. Mutation of the KIT (mast/stem cell growth factor receptor) protooncogene in human piebaldism. Proc Natl Acad Sci U S A. 1991 Oct 1;88(19):8696-9.

29. Gleixner KV, Rebuzzi L, Mayerhofer M, Gruze A, Hadzijusufovic E, Sonneck K, Vales A, Kneidinger M, Samorapoompichit P, Thaiwong T, Pickl WF, Yuzbasiyan-Gurkan V, Sillaber C, Willmann M, Valent P. 2007. Synergistic antiproliferative effects of KIT tyrosine kinase inhibitors on neoplastic canine mast cells. Exp Hematol. 35(10): 1510-21.

30. Gregory-Bryson E, Bartlett E, Kiupel M, Hayes S, Yuzbasiyan-Gurkan V. Canine and human gastrointestinal stromal tumors display similar mutations in c-KIT exon 11. BMC Cancer. 2010 Oct 15;10:559.

31. Gurish MF, Austen KF. 2001. The diverse roles of mast cells. J Exp Med. 194(1): F1-5.

32. Hahn WC, Counter CM, Lundberg AS, Beijersbergen RL, Brooks MW, Weinberg RA. 1999. Creation of human tumour cells with defined genetic elements. Nature, 400:464-468.

33. Hahn WC, Dessain SK, Brooks MW, King JE, Elenbaas B, Sabatini DM, DeCaprio JA, Weinberg RA. 2002. Enumeration of the simian virus 40 early region elements necessary for human cell transformation. Mol Cell Biol. 22:2111-2123.

34. Hanahan D and Weinberg RA. 2011. Hallmarks of cancer: the next generation. Cell. 4;144(5):646-74.

35. Hanahan D, Weinberg RA. The hallmarks of cancer. Cell. 2000 Jan 7;100(1):57-70.

36. Hassan S, Kinoshita Y, Kawanami C, Kishi K, Matsushima Y, Ohashi A, Funasaka Y, Okada A, Maekawa T, He-Yao W, Chiba T. Expression of protooncogene c-kit and its ligand stem cell factor (SCF) in gastric carcinoma cell lines. Dig Dis Sci. 1998 Jan;43(1):8-14.

37. Heeg S, Doebele M, von Werder A, Opitz OG. 2006. In vitro transformation models: modeling human cancer. Cell Cycle. 5(6):630-4.

38. Heinrich M, Blanke CD, Druker BJ, Corless CL. 2002. Inhibition of KIT tyrosine kinase activity: a novel molecular approach to the treatment of KIT-positive malignancies. J Clin Oncol 20: 1692–1703.

39. Heinrich MC, Corless CL, Duensing A, McGreevey L, Chen CJ, Joseph N, Singer S, Griffith DJ, Haley A, Town A, Demetri GD, Fletcher CD, Fletcher JA. PDGFRA activating mutations in gastrointestinal stromal tumors. Science. 2003 Jan 31;299(5607):708-10.

40. Hirota S, Isozaki K, Moriyama Y, Hashimoto K, Nishida T, Ishiguro S, Kawano K, Hanada M, Kurata A, Takeda M, Muhammad Tunio G, Matsuzawa Y, Kanakura Y, Shinomura Y, Kitamura Y. Gain-of-function mutations of c-kit in human gastrointestinal stromal tumors. Science. 1998 Jan 23;279(5350):577-80.

41. Holland AJ, Cleveland DW. 2009. Boveri revisited: chromosomal instability, aneuploidy and tumorigenesis. Nat Rev Mol Cell Biol. 2009 Jul;10(7):478-87.

42. Hongyo T, Li T, Syaifudin M, Baskar R, Ikeda H, Kanakura Y, Aozasa K, Nomura T. Specific c-kit mutations in sinonasal natural killer/T-cell lymphoma in China and Japan. Cancer Res. 2000 May 1;60(9):2345-7.

43. Huang EJ, Nocka KH, Buck J, Besmer P. Differential expression and processing of two cell associated forms of the kit-ligand: KL-1 and KL-2. Mol Biol Cell. 1992 Mar;3(3):349-62.

44. Isotani M, Tamura K, Yagihara H, Hikosaka M, Ono K, Washizu T, Bonkobara M. Identification of a c-kit exon 8 internal tandem duplication in a feline mast cell tumor case and its favorable response to the tyrosine kinase inhibitor imatinib mesylate. Vet Immunol Immunopathol. 2006 Nov 15;114(1-2):168-72.

45. Jacobs-Helber SM, Penta K, Sun Z, Lawson A, Sawyer ST. 1997. Distinct signaling from stem cell factor and erythropoietin in HCD57 cells. J Biol Chem. 272: 6850-6853.

46. Kalesnikoff J, Galli SJ. New developments in mast cell biology. Nat Immunol. 2008 Nov;9(11):1215-23.

47. Khazaie K, Blatner NR, Khan MW, Gounari F, Gounaris E, Dennis K, Bonertz A, Tsai FN, Strouch MJ, Cheon E, Phillips JD, Beckhove P, Bentrem DJ. The significant role of mast cells in cancer. Cancer Metastasis Rev. 2011 Mar;30(1):45-60.

48. Kimura Y, Jones N, Klüppel M, Hirashima M, Tachibana K, Cohn JB, Wrana JL, Pawson T, Bernstein A. Targeted mutations of the juxtamembrane tyrosines in the Kit receptor tyrosine kinase selectively affect multiple cell lineages. Proc Natl Acad Sci U S A. 2004 Apr 20;101(16):6015-20.

49. Kiupel M, Webster JD, Bailey KL, Best S, DeLay J, Detrisac CJ, Fitzgerald SD, Gamble D, Ginn PE, Goldschmidt MH, Hendrick MJ, Howerth EW, Janovitz EB, Langohr I, Lenz SD, Lipscomb TP, Miller MA, Misdorp W, Moroff S, Mullaney TP, Neyens I, O'Toole D,

Ramos-Vara J, Scase TJ, Schulman FY, Sledge D, Smedley RC, Smith K, W Snyder P, Southorn E, Stedman NL, Steficek BA, Stromberg PC, Valli VE, Weisbrode SE, Yager J, Heller J, Miller R. Proposal of a 2-tier histologic grading system for canine cutaneous mast cell tumors to more accurately predict biological behavior. Vet Pathol. 2011 Jan;48(1):147-55.

50. Kiupel M, Webster JD, Kaneene JB, Miller RA, Yuzbasiyan-Gurkan V. 2004. The Use of KIT and Tryptase Expression Patterns as Prognostic Tools for Canine Cutaneous Mast Cell Tumors. Vet Pathol 41: 371-377.

51. Knol EF, Olszewski M. Basophils and mast cells: Underdog in immune regulation? Immunol Lett. 2011 Jul;138(1):28-31.

52. Krystal GW, DeBerry CS, Linnekin D, Litz J. 1998. Lck associates with and is activated by Kit in a small cell lung cancer cell line: inhibition of SCF-mediated growth by the Src family kinase inhibitor PP1. Cancer Res. 58(20): 4660-6.

53. Kurosawa K, Miyazawa K, Gotoh A, Katagiri T, Nishimaki J, Ashman LK, Toyama K. Immobilized anti-KIT monoclonal antibody induces ligand-independent dimerization and activation of Steel factor receptor: biologic similarity with membrane-bound form of Steel factor rather than its soluble form. Blood. 1996 Mar 15;87(6):2235-43.

54. Lennartsson J, Jelacic T, Linnekin D, Shivakrupa R. Normal and oncogenic forms of the receptor tyrosine kinase kit. Stem Cells. 2005;23(1):16-43.

55. Lennartsson J, Rönnstrand L. The stem cell factor receptor/c-Kit as a drug target in cancer. Curr Cancer Drug Targets. 2006 Feb;6(1):65-75.

56. Lenos K, de Lange J, Teunisse AF, Lodder K, Verlaan-de Vries M, Wiercinska E, van der Burg MJ, Szuhai K, Jochemsen AG. 2011. Oncogenic functions of hMDMX in in vitro transformation of primary human fibroblasts and embryonic retinoblasts. Mol Cancer. 12;10:111.

57. Levina V, Marrangoni A, Wang T, Parikh S, Su Y, Herberman R, Lokshin A, Gorelik E. Elimination of human lung cancer stem cells through targeting of the stem cell factor-c-kit autocrine signaling loop. Cancer Res. 2010 Jan 1;70(1):338-46.

58. Lin TY, Bear M, Du Z, Foley KP, Ying W, Barsoum J, London C. The novel HSP90 inhibitor STA-9090 exhibits activity against Kit-dependent and –independent malignant mast cell tumors. Exp Hematol. 2008 Oct;36(10):1266-77.

59. Lin TY, Fenger J, Murahari S, Bear MD, Kulp SK, Wang D, Chen CS, Kisseberth WC, London CA. AR-42, a novel HDAC inhibitor, exhibits biologic activity against malignant mast cell lines via down-regulation of constitutively activated Kit. Blood. 2010 May 27;115(21):4217-25.

60. Linnekin D. 1999. Early signaling pathways activated by c-Kit in hematopoietic cells. Int J Biochem Cell Biol. 31(10): 1053-1074.

61. Liu J, Zhang Y, Zhao J, Yang Z, Li D, Katirai F, Huang B. Mast cell: insight into remodeling a tumor microenvironment. Cancer Metastasis Rev. 2011 Jun;30(2):177-84.

62. London CA, Galli SJ, Yuuki T, Hu ZQ, Helfand SC, Geissler EN. Spontaneous canine mast cell tumors express tandem duplications in the proto-oncogene c-kit. Exp Hematol. 1999 Apr;27(4):689-97.

63. Longley BJ, Reguera MJ, Ma Y. Classes of c-KIT activating mutations: proposed mechanisms of action and implications for disease classification and therapy. Leuk Res. 2001 Jul;25(7):571-6.

64. Ma Y, Longley BJ, Wang X, Blount JL, Langley K, Caughey GH. Clustering of activating mutations in c-KIT's juxtamembrane coding region in canine mast cell neoplasms. J Invest Dermatol. 1999 Feb;112(2):165-70.

65. Ma Y, Zeng S, Metcalfe DD, Akin C, Dimitrijevic S, Butterfield JH, McMahon G, Longley BJ. The c-KIT mutation causing human mastocytosis is resistant to STI571 and other KIT kinase inhibitors; kinases with enzymatic site mutations show different inhibitor sensitivity profiles than wild-type kinases and those with regulatory-type mutations. Blood. 2002 Mar 1;99(5):1741-4.

66. Miettinen M, Lasota J. KIT (CD117): a review on expression in normal and neoplastic tissues, and mutations and their clinicopathologic correlation. Appl Immunohistochem Mol Morphol. 2005 Sep;13(3):205-20.

67. Misdorp W. 2004. Mast cells and canine mast cell tumours. A review. Vet Q. 26: 156-169.

68. Miyazawa K, Williams DA, Gotoh A, Nishimaki J, Broxmeyer HE, Toyama K. Membrane-bound Steel factor induces more persistent tyrosine kinase activation and longer life span of c-kit gene-encoded protein than its soluble form. Blood. 1995 Feb 1;85(3):641-9.

69. Molderings GJ, Brettner S, Homann J, Afrin LB. Mast cell activation disease: a concise practical guide for diagnostic workup and therapeutic options. J Hematol Oncol. 2011 Mar 22;4:10.

70. Muciaccia B, Sette C, Paronetto MP, Barchi M, Pensini S, D'Agostino A, Gandini L, Geremia R, Stefanini M, Rossi P. Expression of a truncated form of KIT tyrosine kinase in human spermatozoa correlates with sperm DNA integrity. Hum Reprod. 2010 Sep;25(9):2188-202.

71. Nagata H, Worobec AS, Oh CK, Chowdhury BA, Tannenbaum S, Suzuki Y, Metcalfe DD. Identification of a point mutation in the catalytic domain of the protooncogene c-kit in

peripheral blood mononuclear cells of patients who have mastocytosis with an associated hematologic disorder. Proc Natl Acad Sci U S A. 1995 Nov 7;92(23):10560-4.

72. Nardella C, Clohessy JG, Alimonti A, Pandolfi PP. Pro-senescence therapy for cancer treatment. Nat Rev Cancer. 2011 Jun 24;11(7):503-11.

73. Natali PG, Berlingieri MT, Nicotra MR, Fusco A, Santoro E, Bigotti A, Vecchio G. Transformation of thyroid epithelium is associated with loss of c-kit receptor. Cancer Res. 1995 Apr 15;55(8):1787-91.

74. Natali PG, Nicotra MR, Sures I, Mottolese M, Botti C, Ullrich A. Breast cancer is associated with loss of the c-kit oncogene product. Int J Cancer. 1992 Nov 11;52(5):713-7.

75. Nicholson JM, Cimini D. 2011. How mitotic errors contribute to karyotypic diversity in cancer. Adv Cancer Res. 112:43-75.

76. Ning ZQ, Li J, Arceci RJ. Activating mutations of c-kit at codon 816 confer drug resistance in human leukemia cells. Leuk Lymphoma. 2001 May;41(5-6):513-22.

77. O'Keefe DA. 1990. Canine mast cell tumors. Vet Clin North Am Small Anim Pract. 20: 1105-1115.

78. Paronetto MP, Farini D, Sammarco I, Maturo G, Vespasiani G, Geremia R, Rossi P, Sette C. Expression of a truncated form of the c-Kit tyrosine kinase receptor and activation of Src kinase in human prostatic cancer. Am J Pathol. 2004 Apr;164(4):1243-51.

79. Patnaik AK, Ehler WE, MacEwen EG, 1984. Canine cutaneous mast cell tumors: morphological grading and survival time in 83 dogs. Vet Pathol 21: 469-474.

80. Rapley EA, Hockley S, Warren W, Johnson L, Huddart R, Crockford G, Forman D, Leahy MG, Oliver DT, Tucker K, Friedlander M, Phillips KA, Hogg D, Jewett MA, Lohynska R, Daugaard G, Richard S, Heidenreich A, Geczi L, Bodrogi I, Olah E, Ormiston WJ, Daly PA, Looijenga LH, Guilford P, Aass N, Fossa SD, Heimdal K, Tjulandin SA, Liubchenko L, Stoll H, Weber W, Einhorn L, Weber BL, McMaster M, Greene MH, Bishop DT, Easton D, Stratton MR, 2004. Somatic mutations of KIT in familial testicular germ cell tumours. Br J Cancer 90: 2397–2401.

81. Ried T, Heselmeyer-Haddad K, Blegen H, Schrock E, Auer G. 1999. Genomic changes defining the genesis, progression, and malignancy potential in solid human tumors: a phenotype/genotype correlation. Genes Chromosomes Cancer. 25(3):195–204.

82. Rönnstrand L. Signal transduction via the stem cell factor receptor/c-Kit. Cell Mol Life Sci. 2004 Oct;61(19-20):2535-48.

83. Sette C, Dolci S, Geremia R, Rossi P. The role of stem cell factor and of alternative c-kit gene products in the establishment, maintenance and function of germ cells. Int J Dev Biol. 2000;44(6):599-608.

84. Sfiligoi G, Rassnick KM, Scarlett JM, Northrup NC, Gieger TL. 2005. Outcome of dogs with mast cell tumors in the inguinal or perineal region versus other cutaneous locations: 124 cases (1990–2001). Journal of the American Veterinary Medical Association 226: 1368–74.

85. Shay JW, Van Der Haegen BA, Ying Y, Wright WE. 1993. The frequency of immortalization of human fibroblasts and mammary epithelial cells transfected with SV40 large T-antigen. Exp Cell Res. 209(1):45-52.

86. Sihto H, Sarlomo-Rikala M, Tynninen O, Tanner M, Andersson LC, Franssila K, Nupponen NN, Joensuu H. 2005. KIT and platelet-derived-growth factor receptor alpha tyrosine kinase mutations and KIT amplifications in human solid tumors. J Clin Oncol 23: 49–57.

87. Sun H and Taneja R. 2007. Analysis of transformation and tumorigenicity using mouse embryonic fibroblast cells. Methods Mol Biol. 383:303-10.

88. Tajima, Y., Huang, E. J., Vosseller, K., Ono, M., Moore, M. A. S.,and Besmer, P. (1998). Role of dimerization of the membraneassociated growth factor kit ligand in juxtacrine signaling: The Sl 17H mutation affects dimerization and stability phenotypes in hematopoiesis. J. Exp. Med. 187, 1451–1461.

89. Takaoka A, Toyota M, Hinoda Y, Itoh F, Mita H, Kakiuchi H, Adachi M, Imai K. Expression and identification of aberrant c-kit transcripts in human cancer cells. Cancer Lett. 1997 May 19;115(2):257-61.

90. Théou-Anton N, Tabone S, Brouty-Boyé D, Saffroy R, Ronnstrand L, Lemoine A, Emile JF. Co expression of SCF and KIT in gastrointestinal stromal tumours (GISTs) suggests an autocrine/paracrine mechanism. Br J Cancer. 2006 Apr 24;94(8):1180-5.

91. Tian Q, Frierson HF Jr, Krystal GW, Moskaluk CA. Activating c-kit gene mutations in human germ cell tumors. Am J Pathol. 1999 Jun;154(6):1643-7.

92. Toksoz D, Zsebo KM, Smith KA, Hu S, Brankow D, Suggs SV, Martin FH, Williams DA. Support of human hematopoiesis in long-term bone marrow cultures by murine stromal cells selectively expressing the membrane-bound and secreted forms of the human homolog of the steel gene product, stem cell factor. PNAS USA. 1992 Aug 15;89(16):7350-4.

93. Toyota M, Hinoda Y, Itoh F, Takaoka A, Imai K, Yachi A. Complementary DNA cloning and characterization of truncated form of c-kit in human colon carcinoma cells. Cancer Res. 1994 Jan 1;54(1):272-5.

94. Tsujimura T, Furitsu T, Morimoto M, Isozaki K, Nomura S, Matsuzawa Y, Kitamura Y, Kanakura Y. 1994. Ligand-independent activation of c-kit receptor tyrosine kinase in a murine mastocytoma cell line P-815 generated by a point mutation. Blood. 83(9): 2619-26.

95. Tsujimura T, Furitsu T, Morimoto M, Kanayama Y, Nomura S, Matsuzawa Y, Kitamura Y, Kanakura Y.Substitution of an aspartic acid results in constitutive activation of c-kit receptor tyrosine kinase in a rat tumor mast cell line RBL-2H3. Int Arch Allergy Immunol. 1995. 106(4): 377-85.

96. Tuveson DA, Willis NA, Jacks T, Griffin JD, Singer S, Fletcher CD, Fletcher JA, Demetri GD. STI571 inactivation of the gastrointestinal stromal tumor c-KIT oncoprotein: biological and clinical implications. Oncogene. 2001 Aug 16;20(36):5054-8.

97. Valent P, Akin C, Sperr WR, Horny HP, Arock M, Lechner K, Bennett JM, Metcalfe DD. Diagnosis and treatment of systemic mastocytosis: state of the art. Br J Haematol. 2003 Sep;122(5):695-717.

98. Valent P, Cerny-Reiterer S, Herrmann H, Mirkina I, George TI, Sotlar K, Sperr WR, Horny HP. Phenotypic heterogeneity, novel diagnostic markers, and target expression profiles in normal and neoplastic human mast cells. Best Pract Res Clin Haematol. 2010 Sep;23(3):369-78.

99. Vogelstein B, Kinzler KW. The multistep nature of cancer. Trends Genet. 1993 Apr;9(4):138-41.

100. Weaver, B. A. & Cleveland, D. W. 2006. Does aneuploidy cause cancer? Curr. Opin. Cell Biol. 18, 658–667.

101. Webster JD, Yuzbasiyan-Gurkan V, Kaneene JB, Miller R, Resau JH, Kiupel M. The role of c-KIT in tumorigenesis: evaluation in canine cutaneous mast cell tumors. Neoplasia. 2006 Feb;8(2):104-11.

102. Webster JD, Yuzbasiyan-Gurkan V, Miller RA, Kaneene JB, Kiupel M. Cellular proliferation in canine cutaneous mast cell tumors: associations with c-KIT and its role in prognostication. Vet Pathol. 2007 May;44(3):298-308.

103. Wehrle-Haller B, Weston JA. Altered cell-surface targeting of stem cell factor causes loss of melanocyte precursors in Steel17H mutant mice. Dev Biol. 1999 Jun 1;210(1):71-86.

104. Williams DE, de Vries P, Namen AE, Widmer MB, Lyman SD. The Steel factor. Dev Biol. 1992 Jun;151(2):368-76.

105. Willmore-Payne C, Holden JA, Tripp S, Layfield LJ. Human malignant melanoma: detection of BRAF- and c-kit-activating mutations by high-resolution amplicon melting analysis. Hum Pathol. 2005 May;36(5):486-93.

106. Yared MA, Middleton LP, Meric F, Cristofanilli M, Sahin AA. Expression of c-kit proto-oncogene product in breast tissue. Breast J. 2004 Jul-Aug;10(4):323-7.

107. Yeh E, Cunningham M, Arnold H, Chasse D, Monteith T, Ivaldi G, Hahn WC, Stukenberg PT, Shenolikar S, Uchida T, Counter CM, Nevins JR, Means AR, Sears R. 2004. A signalling pathway controlling c-Myc degradation that impacts oncogenic transformation of human cells. Nat Cell Biol. 6:308-18.

108. Yuzawa S, Opatowsky Y, Zhang Z, Mandiyan V, Lax I, Schlessinger J. Structural basis for activation of the receptor tyrosine kinase KIT by stem cell factor. Cell. 2007 Jul 27;130(2):323-34.

109. Zayas J, Spassov DS, Nachtman RG, Jurecic R. Murine hematopoietic stem cells and multipotent progenitors express truncated intracellular form of c-kit receptor. Stem Cells Dev. 2008 Apr;17(2):343-53.

110. Zemke D, Yamini B, Yuzbasiyan-Gurkan V. 2002. Mutations in the juxtamembrane domain of c-KIT are associated with higher grade mast cell tumors in dogs. Vet Pathol 39: 529-535.

111. Zhang H. Molecular signaling and genetic pathways of senescence: Its role in tumorigenesis and aging. J Cell Physiol. 2007 Mar;210(3):567-74.

CHAPTER 2

ESTABLISHMENT OF MUTANT C-KIT TRANSFECTED CANINE FIBROBLATS

ABSTRACT

Mast cell tumors (MCTs) represent the most common cutaneous tumors in dogs. They tend to occur in middle-aged dogs of either gender, with predominance in Boxers, Boston terriers, Bull terriers, Weimaraners and Labrador retrievers. Our laboratory has documented that some MCTs have mutations in the c-*KIT* gene, which are associated with poor prognosis. The mutational spectrum observed in c-KIT in dogs is slightly different than in humans and ranges from deletion mutations to a varying set of tandem repeat mutations in the juxtamembrane domain. The mutations observed in the MCTs are thought to be activating mutations, based on some limited studies in one cell line. To date, the direct role of mutant c-KIT isoforms in canine tumorigenesis has not been investigated. To study the molecular and cellular changes resulting directly from mutations in c-KIT, expression vectors containing normal and mutant canine KIT genes were constructed in the plasmid vector, pACGFP1N1, and transfected into canine primary fibroblasts with the resultant cells and progeny selected for stable expression of the plasmid. The mutations included three deletion mutations and three internal tandem duplications, all within exon 11. Site-directed mutagenesis was employed to generate the deletion mutants, while megaprimer PCR was employed to modify the clones to include tandem repeat mutations. These constructs were transfected into cultured canine primary fibroblasts. As fibroblasts do not constitutively express c-KIT, any effect on phenotype can be attributed to the experimentally induced expression. By studying the resulting transfectants, we proposed to test the hypothesis that expression of each mutant c-KIT variant is sufficient to transform fibroblasts. Here we report that after selection with G418 for stable transfectants, we observed GFP expression by fluorescence microscopy and detected c-KIT expression by RT-PCR. Compared with the normal c-KIT transfectant, the life spans of transfected c-KIT mutants were prolonged. Microscopic

analysis of the morphology of all cells transfected with mutant c-KIT isoforms showed that not one of those transfected cells with wild type c-KIT showed dense, multi-layered growth characteristic of a loss of contact inhibition. These cell lines are now available for use in further studies. The functional consequences of the c-KIT mutations will elucidate their role in tumorigenesis, and the cell lines generated will have therapeutic relevance in the assessment of c-KIT driven cancers.

INTRODUCTION

The c-KIT protein, one of type III tyrosine kinase receptors, plays a key role in hematopoiesis, gametogenesis, melanogenesis, and mast cell proliferation. Binding of the ligand, stem cell factor (SCF), to the extracellular domain of the c-KIT receptor induces the dimerization of the receptors and thereby activates the tyrosine kinase cascade through the autophosphorylation of tyrosine residues in the juxtamembrane domain and the kinase domain of the receptor (Lennartsson and Rönnstrand, 2006). Mutations in c-KIT have been reported in many disorder and tumors in various species. Genetic alteration causing loss-of-function of c-KIT results in piebaldism syndrome (Giebel and Spritz, 1991), whereas overexpression or constitutive activation of c-KIT is associated with tumorigenesis (Edling and Hallberg, 2007). More specifically, there is a signal sequence located in the N-terminal end of the receptor. This sequence is followed by the five Ig-like motifs. The second and third Ig-like motifs together are proposed to constitute the ligand binding pocket (Zhang ei al., 2000). The fourth Ig-like motif contains the dimerisation site. Deletion of the fourth Ig-like motif completely abolishes dimerisation and the subsequent downstream signal transduction events. A defective dimerisation site results in accelerated ligand dissociation, indicating that the ligand affinity is dependent on dimerisation of the receptors (Blechman et al., 1995). The intracellular part of c-KIT is composed of the autoinhibitory juxta-membrane domain and the two kinase domains with the insert domain in between them. The kinase domains, with the activation loop located in the distal kinase domain, are responsible for catalysing the transfer of a phosphate group from ATP to the substrate (Roskoski, 2005).

The activating mutantions of c-KIT confer constitutive tyrosine phosphorylation and ligand-independent downstream activation. These mutations expose a strong oncogenic potential

of c-KIT (Edling and Hallberg, 2007). Tumors caused by constitutively activated c-KIT include different types of mast cell neoplasms, gastrointestinal stromal tumors (GISTs), germ cell tumors and some leukemias. In addition, aberrant expression of c-KIT has been observed in many types of tumors such as small cell lung carcinomas, colon cancers, and prostate cancers (Miettinen & Lasota, 2005, Sattler and Salgia, 2004).

Although mechanisms of c-KIT mutation in exon 11 in signaling pathway activation have been described (Lennartsson and Ronnstrand, 2006; Nakai et al., 2005;) , it is unknown whether or not mutant c-KIT isoforms result in *de novo* transformation and tumorigenesis potential of each mutant c-KIT isoforms. Neither study investigated the direct effect of mutant c-KIT isoforms on neoplastic transformation, especially *de novo* transformation in primary fibroblasts. In this study, a series of c-KIT mutations in exon 11 reported in canine GISTs (Gregory-Bryson et al., 2011) and canine mast cell tumors (Zemke et al., 2002) were introduced into normal canine primary fibroblasts. The objective of this study was to establish a model system to investigate the tumorigenic transformation potentials directly driven by mutant c-KIT isoforms with a view toward determining the roles they might play in cancers. Thus, fibroblasts, which do not have constitutive c-KIT expression and are not easily transformed, were selected as the cells with which to observe the effects of expression of normal and mutant c-KIT isoforms.

MATERIALS AND METHODS

Canine Primary Fibroblast Isolation

Canine primary fibroblasts (CAF) were derived from discarded tissues obtained from Veterinary Teaching Hospital, Michigan State University, in accordance with the Institutional Animal Care and Use Committee (IACUC) approved procedures. Small excisions of skin were harvested, while the dogs were under anesthesia during spay-neuter surgery in accordance with approved standard procedures. Samples from the incision site were placed in Dulbecco's Modified Eagle Medium (DMEM) with 10% fetal bovine serum (FBS). Samples were minced into small pieces, washed twice by Dulbecco's Phosphate Buffer Saline (DPBS), and then plated in DMEM supplemented with L-glutamine, penicillin/streptomycin, and 10% FCS (as referred to complete medium) at 37 degree Celsius (°C) in a 5% carbon dioxide (CO_2) incubator. Media were changed twice a week. After cells became confluent, they were trypsinized by 0.05% trypsin-ethylenediaminetetraacetic acid (EDTA) (Invitrogen) and frozen down in freezing medium (10% FBS and 10% dimethyl sulfoxide; DMSO) for further studies.

Plasmid construction

Full length wild type canine c-KIT complementary DNA (cDNA; Pubmed Reference Accession: AF448148) cloned in the expression vector, pAcGFP1N1 (Stratagene) was previously constructed and available in our lab (referred to pAcGFP1N1-wt, Figure 3). In addition, plasmids were transformed into *Escherichai coli* (E. coli) TOP10 cells (Invitrogen), which was chemically made competent cells (Inoue et al., 1980), and selected using blue-white screening.

Figure 3: Map of expression vector, pAcGFP1N1. Vector containing full length wild type c-KIT cDNA was used as a template for mutagenesis. Transgene expression was driven by the CMV promoter, and a green fluorescence protein (GFP) reporter gene was tagged at 3' of the insert.

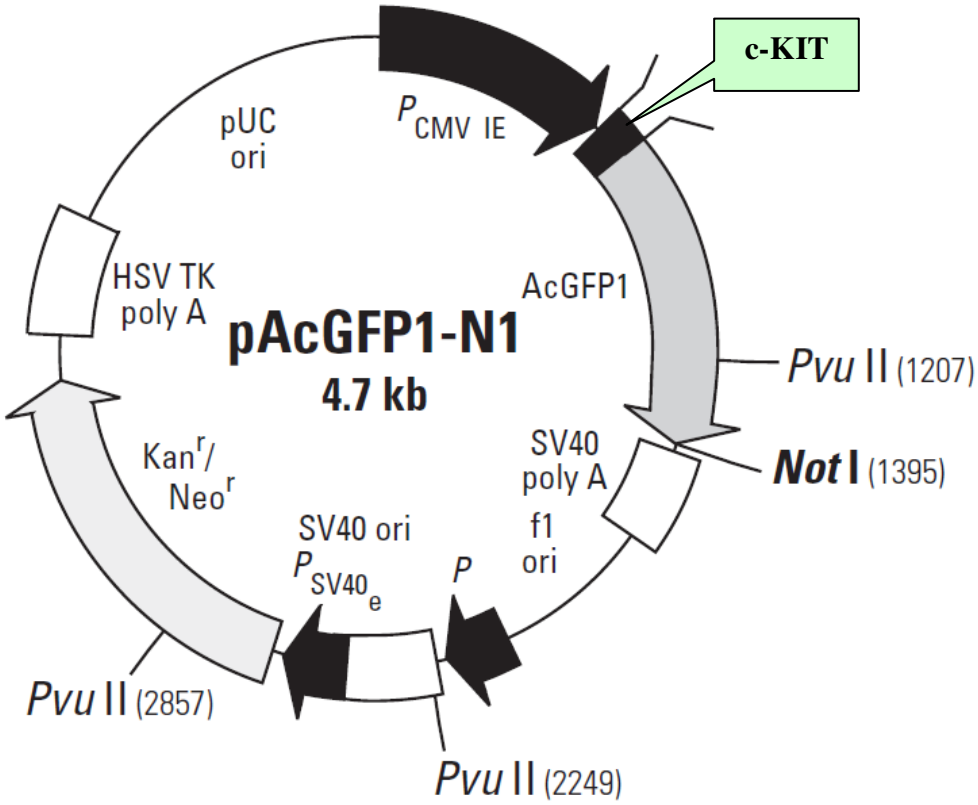

Transformant of colonies in white color, which was representing the presence of the plasmid in the cells were selected after growing on Luria-Bertani (LB) agar supplemented with kanamycin (50 milligrams/liter; mg/ml). Colonies were screened by PCR to confirm that they were harboring wild type c-KIT using these following primers: 5'-CAG ATC GTG CAG CTA ATT GA-3' and 5'-CAG ATG AAC TTC AGG GTC AGC-3'. Positive colonies were selected and grown overnight in 5 milliliters (ml) of LB broth supplemented with kanamycin.

Plasmids were extracted from overnight cultures using a QIAprep Spin Miniprep Kit (Qiagen) The full sequence and orientation of full length c-KIT insert was determined using an

ABI 3730 Genetic Analyzer (AppliedBiosystems, Inc.) by sequencing with primers flanking the insertion site as shown in Table 1.

Table 1: Primers flanking wild type c-KIT insert in expression vector, plasmid pAcGFP1N1.

Primer name	**Location**	**Sequence 5'-3'**
VYG1338 - forward	5' MCS	AAT GTC GTA ACA ACT CCG CCC
VYG966 - forward	at 715 bp	GAT GTG TCT AGT TTC GTG GA
VYG1332 - forward	at 1566 bp	CAC CCT GTT CAC ACC TTT GCT GAT
VYG1334 - forward	at 2370 bp	TTG TAT TCA CAG AGA CTT GGC TGC T
VYG1932 - reverse	3' MCS	CAG ATG AAC TTC AGG GTC AGC
VYG984 - reverse	at 2202 bp	AAC GTA AGA AAC GCC GGG TT
VYG975 - reverse	at 1408 bp	ACA GAG ACG AGT TTT GCA TC

A clone harboring the wild type c-KIT plasmids confirmed by sequencing was used as a template for mutagenesis to obtain other c-KIT mutant isoform constructs. Six different c-KIT mutant isoforms all within exon 11 (Zemke et al., 2002) were constructed (as shown in Figure 4). These included three distinct deletion and three distinct internal tandem duplication mutations.

Figure 4: Scheme of c-KIT mutations used in the study. Three different deletion mutations were located at codon 560-562 (Deletion 2), codon 559-561 (Deletion 3), and codon 560-561 (Deletion 9), resulted in deletion of two amino acids (the mutation numbering system is from Zemke et al., 2002). Three different duplication mutations were 15-16 amino acids-repeating codon, involved at codon 575-591. All mutations are in-frame mutation.

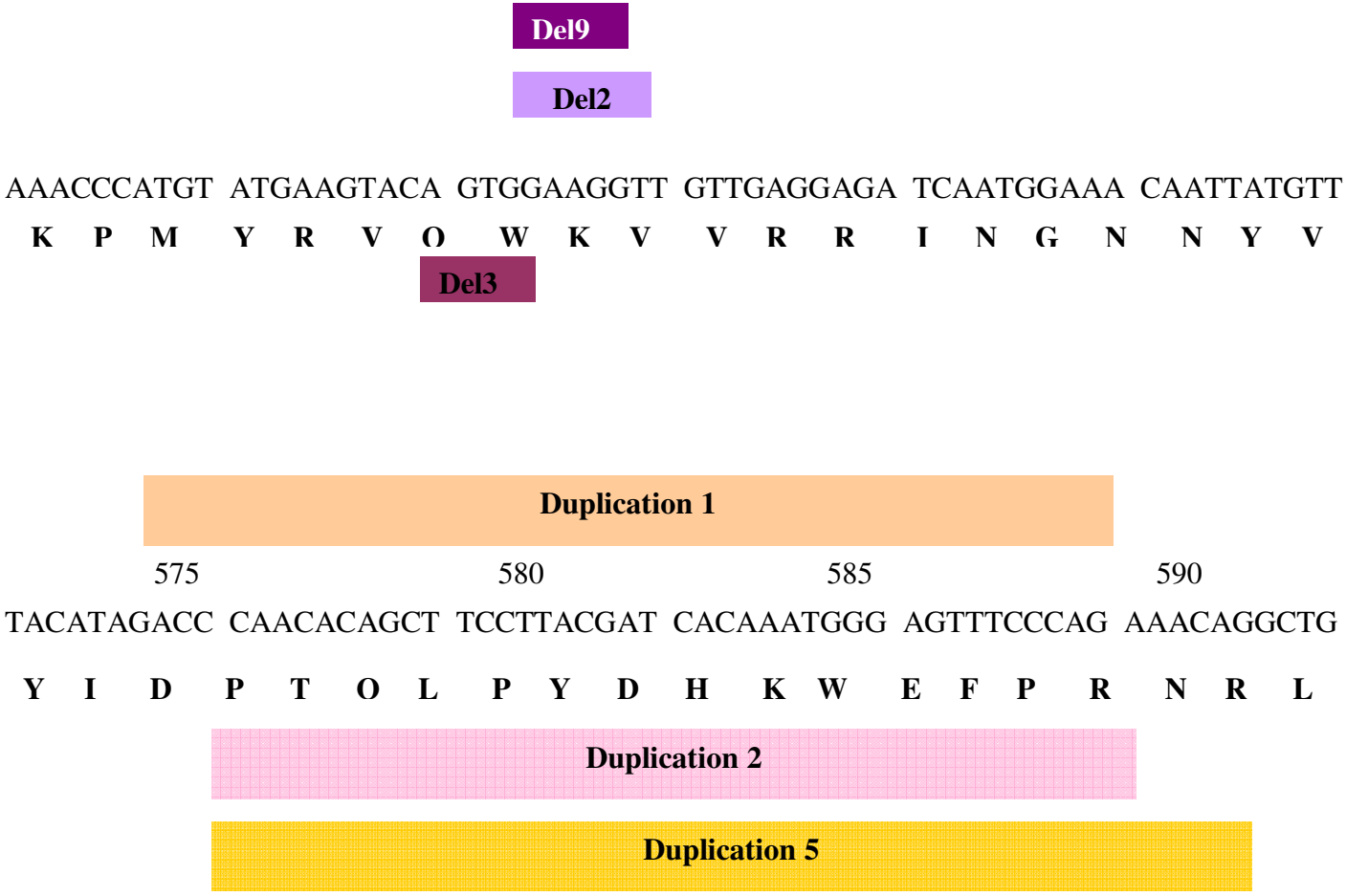

The deletion mutantion plasmids were constructed using the QuikChange Site-Directed Mutagenesis kit (Stratagene) according to the manufacturer's instructions. Duplication mutantion plasmids were constructed by the polymerase chain reaction (PCR)-based megaprimer mutagenesis method. Megaprimer amplication was performed in two steps. The first step was to generate the duplication megaprimer (171 base pairs DNA fragments) amplified with the following primers: VYG1296 5'-CCA TGT ATG AAG TAC AGT GGA AG-3' and VYG1564 5'-CAA AGC TCA GCC TGT TTC TGG-3'.

The PCR products were purified using a QIAquick PCR Purification kit (Qiagen), and used as primer for the second step. Megaprimer PCR mutagenesis was then performed using 200 nanograms (ng) of the purified PCR products generated from the first step and 5 ng of wild type c-KIT plasmid as a template, using an iProof™ High Fidelity DNA Polymerase kit (Biorad). Thermal cycle conditions were: 1 cycle of 98 °C for 30 seconds, 40 cycles of 98 °C for 10 seconds, 72 °C for 30 seconds, 72 °C for 3.5 minutes, followed by 72 °C for 10 minutes. Following the mutagenesis, the DNA was restriction digested by DpnI restriction enzyme (New England Biolabs, Inc.) for 2 hours at 37°C to digest un-mutagenized parental plasmid, and the resulting DNA was then transformed into XL-1 Blue *E. Coli* (Quickchange® II, Stratagene). Plasmids were purified from the bacteria (Miniprep®, Qiagen) and all constructs were confirmed by direct DNA sequencing to verify that the correct mutations had been produced with no unexpected mutations.

Cell Transfection

Early passage (P3-P6) canine fibroblasts grown in 6-well culture plates were transfected with each mutant c-KIT plasmid construct, using Lipofectamine™ 2000 (Invitrogen, USA) according to the manufacturer's instructions. In brief, $5x10^5$ cells were seeded on 6-well-plates

overnight until 90% to 95% confluence was reached. Plasmids containing mutant c-KIT isoforms (5 micrograms; µg) was mixed with 250 microliters (µl) of DMEM, then 10 µl of Lipofectamine 2000 mixed with 250 µl of DMEM was added and incubated for 20 min at room temperature. Finally, transfection reagent and plasmid complex were added drop wise to the cultured canine primary. Twenty four hours post transfection, the cells were passaged at a 1:10 dilution into fresh complete medium. Then, transfected fibroblasts were cultured in fresh complete medium containing 200 µg/ml G418 (Geneticin, Invitrogen) for three weeks. Cells transfected with the empty pAcGFP1N1 vector and the c-KIT wild type plasmid were processed similarly as controls. Transfection efficiency and c-KIT localization were determined by Green Fluorescence Protein (GFP) expression using cell sorting and fluorescence microscopy.

Flow cytometry-fluorescence activated cell sorting (FACs)

In this vector, the protein expression is driven by the constitutively active cytomegalovirus (CMV) promoter resulting in different in-frame green fluorescence fused- c-KIT mutant isoforms. G418-resistant transfected fibroblasts were harvested by trypsin-EDTA treatment, and washed three times by DPBS. FACs for GFP expression was performed at the Michigan State University flow cytometry core using BD FACs Vantage SE turbo sort (BD Biosciences). The sorted cells were plated in 6-well-plate with complete medium until reaching confluence, then slowly frozen overnight in an isopropanol bath freezing container (Nalgene; Nunc, Rochester, NY) at –80°C, transferred to liquid nitrogen, and preserved for further experiments.

Detection of c-KIT mRNA by RT-PCR and Quantitative RT-PCR

Total RNA was isolated from the sorted transfectants using Versagene RNA Tissue Purification Kit (Versagene) following the manufacturer's instructions and treated with DNase I

(DNA-free kit, Ambion) to remove DNA contamination. The RNA was reverse transcribed using SuperScript™ III Reverse Transcriptase (Invitrogen, USA) and the cDNA was amplified by PCR using Taq polymerase (Invitrogen, USA). Primers used are as follows: for c-KIT expression, VYG1284 5'-TAC ACA TTT CAA GTG TCC AAT TCC-3' and VYG980 5'-TAG GGC TTC TCG TTC GGT TA-3'; for β2MG (housekeeping gene) expression, VYG1487 5'- AGA AGG TAG TGA AGC AGG CAT C -3' and VYG1488 5'- GTG GAA GAG TGG GTG TCA TTG -3'. cDNA was PCR-amplified under the following conditions: 94°C for 4 min followed by 40 cycles denaturing at 94°C for 1 minute, annealing at 58°C for 1 minute, elongation at 72°C for 1 minute, and a final extension at 72°C for 5 min. PCR products were analyzed by 2.0% agarose gel electrophoresis and stained with ethidium bromide for detection of the appropriate fragment.

Quantitative real-time PCR using SYBR Green (Applid Biosystems) for amplification of c-KIT was also performed using a StepOnePlus™ Real-Time PCR System (Applied Biosystems). All analyses were done in quadruplicate, and the mean was used for further calculations. The baseline was set automatically by the StepOnePlus software, and the threshold Ct was defined as the number of cycles in which the fluorescence exceeded the automatically set threshold. The c-KIT mRNA expression was normalized by the expression of β2MG. The mRNA relative quantitation was done using the ΔCt method. The difference (ΔCt) between the average of c-KIT and the housekeeping gene (β2MG) was calculated. Fold changes in c-KIT expression of each CAF-KIT cell line as compared to primary canine fibroblasts were calculated using the delta-delta Ct (ΔΔCt) method using β2MG as the normalization control.

RESULTS

Canine primary fibroblasts were successfully isolated using the culture conditions described in Materials and Methods. Five to seven days after plating minced dog skin, cells were attached to the cell culture plate, and fibroblast colonies were formed. Then the cells were trypsinized and re-plated to obtain cell monolayers. Fibroblast morphology was observed, characterized by a stellate/elongated shape (Figure 5, left panel). Cells had a limited lifespan and became senescence after growing in culture more than a month (Figure 5, right panel).

Figure 5: Microscopic images of growing and senescent canine primary fibroblasts. Canine primary fibroblasts (active, left panel) show a normal morphology, characterized by elongated, spindle shape, with oval or round nucleus. Cells grew as monolayer on the cell culture plate. After growing in culture for more than a month, cells were underwent senescence (right panel), characterized by flat and enlarged cells (Brightfield, 4x magnification)

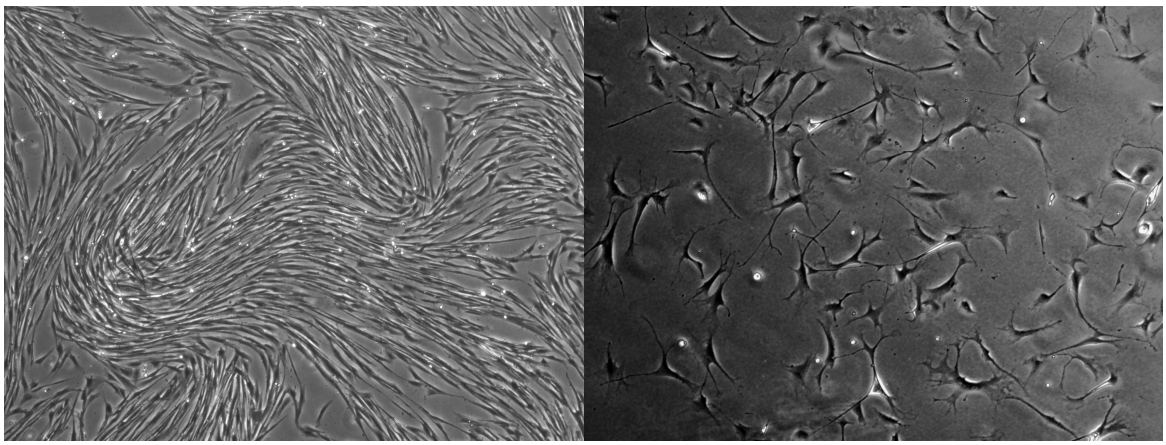

As the result of mutagenesis, plasmids containing deletion 2, deletion 3, deletion 9, duplication 1, duplication 2, and duplication 5 were used for transfection into canine primary fibroblasts. The locations and changes of each plasmid constructed are described in Table 2.

Table 2: The genetic alteration and location of c-KIT mutations used in this study.

Name	Location*	Changing
Del2	Deletion at 560-562	VQWKVV to VQFV
Del3	Deletion at 559-561	VQWKVV to VRVV
Del9	Deletion at 560-561	VQWKVV to VQVV
Dup1	Repeating of 575-589	Adding D P T Q L P Y D H K W E F P R
Dup2	Adding N plus repeating 576-589	Adding N P T Q L P Y D H K W E F P R
Dup5	Repeating of 576-591	Adding P T Q L P Y D H K W E F P R N R

* Codon numbers are based on the shorter isoform of canine full length c-KIT mRNA (without GNSK amino acid).

Before transfection, all constructs were verified by restriction digestion and sequencing, and then transfected into cells in 24-well-plates using Lipofectamine 2000 (Invitrogen). Passages 2-4 of canine primary fibroblasts were plated to obtain 90% confluence in 9 wells of 24-well-plates. Eight wells were transfected either with empty vector (pAcGFP1N1 without insert), vector with wild type c-KIT (wt-KIT), vector with deletion 2 (Del2), vector with deletion 3(Del3), vector with deletion 9 (Del9), vector with duplication 1 (Dup1), vector with duplication 2 (Dup2), or vector with duplication 5 (Dup5). Cells in one well were mocked transfected with PBS to serve as a control. The mixture of plasmid and lipofectamine was incubated overnight with fibroblasts. The next day, cells were trypsinized and passaged at a 1:10 dilution in a 60 mm plate. G418 (Geneticin, Invitrogen) was added into the complete medium at 200 μg/ml for 14 days to select cells that had taken up the plasmids, which was decreased to 25 μg/ml to maintain stable transfectants .

Figure 6: Detection of transfection in control group. Mock transfected-canine primary fibroblasts (Panel A) were died after antibiotic selection and have no GFP signal. Empty vector-transfected fibroblasts (Panel B) served as a control group, GFP signals were observed, but cells underwent senescence after G418 selection. Canine primary fibroblasts transfected with wt-GFP plasmids (Panel C and D) also served as control groups, and GFP signals were observed (Panel C; at 1 week after selection). Cells went senescent after three months in culture (Panel D). Fluorescence microscope, 10x magnifications

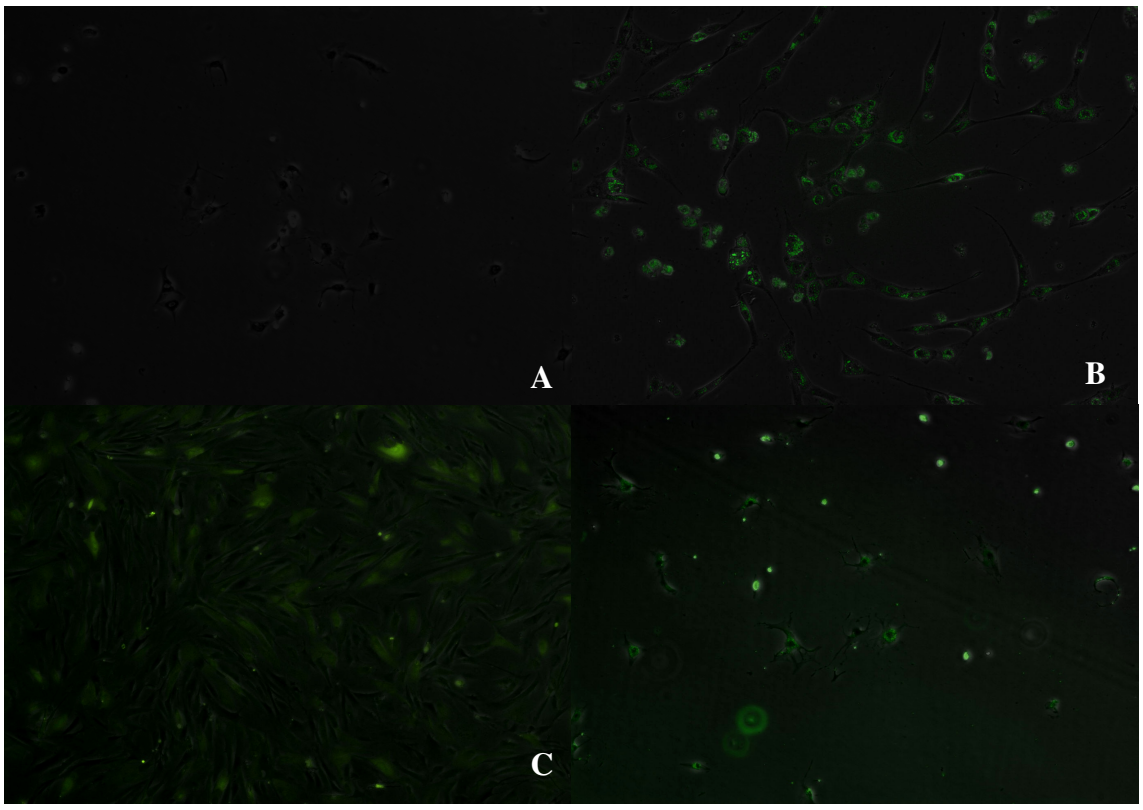

Transfection efficiency was examined by observing the number of GFP-positive cells. At the same concentration of plasmid, the transfection efficiency using lipofectamine 2000 (Invitrogen) of all mutant c-KIT plasmid in canine primary fibroblasts was about 5-10% and increased to 85-90% when cells were transfected by pAcGFP1N1 empty vector.

Figure 7: Detection of mutant c-KIT plasmid transfection. Expression of c-KIT transgene was detected by GFP reporter gene expression in Del 2, Del3, Del9, and Dup2 cell lines (picture A, B, C, and D, respectively). GFP signals were shown in the cytoplasm of cells. (Fluorescence, 20 x magnification).

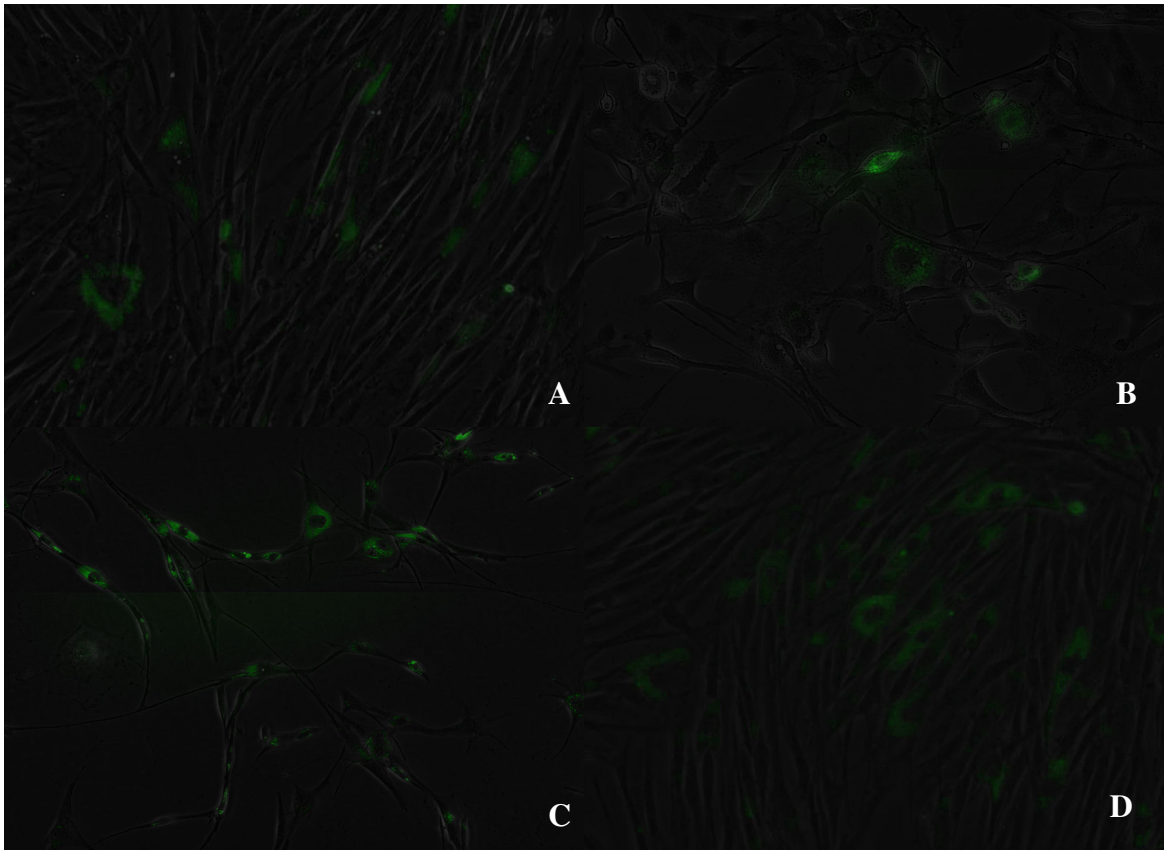

After 2 weeks of antibiotic selection, all mock transfected fibroblasts died, whereas 5-10% of vector-transfected cells survived. Cells were fed twice per week with complete medium supplemented with 25 µg/ml G418. Three months after transfection, empty vector, wt, Dup1, and Dup5 cells reached their replicative senescence, whereas Del2, Del3, Del9, Dup2 cells showed proliferation foci. Low level of GFP expression was observed under fluorescence microscope in all proliferating cell lines.

Proliferative foci from Del2, Del3, De l9, and Dup2 cell lines were trypsinized and diluted in 2%FBS/PBS at a concentration of $1x10^6$ cells/ml. Each cell line was sorted to collect the GFP-positive cells. Very small percentages of GFP positive cells were detected (Del2: 1.2%. Del3: 0.8%, Del9: 1.1%, and Dup2: 1.0%), selected, and grown in complete medium. All cell lines continued to divide rapidly and indefinitely without any sign of senescence.

RNA isolation and cDNA synthesis from each cell line was performed, and the expression level of c-KIT was determined by quantitative real-time PCR. The results from RT-PCR showed that c-KIT transgene was detected at 126 bp in all cell lines, and no c-KIT expression in normal canine fibroblast cDNA (Figure 8).

Figure 8: Expected RT-PCR fragments of 126 base pairs of c-KIT mRNA were detected. Lane 1: CAF-KIT-Del2 transfectant; Lane 2: CAF-KIT-Del3 transfectant ; Lane 3: CAF-KIT-Del9 transfectant ; Lane 4: CAF-KIT-Dup2 transfectant ; Lane 5: normal canine fibroblast (CAF); Lane +: RNA from MCTs (positive control); Lane - : A water blank (negative control) Lane M: 100 bp ladder size standard (Invirogen).

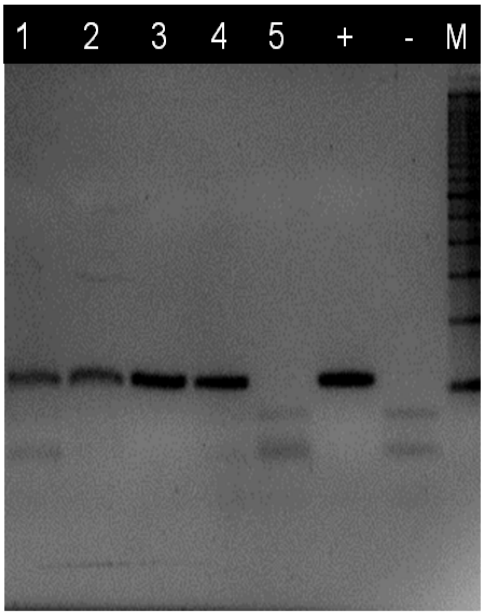

Quantificative real-time PCR showed a relatively high level of expression of c-KIT mRNA in Del2, Del9, and Dup2 cell lines (Table 3). As compared to canine primary fibroblast cDNA, Del2, Del9, Dup2 revealed their relative quantification (RQ) of c-KIT expression at 42.6, 1.8, and 8.1 time, respectively. The Del3 cell line showed under expression of c-KIT with RQ at 0.1 as compared to canine primary fibroblasts.

Table 3: Quantitative real-time RT-PCR of c-KIT mRNA expression in CAF-KIT mutant cells. * Relative quantification (RQ) shown in fold change calibrated to canine primary fibroblasts.

Primary fibroblasts as a calibrator	**RQ* measured at 3 years**			**RQ* measured at 2 years**		
	RQ Average	**RQ min**	**RQ max**	**RQ Average**	**RQ min**	**RQ max**
Del2	42.6	26.8	67.6	92.7	80.8	106.2
Del3	0.1	0.08	0.2	33.8	29.8	38.34
Del9	1.8	1.5	2.2	25.8	12.7	52.3
Dup2	8.1	6.3	10.4	1237.2	1124.6	1361.1

Figure 9: Relative quantification of c-KIT mRNA expression. Quantitative real-time RT-PCR of c-KIT mRNA expression in CAF-KIT mutant cells comparing the measurement performed at 3 years and 2 years after transfection.

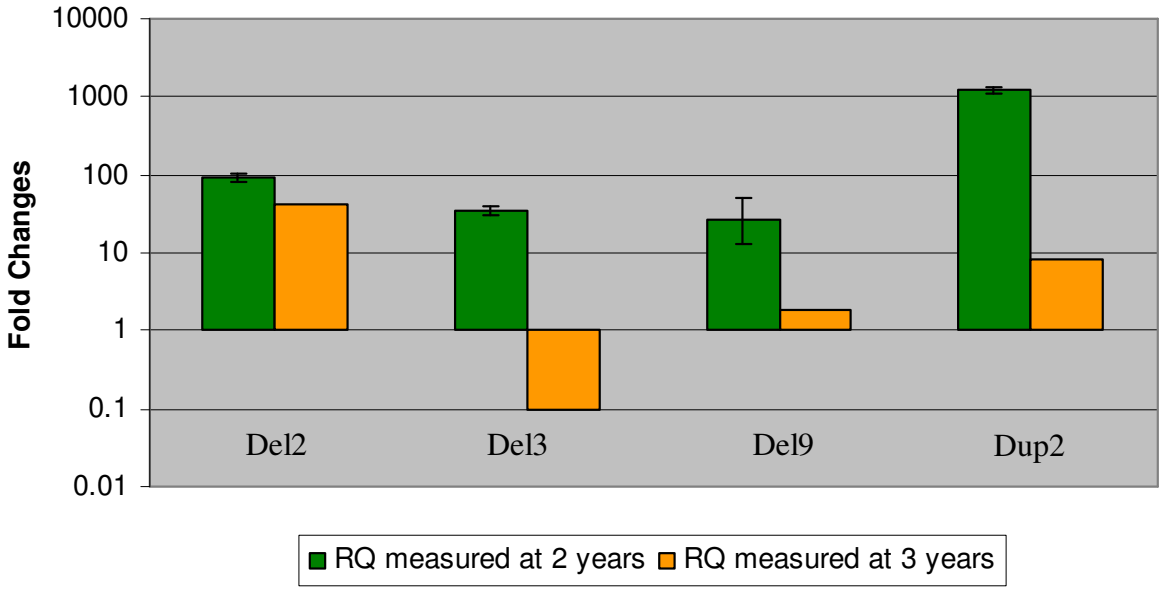

In summary, we are able to conclude the chronology of cellular changes mediated by mutant c-KIT transfection in canine primary fibroblasts. At three months after transfection and antibiotic selection, untransfected canine fibroblasts, empty vector-transfected fibroblasts, and wild type c-KIT-transfected fibroblasts went senescence by showing an enlarged, flat cell morphology, follwed by death. In contrast, cells transfected by four of six mutant c-KIT including deletion 2, deletion 3, deletion 9, and duplication 2 plasmid were alive and in their growth arrest for eight months. During this arrest period, cells maintained their normal phenotype but did not divide. Then, proliferation foci were observed and harvested for fluorescence cell sorting to select c-KIT mutant expressing cells for further study.

DISCUSSION

In this study, we were able to test the ability of deletion and duplication mutation of c-KIT identified in human GISTs (Del2 and Del9; Taniguch et al., 1999, Agaimy et al., 2008), canine GISTs (Del2 and Del9; Gregory-Bryson et al., 2010), and canine mast cell tumors (Del2, Del3, Del9, Dup2; Zemke et al., 2002) to cause the immortalization in canine primary fibroblast. *In vitro* studies provide important insights into gene functions in cellular and developmental events (Uetake et al., 2011). Mutant c-KIT isoforms were shown in previous studies to be activated without the presence of the ligand in tumor cell lines (Furitsu et al., 1993; Tsujimura et al., 1994; Xiang et al., 2006). Although these studies did not determine if each c-KIT isoform could cause tumorigenesis, the novel aspect of this study was to show that a normal, i.e. non-neoplastic, primary cells could be transformed through the introduction and expression of various mutant c-KIT isoforms. Through our research, we were able to show that we could generate wild type and mutant c-KIT constructs in plasmids and transfect them into canine primary fibroblasts. The transfection efficiency of the mutant and wild type c-KIT constructs were uniformly lower than that of the empty vector in canine primary fibroblasts. It is known that plasmid DNA size greatly affects the transfection efficiency, and our findings are consistent with other studies (Darquet et al., 1997; Ross and Hui, 1999). This result could have several possible factors. Using Lipofectamine may cause lipoplexes resulting from the association of cationic lipids with small plasmid, which might be smaller than those obtained with larger plasmids and might cause the differences in processing of the plasmid (Rao and Gopal, 2006). Smaller size of plasmid DNA may account for either an easier DNA release from cationic lipids, a better facilitation of the intracellular migration of DNA from the cytoplasm to the nucleus or better penetration into the nuclear pore by a smaller size particle (Kreiss et al., 1999)

After the G418 antibiotic selection and FACs, the GFP-positive cells were able to be continually passaged twice a week for more than three years. This study clearly showed that introduction of each mutant c-KIT proto-oncogene in the absence of other drivers, is able to immortalize canine primary fibroblasts. Moreover, cells ectopically expressing the wild type c-KIT and cells transfected with the empty vector senescence at three months after transfection, antibiotic selection, and FACs. In addition, all transfected cells exhibited morphological crisis and cell growth arrest after the initial FACs. The cells remained arrested (not dying, but not proliferating) for nearly 8 months. Later on, the c-KIT mutant transfected cells including CAF-KIT-Del2, CAF-KIT-Del3, CAF-KIT-Del9, and CAF-KIT-Dup2, overcame proliferative senescence after 8 months period of crisis and produced immortalization-cell colonies. These CAF-KIT mutant cell lines including CAF-KIT-Del2, CAF-KIT-Del3, CAF-KIT-Del9, and CAF-KIT-Dup2 have been cultured in complete media for more than three years by splitting them two or four times every week. Based on the criteria for defining the extended lifespan and immortalization proposed by Wright et al., 1989 and Shay et al., 1991, in which extended lifespan conferred the extended lifespan by about 20 population doubling (PD) of normal cell lifespan (20-60 PD) and where "the immortalization" is more than 150 PD, we can conclude that these CAF-KIT mutant cell lines were clearly immortalized.

To determine whether the c-KIT transgene was stably integrated and expressed in the host genome, expression of c-KIT mRNA was analyzed at two years and three years after transfection. The low level expression of c-KIT, detectable only by RT-PCR and quantitative real-time RT-PCR, was confirmed. Quantitative real-time RT-PCR was used to quantify the amount of c-KIT expression. As calibrated to c-KIT expression in canine primary fibroblasts, CAF-KIT mutant cell lines showed elevated expression levels of c-KIT. However, canine

primary fibroblasts do not normally express c-KIT, which might make them a less than ideal calibrator.

The expression of c-KIT was monitored at the protein level by fluorescence microscopy using a GFP reporter and at the mRNA level by RT-PCR. As we selected GFP positive cells and expanded them for further study, the levels of c-KIT expression were high at early time points. Even though the cytomegalovirus (CMV) promoter is a strong promoter and capable of driving the constitutive transgene expression (Xia et al., 2006), results showed that c-KIT and GFP expression gradually decreased over time. This effect might have occurred because the CMV promoter was turned off by poorly understood cellular mechanism (wright et al., 2005). Several studies conducted in human stem cells also show that CVM promoter appeared to drive only transient transcriptional activities and could not maintain stable gene and protein expression upon subsequent passage in the SNUhES3 hES cell line (Kim et al., 2005). For stable transfection, it might be necessary to give the transformed cell a growth advantage over the untransformed by using a CMV promoter encoding bicistronic mRNA (IRES, for example) from which both transgene and an antibiotic resistant gene are simultaneously transcribed but separated from the same RNA transcript (Barrow et al., 2006; Hellen and Sarnow, 2001).

Our results were consistent with results from studies in K562 cells (Migliaccio et al., 2000) from a human immortalised myelogenous leukemia line, which showed that K562 cell contains two types of transgene integration sites: (1) abundant unstable sites that permit transcription but not long-term integration of the transgenes and (2) rare stable sites that permit both efficient transcription and long-term stable integration of the transgenes. Eventually, most of transfected plasmids integrated mainly into abundant, unstable host sites, which gradually eliminated the expressed transgene so that progeny cells became progressively less fluorescent

and ultimately non-fluorescent in 80–250 cell generations (10–40 weeks). Their findings also indicated that extinction of transgenic expression in these progeny cells over time was due, at least in part, to elimination of the transgene from the host genome and not entirely to transcriptional silencing of the transgene (Pamler et al., 1991).

It is possible in this study that stable transfection had happened in these c-KIT mutant transfected cells. However, the cells that bypassed senescence were still subjected to telomeric shortening, continued aging, the accumulation of chromosomal abnormalities, and eventually, a second mortality check point referred to as a crisis. Then, the constitutively ectopic expression of c-KIT made cells overcome the crisis and caused the transformation of canine primary canine fibroblast. The structural and numerical alterations happened at transformational steps such as other acquired mutations, mitotic stress-induced mutations, or chromosomal instability, which may have contributed to the deletion or depletion of transgene expression.

It is known that deletions and internal tandem duplication (ITD) mutations in the juxtamembrane domain of c-KIT at exon 11 cause the c-KIT protein to be constitutively active. The juxtamembrane domain of c-KIT functions as an allosteric regulation of protein dimerization and enzymatic activity. The disruption in function of this domain from the mutations leads to receptor dimerization even in the absence of ligand, with constitutive aberrant phosphorylation of several downstream signaling pathways (Kitayama et al., 1995; Tsujimura et al., 1996; Moskaluk et al., 1999; Corbacioglu et al., 2006).

Collectively, these results demonstrated the ectopic expression of single mutant c-KIT proto-oncogenes. Even though CAF-KIT mutant cell lines showed a low expression of c-KIT mutant transgene, it was enough to drive the immortalization and potential transformation in normal canine primary fibroblasts. However, there is a need to further identify the tumorigenic

properties in these CAF-KIT mutant cell lines to understand the basis of c-KIT driven tumorigenesis.

REFERENCES

REFERENCES

1. Agaimy A, Dirnhofer S, Wünsch PH, Terracciano LM, Tornillo L, Bihl MP. Multiple sporadic gastrointestinal stromal tumors (GISTs) of the proximal stomach are caused by different somatic KIT mutations suggesting a field effect. Am J Surg Pathol. 2008 Oct;32(10):1553-9.

2. Barrow KM, Perez-Campo FM, Ward CM. Use of the cytomegalovirus promoter for transient and stable transgene expression in mouse embryonic stem cells. Methods Mol Biol. 2006;329:283-94.

3. Blechman JM, Lev S, Barg J, Eisenstein M, Vaks B, Vogel Z, Givol D, Yarden Y. The fourth immunoglobulin domain of the stem cell factor receptor couples ligand binding to signal transduction. Cell. 1995 Jan 13;80(1):103-13.

4. Corbacioglu S, Kilic M, Westhoff MA, Reinhardt D, Fulda S, Debatin KM. Newly identified c-KIT receptor tyrosine kinase ITD in childhood AML induces ligand-independent growth and is responsive to a synergistic effect of imatinib and rapamycin. Blood. 2006 Nov 15;108(10):3504-13.
5. Darquet AM, Cameron B, Wils P, Scherman D, Crouzet J. A new DNA vehicle for nonviral gene delivery: supercoiled minicircle. Gene Ther. 1997 Dec;4(12):1341-9.

6. Edling CE, Hallberg B. c-Kit--a hematopoietic cell essential receptor tyrosine kinase. Int J Biochem Cell Biol. 2007;39(11):1995-8.

7. Furitsu T, Tsujimura T, Tono T, Ikeda H, Kitayama H, Koshimizu U, Sugahara H, Butterfield JH, Ashman LK, Kanayama Y, et al. Identification of mutations in the coding sequence of the proto-oncogene c-kit in a human mast cell leukemia cell line causing ligand-independent activation of c-kit product. J Clin Invest. 1993 Oct;92(4):1736-44.

8. Giebel LB, Spritz RA. Mutation of the KIT (mast/stem cell growth factor receptor) protooncogene in human piebaldism. Proc Natl Acad Sci U S A. 1991 Oct 1;88(19):8696-9.

9. Gregory-Bryson E, Bartlett E, Kiupel M, Hayes S, Yuzbasiyan-Gurkan V. Canine and human gastrointestinal stromal tumors display similar mutations in c-KIT exon 11. BMC Cancer. 2010 Oct 15;10:559.

10. Hellen CU, Sarnow P. Internal ribosome entry sites in eukaryotic mRNA molecules. Genes Dev. 2001 Jul 1;15(13):1593-612.

11. Inoue H, Nojima H, Okayama H. High efficiency transformation of Escherichia coli with plasmids. Gene. 1990 Nov 30;96(1):23-8.

12. Kim JH, Do HJ, Choi SJ, Cho HJ, Park KH, Yang HM, Lee SH, Kim DK, Kwack K, Oh SK, Moon SY, Cha KY, Chung HM. 2005. Efficient gene delivery in differentiated human embryonic stem cells. Exp Mol Med 37: 36–44.

13. Kitayama H, Kanakura Y, Furitsu T, Tsujimura T, Oritani K, Ikeda H, Sugahara H, Mitsui H, Kanayama Y, Kitamura Y, et al. Constitutively activating mutations of c-kit receptor tyrosine kinase confer factor-independent growth and tumorigenicity of factor-dependent hematopoietic cell lines. Blood. 1995 Feb 1;85(3):790-8.

14. Kreiss P, Cameron B, Rangara R, Mailhe P, Aguerre-Charriol O, Airiau M, Scherman D, Crouzet J, Pitard B. Plasmid DNA size does not affect the physicochemical properties of lipoplexes but modulates gene transfer efficiency. Nucleic Acids Res. 1999 Oct 1;27(19):3792-8.

15. Lennartsson J, Rönnstrand L. The stem cell factor receptor/c-Kit as a drug target in cancer. Curr Cancer Drug Targets. 2006 Feb;6(1):65-75.

16. Miettinen M, Lasota J. KIT (CD117): a review on expression in normal and neoplastic tissues, and mutations and their clinicopathologic correlation. Appl Immunohistochem Mol Morphol. 2005 Sep;13(3):205-20.

17. Migliaccio AR, Bengra C, Ling J, Pi W, Li C, Zeng S, Keskintepe M, Whitney B, Sanchez M, Migliaccio G, Tuan D. Stable and unstable transgene integration sites in the human genome: extinction of the Green Fluorescent Protein transgene in K562 cells. Gene. 2000 Oct 3;256(1-2):197-214.

18. Moskaluk CA, Tian Q, Marshall CR, Rumpel CA, Franquemont DW, Frierson HF Jr. Mutations of c-kit JM domain are found in a minority of human gastrointestinal stromal tumors. Oncogene. 1999 Mar 11;18(10):1897-902.

19. Nakai Y, Nonomura N, Oka D, Shiba M, Arai Y, Nakayama M, Inoue H, Nishimura K, Aozasa K, Mizutani Y, Miki T, Okuyama A. KIT (c-kit oncogene product) pathway is constitutively activated in human testicular germ cell tumors. Biochem Biophys Res Commun. 2005 Nov 11;337(1):289-96.

20. Palmer TD, Rosman GJ, Osborne WR, Miller AD. Genetically modified skin fibroblasts persist long after transplantation but gradually inactivate introduced genes. Proc Natl Acad Sci U S A. 1991 Feb 15;88(4):1330-4.

21. Rao NM, Gopal V. Cell biological and biophysical aspects of lipid-mediated gene delivery. Biosci Rep. 2006 Aug;26(4):301-24.

22. Roskoski R Jr. Structure and regulation of Kit protein-tyrosine kinase—the stem cell factor receptor. Biochem Biophys Res Commun. 2005 Dec 23;338(3):1307-15.

23. Ross PC, Hui SW (1999) Lipoplex size is a major determinant of in vitro lipofection efficiency. Gene Ther 6:651–659.

24. Sattler M, Salgia R. Targeting c-Kit mutations: basic science to novel therapies. Leuk Res. 2004 May; 28:S11-20.

25. Shay JW, Wright WE, Werbin H. Defining the molecular mechanisms of human cell immortalization. Biochim Biophys Acta. 1991 Apr 16;1072(1):1-7.

26. Taniguchi M, Nishida T, Hirota S, Isozaki K, Ito T, Nomura T, Matsuda H, Kitamura Y. Effect of c-kit mutation on prognosis of gastrointestinal stromal tumors. Cancer Res. 1999 Sep 1;59(17):4297-300.

27. Tsujimura T, Furitsu T, Morimoto M, Isozaki K, Nomura S, Matsuzawa Y, Kitamura Y, Kanakura Y. Ligand-independent activation of c-kit receptor tyrosine kinase in a murine mastocytoma cell line P-815 generated by a point mutation. Blood. 1994 May 1;83(9):2619-26.

28. Tsujimura T, Morimoto M, Hashimoto K, Moriyama Y, Kitayama H, Matsuzawa Y, Kitamura Y, Kanakura Y. Constitutive activation of c-kit in FMA3 murine mastocytoma cells caused by deletion of seven amino acids at the juxtamembrane domain. Blood. 1996 Jan 1;87(1):273-83.

29. Uetake H, Oka K, Niki Y. Stable transformation and cloning mediated by piggyBac vector and RNA interference knockdown of Drosophila ovarian cell line. In Vitro Cell Dev Biol Anim. 2011 Dec;47(10):689-94.

30. Wright WE, Pereira-Smith OM, Shay JW. Reversible cellular senescence: implications for immortalization of normal human diploid fibroblasts. Mol Cell Biol. 1989 Jul;9(7):3088-92.

31. Wright A, Semyonov A, Dawes G, Crameri A, Lyons R, Stemmer WP, Apt D, Punnonen J. Diverse plasmid DNA vectors by directed molecular evolution of cytomegalovirus promoters. Hum Gene Ther. 2005 Jul;16(7):881-92.

32. Xia W, Bringmann P, McClary J, Jones PP, Manzana W, Zhu Y, Wang S, Liu Y, Harvey S, Madlansacay MR, McLean K, Rosser MP, MacRobbie J, Olsen CL, Cobb RR. High levels of protein expression using different mammalian CMV promoters in several cell lines. Protein Expr Purif. 2006 Jan;45(1):115-24.

33. Xiang Z, Kreisel F, Cain J, Colson A, Tomasson MH. Neoplasia driven by mutant c-KIT is mediated by intracellular, not plasma membrane, receptor signaling. Mol Cell Biol. 2007 Jan;27(1):267-82.

34. Zemke D, Yamini B, Yuzbasiyan-Gurkan V. Mutations in the juxtamembrane domain of c-KIT are associated with higher grade mast cell tumors in dogs. Vet Pathol. 2002 Sep;39(5):529-35.

35. Zhang Z, Zhang R, Joachimiak A, Schlessinger J, Kong XP. Crystal structure of human stem cell factor: implication for stem cell factor receptor dimerization and activation. Proc Natl Acad Sci U S A. 2000 Jul 5;97(14):7732-7.

CHAPTER 3

IN VITRO STUDIES OF TUMORIGENIC PHENOTYPES OF CAF-KIT MUTANT CELL LINES

ABSTRACT

While c-KIT mutations observed in canine mast cell tumors (MCTs) are significantly associated with poor prognosis, the functional significance of c-KIT activating mutations in tumorigenesis has not been elucidated. To explore the role of a range of c-KIT mutations observed in various types of human and canine cancers, expression constructs bearing wild type and mutant c-KIT-GFP fusion genes were generated in a plasmid vector (pAcGFP1N1). These plasmids were then each transfected into canine primary fibroblasts along with negative and mock controls. The fibroblasts were then grown under constant selective pressure. As fibroblasts do not normally express c-KIT, changes in cellular phenotype could be directly attributed to the c-KIT expression. The cellular phenotype of each set of transfected fibroblasts was evaluated via a number of assays and compared to that of canine primary fibroblasts. Mutant c-KIT transfected fibroblasts were found to have prolonged lifespan, anchorage-independent growth in soft agar, and an ability to grow in low density and low serum. They also demonstrated the abilities to invade the basement membrane and to spread and close a wound generated in a monolayer. In addition, these cells have a higher saturation density and shorter population doubling time. This is the first study to directly implicate expression of mutant c-KIT in the tumorigenic process, showing that mutant KIT isoforms observed in cancers are sufficient to drive tumorigenesis.

INTRODUCTION

The c-KIT protein, a 145-kDa transmembrane glycoprotein, is the normal cellular homologue of the viral oncoprotein v-KIT (Besmer et al., 1986), and is normally expressed by hematopoietic progenitor cells, mast cells, germ cells, interstitial cells of Cajal, and also by certain human tumors (Natali et al. 1992; Turner et al., 1992). This c-KIT-mediated signal transduction is known to play a crucial role in proliferation, differentiation, migration, and survival of these cells.

Gain-of-function mutations in the proto-oncogene c-KIT that induce constitutive kinase activity of c-KIT protein leading to disregulated growth are believed to play a central role in of many types of human tumors including acute amyeloid leukemia (AML) (Ashman et al., 2000), melanoma (Willmore-Payne et al., 2005), gastrointestinal stromal tumors (GISTs) (Hirota et al., 1998), germ cell tumors (Tian et al, 1999), and mast cell disorders (Longley et al., 1999).

To investigate the transforming activity and tumorigenesis of mutant c-KIT, in vitro model systems have been widely employed. Expression and state of tyrosine phosphorylation of c-KIT point mutations (V559G and D814V) hematopoietic cell lines caused ligand-independent growth of mixed erythroid/myeloid colonies and development of tumors in transplanted mice, although not in cells carrying wild-type c-KIT (Kitayama et al., 1995). Using the human embryonic kidney cell line, 293, transfection of D816H mutant c-KIT signaling through activation of STAT3 can induce anchorage-independent growth in vitro and tumor formation in vivo (Ning et al., 2001). Moreover, an interleukin-3-dependent mast cell line, IC2, expressing D814Y mutation of c-Kit receptor was able to induce ligand-independent mast cell growth *in vitro*, tumorigenicity *in vivo*, and mast cell differentiation (Piao and Bernstein, 1996). Ectopic expression of the normal murine receptor tyrosine kinase, c-KIT, in the mouse fibroblast cell line

induced many phenotypic changes characteristic of transformation including anchorage-independent growth, focus formation and tumorigenicity in nude mice (Caruana et al., 1998). A series of c-KIT mutations in exon 11 reported in canine mast cell tumors (W556R, L575P, deletion of W556- K557, and deletion of V558) was introduced into COS-7 cells. Result showed that all five mutations cause high spontaneous tyrosine phosphorylation of c-KIT and may therefore contribute to the pathogenesis of mast cell neoplasia (Ma et al., 1999).

A number of studies have defined that ectopically expressed c-KIT mutations in several cell lines result in neoplastic transformation and tumorigenicity in vivo. However, the effect of c-KIT mutation expressed in primary cells or in endogenous c-KIT lacking cells has not been well explored. Isolated murine bone marrow progenitor cells infected by plasmid harboring V559G and D814 induced factor-independent growth of various types of hematopoietic progenitor cells and led to development of acute leukemia in xenograft mice (Kitayama et al., 1996). In contrast, constitutive expression of D816VKit in murine primary haemopoietic cells isolated from murine fetal liver was not a sufficient transforming stimulus (Ferrao et al., 2003). Moreover, these experiments were performed while endogenous c-KIT protein was normally expressed. In order to fully understand the direct role of c-KIT mutation in neoplastic transformation, mutant c-KIT isoforms expressed in canine primary fibroblasts lacking endogenous c-KIT expression were examined in a wide range of in vitro studies relevant to tumorigenic transformation ability. This study provides the opportunity to elucidate the molecular mechanisms responsible for neoplastic transformation driven by activated c-KIT tyrosine kinase receptors.

MATERIALS AND METHODS

Cell lines

Established mutant c-KIT-harboring cell lines were used in this study (Chapter 2), including Deletion 2-harboring cells (CAF-KIT-Del2), Deletion 3-harboring cells (CAF-KIT-Del3), Deletion 9-harboring cells (CAF-KIT-Del9), and Duplication 2-harboring cells (CAF-KIT-Dup2). These cells were cultivated in complete medium (DMEM, L-glutamine, penicillin/streptomycin, and 10% FCS), at 37 °C in a humidified atmosphere of 5% CO_2. Isolated primary canine fibroblasts were used as a negative control. C2 mast cell lines were kindly provided by Dr. Elizabeth McNiel (Michigan State University) and used as a positive control.

Anchorage-independent growth

The transfected fibroblasts were assayed for anchorage-independent growth by colony formation in soft agar and loss of contact inhibition by focus-formation. Cells were harvested, and 3.5×10^3 cells were suspended in 2 ml of medium containing 0.33% agar supplemented with growth medium and plated in triplicate. The mixture was seeded to solidify on top of 2 ml of a 0.5% agar base layer containing growth medium in a six-well-plate. Cells were fed twice a week with 0.5 ml of complete medium and maintained in a 37°C, 5% CO_2 incubator. Primary canine fibroblasts served as a positive control. After 4-6 weeks colonies consisting of greater than 50 cells were counted microscopically.

Saturation density assay

To determine the oncogenic potential of the transfectants, saturation density assays were performed by plating cells in triplicate at a density of 5×10^3 cells/well in a 24-well plate in 500 µl of complete medium. Triplicate wells from each group were trypsinized. Total number of cells per well and viability were determined using a hemocytometer and Trypan blue exclusion every

day for 14 days with regular media replenishment. The number of cells per cm^2 within 2 weeks after plating, with no further increase in numbers observed, was designated as saturation density. The population doubling time during the exponential growth phase was measured by the online website http://www.doubling-time.com/compute.php?lang=en

Growth in the low serum and low density

For low serum and low density stress induction, 100 cells of each cell line were resuspended in 2 ml of complete medium and placed in a 6-well tissue culture plate in the presence of 1% or 10% FBS. Cells were fed twice weekly. After 14 days, number of colonies and total number of cells were counted.

Matrigel invasion assay

Cell invasiveness was evaluated *in vitro* using Matrigel-coated semipermeable-modified Boyden inserts. BioCoat Growth Factor-Reduced Matrigel invasion chambers (24-well cell culture inserts containing an 8.0-μm PET membrane with a uniform layer of Matrigel matrix; BD) were used to assess cell invasion following the manufacturer's instructions. After determination of cell count and viability in a hemocytometer by the trypan blue exclusion test, cells resuspended in DMEM with L-glutamine, penicillin/streptomicin were added to the upper compartment of the chamber (2.5 × 105 cells/chamber) . DMEM supplemented with 10% FBS was placed in the bottom well with 10% FBS providing the chemo-attractants. Incubation was carried out for 20 hours at 37 °C in humidified air with 5% CO2. The cells on the insert were removed by wiping gently with a cotton swab. Cells on the reverse side of the insert were fixed and stained with DiffQuick according to the manufacturer's instructions and mounted on glass slides. Total number of cells that crossed the membrane was counted under a light microscope,

and the average value was calculated. Experiments were performed in a three chambers per cell line.

Wound healing assay

Cells were plated into 6-well-plates to obtain confluent monolayers. Wounds were generated by scratching three straight lines the cell monolayer using 1 ml pipette tip and then washed twice by PBS to remove dislodged cells. Then cells were replaced with fresh complete medium. Migration of cells to seal the wounds was monitored and photographed using a phase contrast microscope every 24 hours.

RESULTS

From the previous chapter, ectopic expression of mutant c-KIT isoforms, including deletion 2, deletion 3, deletion 9, and duplication2, can allow these mutant-harboring cells to bypass senescence. After CAF-KIT-Del2, CAF-KIT-Del3, CAF-KIT-Del9, CAF-KIT-Dup2 had become immortal, *in vitro* growth and tumorigenic phenotypes of these cell types were tested. To characterize their oncogenic phenotype, an anchorage independent growth test via soft agar assay was conducted by seeding 3.5×10^4 cells in 6-well culture dishes in 0.3% agar on top of a base layer containing 0.5% agar. This method shows the ability of cells to grow in the absence of adhesion, a major indicator for cell transformation. Moreover, anchorage- independent colony formation in soft agar has been successfully used to assess the tumorigenicity of cancer cells *in vitro*, which has been positively correlated to *in vivo* tumorigenicity in animal models (Leone et al., 1991). Cells were grown in the low percentage agar for 4-6 weeks, and the results are presented in Figure 10. In addition, all 4 c-KIT mutant-isoform cell lines have the ability to grow in an anchorage-independent manner and form their cell foci on the soft semi-solid agar in the absence of ligands, a hallmark of cellular transformation. The numbers of colonies of 100 cells or more were counted for each cell line. Results are shown in Table 4. There was a difference in size of the foci, ranging from pinpoint to 1.5 mm. CAF-KIT-Del2, CAF-KIT-Del9, and CAF-KIT-Dup2 showed the cell growth colonies that were observable to the naked eye as dots on the agar. In contrast, CAF-KIT-Del3 cells showed monolayer clusters of cell growth on soft agar, which can be observed only by microscope.

Figure 10: Observation of anchorage-independent growth in mutant c-KIT-transformed canine fibroblasts. Anchorage independent growth was determined using soft agar assay by seeding 3.5×10^4 cells in triplicate onto 6-well culture dishes and feeding with growth media twice per week for 3-4 weeks. There was no colony formation observed in canine primary fibroblast (Panel E). CAF-KIT-Del2 (panel A), CAF-KIT-Del9 (panel C), and CAF-KIT-Dup2 (panel D) showed their noticeable colonies at 3 weeks after seeding. CAF-KIT-Del3 (panel B) demonstrated a growth pattern on soft agar as a cluster of monolayer cell growth (panel G, 4 x magnifications). Colonies of CAF-KIT-Del2 (panel F) observed on agar were seen as ball-like structure under microscope.

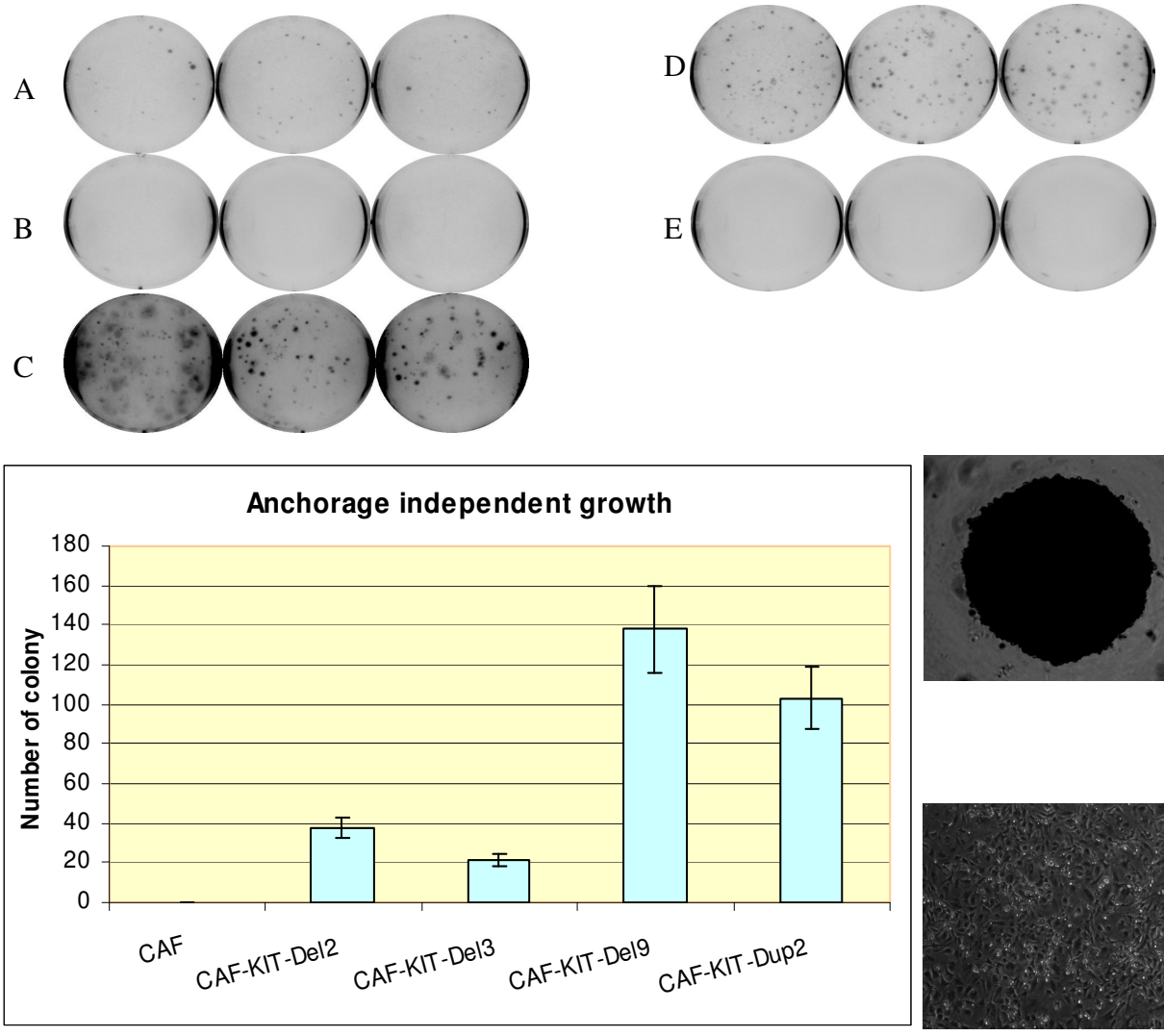

Untransformed CAF-KIT wild type cells did not grow at all in soft agar, and neither untransfected primary canine fibroblasts nor empty vector-transfected fibroblasts were able to induce colony formation.

For the growth in limited resources such as low density and low serum, cells from each cell line were plated at 100 cells/well in triplicate onto a 6-well-plate and then incubated for 2 weeks. Numbers of cells and colonies were counted. The results showed that all 4 c-KIT mutant cell lines are capable of growth in low density conditions with the foci formation from losing contact inhibition (Figure 11 and Table 4). Moreover, three of four cell lines can grow in limited nutrients such as a medium with low serum concentration, except CAF-KIT-Del9 cell lines (Table 4). Normal fibroblasts underwent senescence and had no colony formation after 3 weeks of seeding. CAF-KIT-Del2, CAF-KIT-Del9 and CAF-KIT-Dup2 cells showed a number of noticeable colonies, whereas CAF-KIT-Del3 showed smaller size of growth foci and were observable only under the microscope.

Figure 11: Growth of mutant c-KIT transformed canine fibroblasts in low density cultures. Growth in low density results showed that all c-KIT mutant cell lines, including CAF-KIT-Del2 (panel A), CAF-KIT-Del3 (panel B), CAF-KIT-Del9 (panel C), and CAF-KIT-Dup2 (panel D), had a greater number of colonies grown in low density conditions compared to primary canine fibroblast (panel E). Note that CAF-KIT-Del3 colonies are small and otherwise unnoticeable unless observed under microscope (panel F, 4 x magnifications). Primary canine fibroblast served as a control showing their senescence morphology, characterized by enlarged and flat cells (panel G, 4 x magnifications).

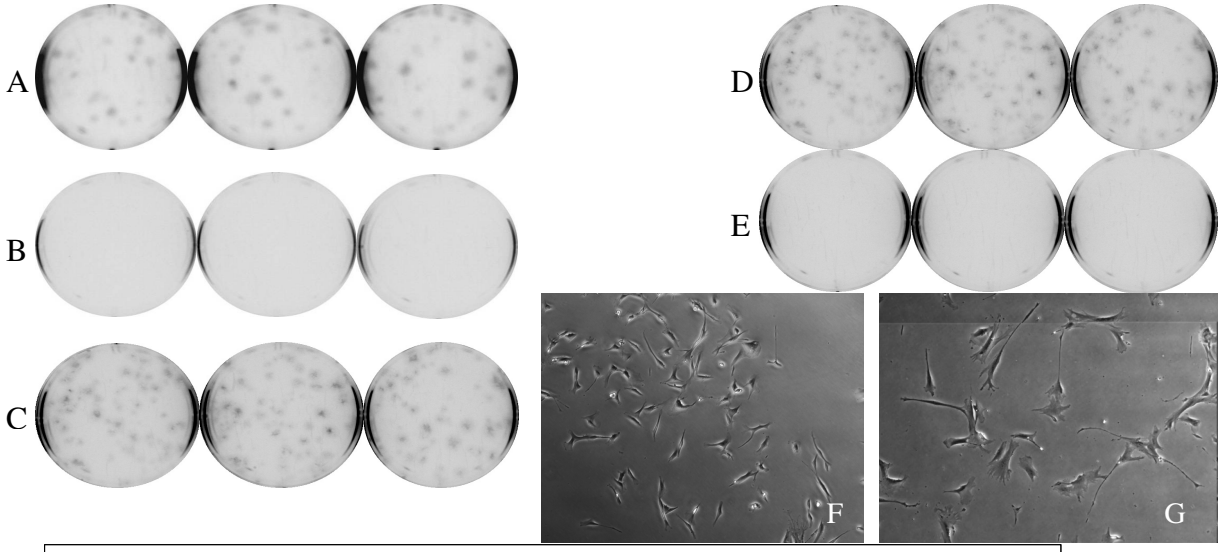

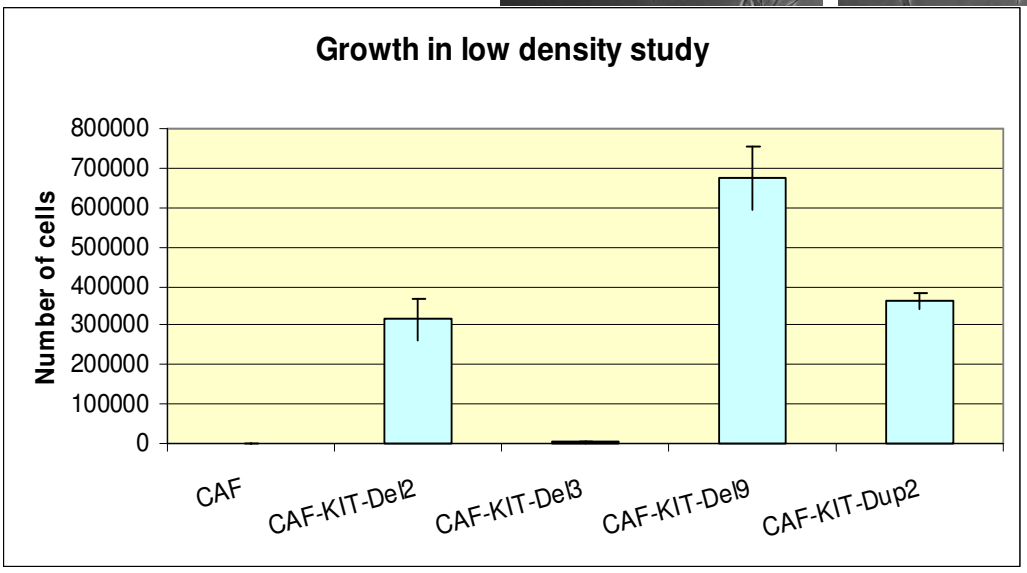

The next experiment was to evaluate the basement membrane invasion ability of mutant c-KIT cells by using matrigel assay. Dual chambered invasion plates containing reconstituted extracellular matrices overlaid on 8 µM pore sized membranes were used. The invasive nature of the cells was measured by their spontaneous ability to migrate from the upper chamber to the lower chamber of the invasion plate. Results showed that mutant cells have the ability to penetrate through the filter, which is a model for migration through the basement membrane (Figure 12). Although CAF-KIT-Del 3 cell lines proved less invasive than other mutant cells, they are still more invasive than normal fibroblasts.

Figure 12: The effect of mutant c-KIT isoforms on invasiveness examined by the Matrigel invasion assay. Cells were seeded at 2.5×10^4 cells in the upper chamber in serum free media with serum added in the lower chamber as a chemo-attractant. After 24 hours, the cells in the lower chamber were fixed, stained, and counted under a microscope. Results showed that the number of cells of all mutant c-KIT-isoform cell lines that invaded through membranes is greater than of that canine primary fibroblasts (Panel E). Panel A: CAF-KIT-Del2, Panel B: CAF-KIT-Del3, Panel C: CAF-KIT-Del9, Panel D: CAF-KIT-Dup2. All panels at 4 x magnifications.

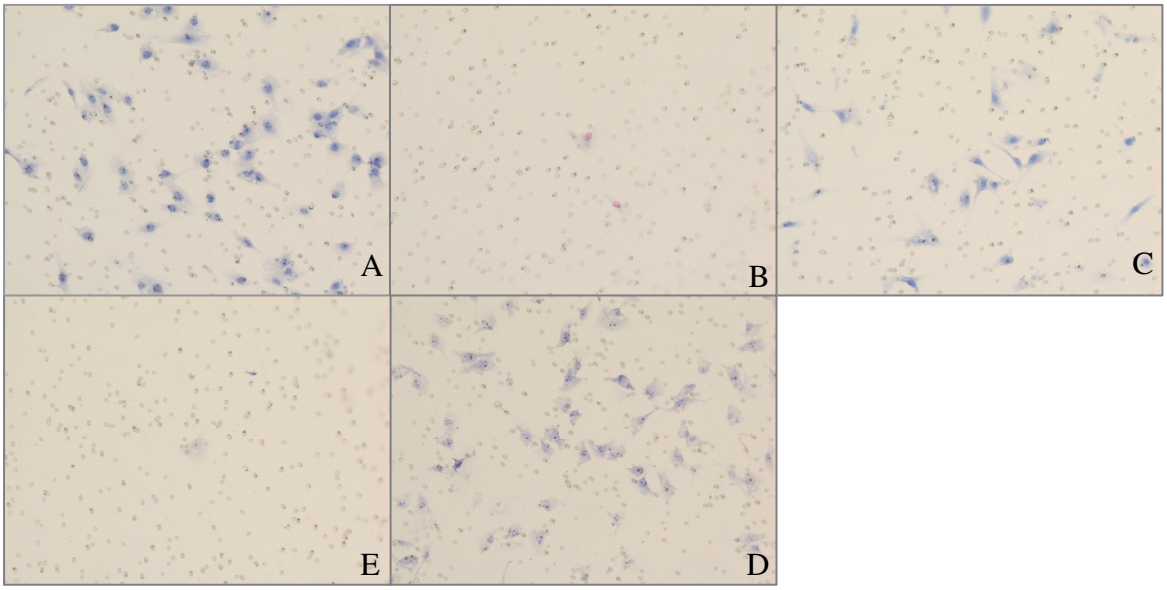

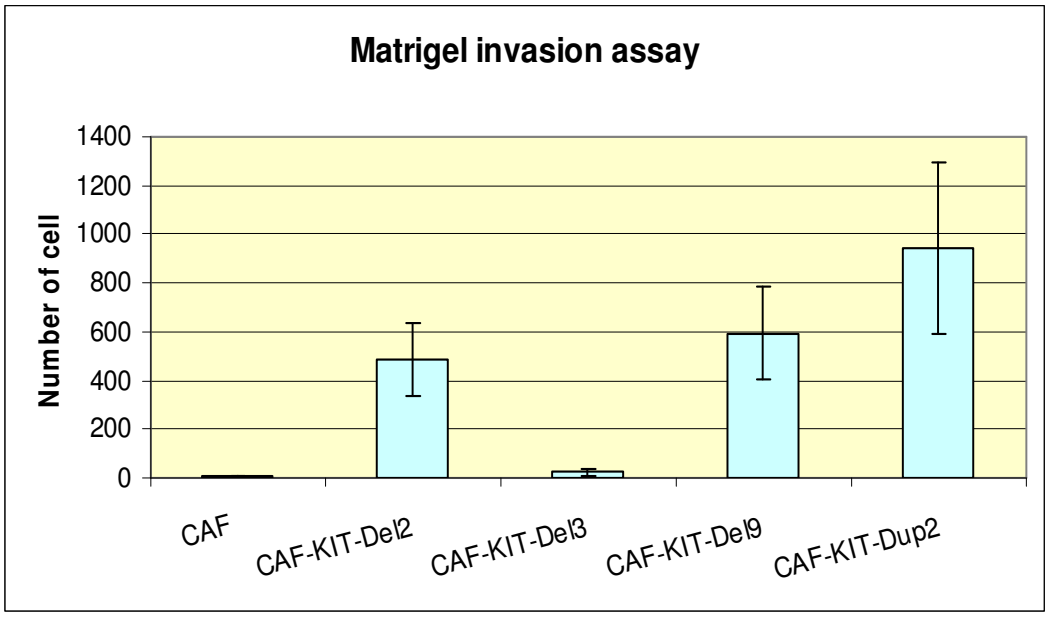

Saturation density showed that all 4 mutant c-KIT cells have a higher density of cells in a limited growth surface area compared to normal fibroblasts (Figure 13). CAF-KIT-Del 9 showed the highest cell density at 3.0 x 10^5cells/cm^2 surface area. Compared to primary canine fibroblasts at saturation density 5,300 cells/cm^2, all c-KIT mutant cell lines, including CAF-KIT-Del2, CAF-KIT-Del3, and CAF-KIT-Dup2, showed a greater saturation density at 2.6 x 10^5cells/cm^2, 1.2 x 10^5cells/cm^2, 2.1 x 10^5cells/cm^2, respectively.

Figure 13: Growth curves for c-KIT cell lines under limited surface area conditions. Saturation density: Each cell line was seeded at 5,000 cells/well in duplicate onto 24 well-plates. Cells were fed twice per week with complete medium. Every 24 hours, cells were trypsinized and counted each dayfor 14 days. Daily increases in the number of cells were recorded to calculate the saturation density and the population doubling time. The experiment was repeated in triplicate and the data reported as an average.

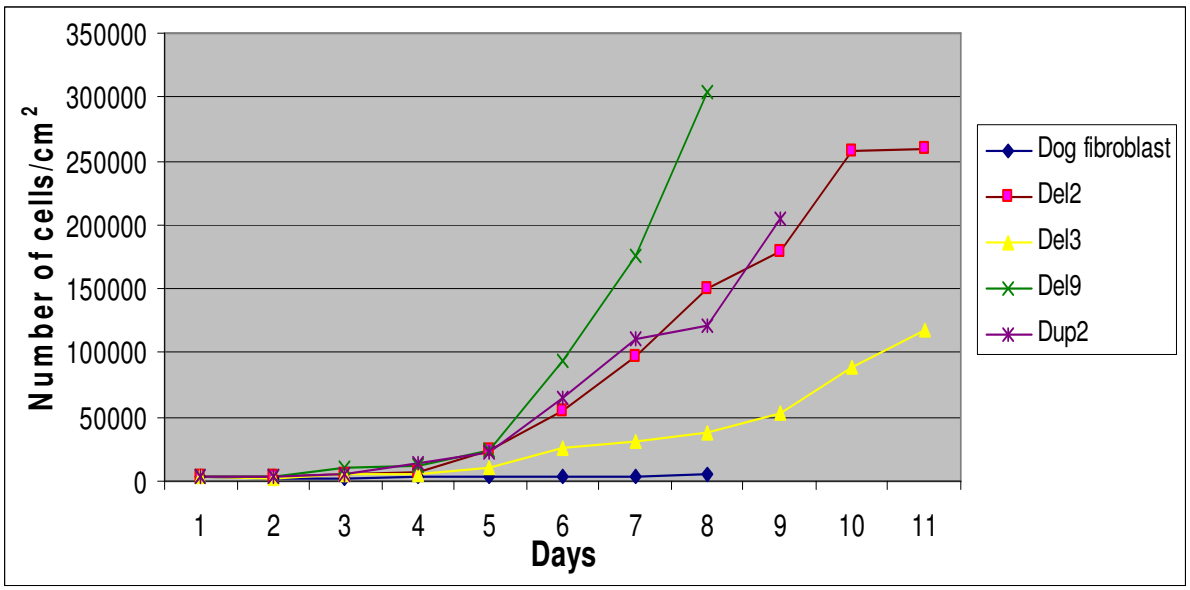

The population doubling times of CAF-KIT-Del2, CAF-KIT-Del3, CAF-KIT-Del9, and CAF-KIT-Dup2 were 42, 43, 31, and 41 hours respectively- all shorter than the 84 hour of canine primary fibroblast cells. There was a two-fold decrease in the doubling times of each of these cell lines from the 84 hours required for canine primary fibroblast cells.

Cell migration is a process that is critical during many stages of cancer cell metastasis. In order to monitor cell movement into wounded areas, three fields of each of the 3 wounds analyzed per condition were photographed immediately after the scratches were made (0 hour) and 24, 48, and 120 hours later. Microscopic analysis evaluating cell capacity to migrate and fill these wounded areas at different times showed that all 4 mutant c-KIT cell lines can migrate faster than primary canine fibroblast via wound healing assay (as shown in Figure 14). All c-KIT mutant cell lines can migrate, thus completely healing gaps made by the tip of 1000 ul pipette tip, within 48 hours, which is five days in canine primary fibroblasts.

Figure 14: Wound healing assay showing the migration paths of mutant c-KIT cell lines (Panel A: CAF-KIT-Del2; Panel B: CAF-KIT-Del3; Panel C: CAF-KIT-Del9; Panel D: CAF-KIT-Dup2) at wound points during 120 hours assay compared to canine primary fibroblast (Panel E). Phase contrast photograph at 4 x magnification.

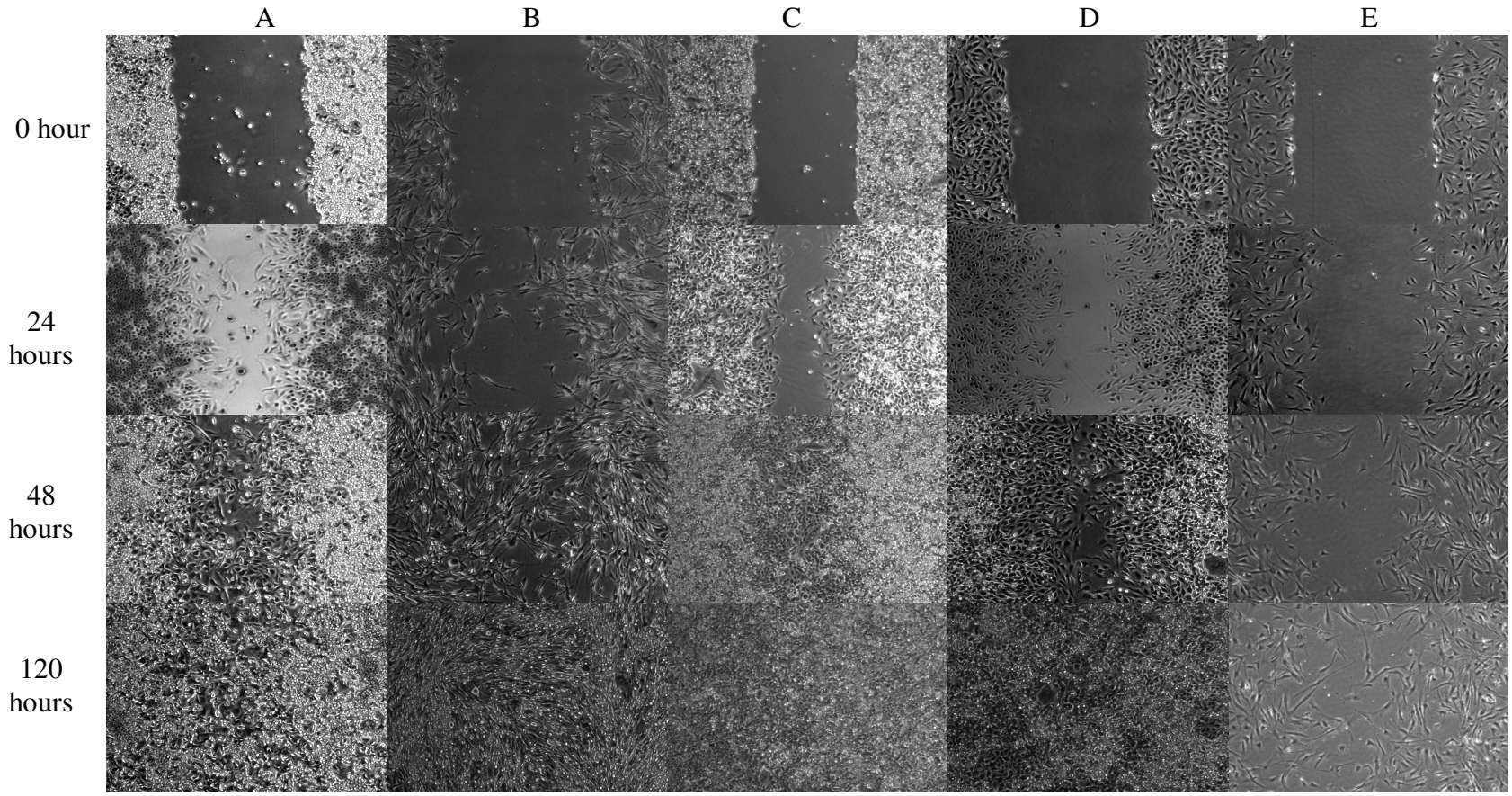

Table 4: Summary of *in vitro* studies for mutant c-KIT transformed canine fibroblasts.

	Soft agar assay	**Saturation density**	**Growth in low serum**		**Growth in low density**		**c-KIT mRNA expression**	**Quantitative RT-PCR**	**Population doubling time**	**Matrigel invasion assay**	**Wound healing assay**
	No. of colonies	Cells/cm^2	No. of cells	No. of colonies	No. of cells	No. of colonies		Fold change	Hours	No. of cells	Hours
CAF	0	5333	<1,000*	0	1166	1	No	1	84	8	120
Del2	**38**	**258,771**	**2,500**	**1.3**	**316,000**	**27**	**Yes**	**92**	**42**	**484**	**48**
Del3	**21**	**118,421**	**2,916**	**3**	**4,500**	**12**	**Yes**	**33**	**43**	**24**	**48**
Del9	**138**	**304,386**	**<1,000***	**0**	**674,000**	**93**	**Yes**	**25**	**31**	**594**	**48**
Dup2	**103**	**205,263**	**1,750**	**2**	**362,000**	**41**	**Yes**	**1237**	**41**	**942**	**48**

Data are the mean of three independent experiments.

DISCUSSION

An important step in cellular transformation and tumorigenesis is immortalization, in which cells gain the ability to grow indefinitely by bypassing cellular senescence (Sun and Taneja, 2007). Cellular transformation is a stepwise process, and several successive genetic or epigenetic changes are required for the development of a neoplastic phenotype (Zongaro et al., 2005). In studies presented in the previous chapter, we demonstrated that the introduction of a single c-KIT mutant proto-oncogene was capable of immortalizing canine primary fibroblasts and resulted in CAF-KIT-Del2, CAF-KIT-Del3, CAF-KIT-Del9, and CAF-KIT-Dup2 cell lines.

Mutations in c-KIT exon 11 subjected to this study have been reported in many tumors, including canine mast cell tumors, canine GISTs, and human GISTs (Zemke et al., 2002; Gregory-Bryson et al., 2010; Hirota et al., 1998). These mutations resulted in three different 2-amino acids deletions (deletion 2, deletion 3, and deletion 9) and an internal tandem duplication mutation of 15-amino acids. The previous report has demonstrated that mutation in c-KIT exon 11 caused a constitutive activation of the c-KIT receptor even in the absence of ligand (Kitayama et al., 1995). Reported in canine mast cell tumors (Webster et al., 2006), mutations of the juxtamembrane domain of c-KIT exon 11 have been significantly associated with poor prognosis of disease. However, it is as of yet unknown whether c-KIT mutations reported in tumors truly induce transformation of primary cells and/or are causative of tumorigenesis.

Our findings show that c-KIT mutant transfected cells can become neoplastically transformed. Unlike other studies, which were performed in immortalized cell lines, these data are the first to demonstrate that a single mutant c-KIT proto-oncogene can cause the tumorigenic transformation in primary cells. Using immortalized mouse embryonic fibroblasts, the ectopic expression of a single oncogene (Ras) resulted in a loss of contact inhibition, anchorage-

independent growth, and tumor formation in nude mice (Zongaro et al., 2005). However, the same oncogene was not able to transform primary mouse embryonic fibroblasts (Zongaro et al., 2005).

Transformed cells are distinguished from nontransformed counterparts by differences in morphology, metabolism, and, most importantly, growth properties (Ryoo et al., 2006). In the previous chapter, results showed that each CAF-KIT mutant cell line revealed their distinct phenotypes and lost their original morphology. Anchorage-independent growth using soft agar assay, which is the best criterion for in vitro transformation (Bouck and Di Mayorcaet al., 1979; Cooper at al., 1980) and is most closely associated with tumorigenicity *in vivo*, was performed (Shin et al., 1975; Coldburn et al., 1978; Hara et al., 1999). The deletion 2, deletion 3, deletion 9, and duplication 2 transformants formed foci in soft agar, which did not occur in the canine primary fibroblasts used as the control.

Other evidence supporting the neoplastic transformation of these CAF-KIT mutant cell lines includes an elevated saturation density, the loss of contact inhibition, and the short cell population doubling time. Whereas normal cells will stop growing and inhibit their neighbor cells through contact with the cell surfaces, referred to as contact inhibition, neoplastic transformed cells usually do not cease their proliferation when they come into contact and often reveal piled-up foci formation. Increased saturation density is associated with loss of contact inhibition and decreased capacity to suppress the expansion of initiated or transformed cells into clonal tumors (Rubin, 2008). High saturation density is regarded an indicator of malignant transformation (Khosravi-Far et a., 1995). Thus the increase in the saturation density of CAF-KIT mutant cell lines indicates the malignancy of these cells. Studies also show the good

association between a loss of contact inhibition and tumor formation in vivo (Esinduy et al., 1995; Abercombie and Ambrose, 1962).

The cloning efficiency of CAF-KIT mutant cell lines was measured by their ability to grow in low density. Cells were plated at very low density such that each individual cell must divide out of contact with other cells. These CAF-KIT mutant cell lines were able to grow in this low density condition and had a much higher cloning efficiency compared to canine primary fibroblasts. As normal cells have very low cloning rates, the increase in cloning efficiency by more than 10 times is indicative of transformation (Hoff et al., 2004).

One of the differences between tumorigenic and non-tumorigenic cells is their ability to grow in low serum without arrest in a state with a G1 DNA content (G0) of tumorgenic cells (Riddle at al., 1979). In the presence of viral oncogene expression, cells will reduce their dependences on growth factor for cell division. Thus, the ability to grow in low serum concentrations serves as a hallmark of virally transformed cells (Hoff et al., 2004). To measure the growth of CAF-KIT mutant cell lines in low serum concentrations, which resembles restrictive environmental conditions *in vivo*, growth in 1% serum experiments, was performed. Results show the all CAF-KIT mutant cells, except CAF-KIT-Del9, grew in low serum conditions and showed lower dependence upon serum for growth.

Increased cell motility and invasion are characteristics of a neoplastic transformation (Botlagunta et al., 2010) that are essential attributes of metastasis (Winnard et al., 2008). All CAF-KIT mutant cell lines demonstrated also an enhanced invasive ability *in vitro* using matrigel invasion assay, mimicking basement membrane invasion. Invasion capability of cells has been shown to correlate with their malignant characteristics *in vivo* (Calaf and Hei, 2000). Furthermore, migration activities of cells *in vitro* are thought to be related to many in

vivo cellular behaviors, including the directed migration of cells during differentiation and the aberrant invasive activities of metastatic tumor cells (Keese at al., 2004). All CAF-KIT mutant cell lines were also able to migrate into cleared areas and heal wounds completely within 48 hr of incubation. On the other hand, normal canine primary fibroblasts showed little migration into the cleared regions during this time period. These data indicate that these CAF-KIT mutant cell lines transformed into a state of tumorigenic potential, including the cell's ability to migrate and invade, i.e., a possible increase in dissemination or metastatic potential.

Given these findings, the introduction of a single mutant c-KIT isoform was capable of overriding the senescence, immortalizing, and transforming the canine primary fibroblasts into potentially tumorigenic CAF-KIT mutant cell lines, which did not happen in wild type c-KIT carrying cells. However, it is unlikely that oncogenic transformation resulting in the malignant phenotypes is solely caused by unregulated ectopic expression of the mutant c-KIT transgenes. On the other hand, spontaneous transformation in canine primary fibroblasts has never been confirmed. Therefore, it would appear that the process of tumorigenic transformation is initiated by gain-of-function mutation occurring in association with, and possibly caused by, ectopic expression of mutant c-KIT.

Taken together, this study demonstrates that malignant transformation occurred in the mutant c-KIT-transfected canine primary fibroblasts *in vitro*.

REFERENCES

REFERENCES

1. Abercombie M and Ambrose EJ. The surface properties of cancer cells: a review. Cancer Res. 1962 Jun;22:525-48.

2. Ashman LK, Ferrao P, Cole SR, Cambareri AC. Effects of mutant c-kit in early myeloid cells. Leuk Lymphoma. 2000 Mar;37(1-2):233-43.

3. Besmer P, Murphy JE, George PC, et al. A new acute transforming feline retrovirus and relationship of its oncogene v-kit with the protein kinase gene family. Nature. 1986;320:415–21.

4. Botlagunta M, Winnard PT Jr, Raman V. Neoplastic transformation of breast epithelial cells by genotoxic stress. BMC Cancer. 2010 Jun 30;10:343.

5. Bouck N, Di Mayorca G. Evaluation of chemical carcinogenicity by in vitro neoplastic transformation. Methods Enzymol. 1979;58:296-302.

6. Calaf GM, Hei TK. (2000) Establishment of a radiation and estrogen-induced breast cancer model. Carcinogenesis 21: 769-76.

7. Caruana G, Cambareri AC, Gonda TJ, Ashman LK. Transformation of NIH3T3 fibroblasts by the c-Kit receptor tyrosine kinase: effect of receptor density and ligand-requirement. Oncogene. 1998 Jan 15;16(2):179-90.

8. Colburn NH, Bruegge WF, Bates JR, Gray RH, Rossen JD, Kelsey WH, Shimada T. Correlation of anchorage-independent growth with tumorigenicity of chemically transformed mouse epidermal cells. Cancer Res. 1978 Mar;38(3):624-34.

9. Cooper GM, Okenquist S, Silverman L. Transforming activity of DNA of chemically transformed and normal cells. Nature. 1980 Apr 3;284(5755):418-21.

10. Esinduy CB, Chang CC, Trosko JE, Ruch RJ. In vitro growth inhibition of neoplastically transformed cells by non-transformed cells: requirement for gap junctional intercellular communication. Carcinogenesis. 1995 Apr;16(4):915-21.

11. Ferrao PT, Gonda TJ, Ashman LK. Constitutively active mutant D816VKit induces megakayocyte and mast cell differentiation of early haemopoietic cells from murine foetal liver. Leuk Res. 2003 Jun;27(6):547-55.

12. Hara K, Kudoh H, Enomoto T, Hashimoto Y, Masuko T. Malignant transformation of NIH3T3 cells by overexpression of early lymphocyte activation antigen CD98. Biochem Biophys Res Commun. 1999 Sep 7;262(3):720-5.

13. Hirota S, Isozaki K, Moriyama Y, et al. Gain-of-function mutations of c-kit in human gastrointestinal stromal tumors. Science 1998;279:577–80.

14. Hoff H, Belletti B, Zhang H, Sell C. The transformed phenotype. Methods Mol Biol. 2004;285:95-104.

15. Keese CR, Wegener J, Walker SR, Giaever I. Electrical wound-healing assay for cells in vitro. Proc Natl Acad Sci U S A. 2004 Feb 10;101(6):1554-9.

16. Khosravi-Far R, Solski PA, Clark GJ, Kinch MS, Der CJ. Activation of Rac1, RhoA, and mitogen-activated protein kinases is required for Ras transformation. Mol Cell Biol. 1995 Nov;15(11):6443-53.

17. Kitayama H, Kanakura Y, Furitsu T, Tsujimura T, Oritani K, Ikeda H, Sugahara H, Mitsui H, Kanayama Y, Kitamura Y, et al. Constitutively activating mutations of c-kit receptor tyrosine kinase confer factor-independent growth and tumorigenicity of factor-dependent hematopoietic cell lines. Blood. 1995 Feb 1;85(3):790-8.

18. Kitayama H, Tsujimura T, Matsumura I, Oritani K, Ikeda H, Ishikawa J, Okabe M, Suzuki M, Yamamura K, Matsuzawa Y, Kitamura Y, Kanakura Y. Neoplastic transformation of normal hematopoietic cells by constitutively activating mutations of c-kit receptor tyrosine kinase. Blood. 1996 Aug 1;88(3):995-1004.

19. Leone A, Flatow U, King CR, Sandeen MA, Margulies IM, Liotta LA, Steeg PS. Reduced tumor incidence, metastatic potential, and cytokine responsiveness of nm23-transfected melanoma cells. Cell. 1991 Apr 5;65(1):25-35.

20. Longley BJ Jr, Metcalfe DD, Tharp M, Wang X, Tyrrell L, Lu SZ, Heitjan D, Ma Y. Activating and dominant inactivating c-KIT catalytic domain mutations in distinct clinical forms of human mastocytosis. Proc Natl Acad Sci U S A. 1999 Feb 16;96(4):1609-14.

21. Ma Y, Longley BJ, Wang X, Blount JL, Langley K, Caughey GH. Clustering of activating mutations in c-KIT's juxtamembrane coding region in canine mast cell neoplasms. J Invest Dermatol. 1999 Feb;112(2):165-70.

22. Natali PG, Nicotra MR, Sures I, Mottolese M, Botti C, Ullrich A. Breast cancer is associated with loss of the c-kit oncogene product. Int J Cancer 1992;52:713–7.

23. Ning ZQ, Li J, McGuinness M, Arceci RJ. STAT3 activation is required for Asp(816) mutant c-Kit induced tumorigenicity. Oncogene. 2001 Jul 27;20(33):4528-36.

24. Piao X, Bernstein A. A point mutation in the catalytic domain of c-kit induces growth factor independence, tumorigenicity, and differentiation of mast cells. Blood. 1996 Apr 15;87(8):3117-23.

25. Riddle VG, Pardee AB, Rossow PW. Growth control of normal and transformed cells. J Supramol Struct. 1979;11(4):529-38.

26. Rubin H. Cell-cell contact interactions conditionally determine suppression and selection of the neoplastic phenotype. Proc Natl Acad Sci U S A2008;105:6215–21.

27. Ryoo ZY, Jung BK, Lee SR, Kim MO, Kim SH, Kim HJ, Ahn JY, Lee TH, Cho YH, Park JH, Kim JK. Neoplastic transformation and tumorigenesis associated with overexpression of IMUP-1 and IMUP-2 genes in cultured NIH/3T3 mouse fibroblasts. Biochem Biophys Res Commun. 2006 Oct 27;349(3):995-1002.

28. Shin SI, Freedman VH, Risser R, Pollack R. Tumorigenicity of virus-transformed cells in nude mice is correlated specifically with anchorage independent growth in vitro. Proc Natl Acad Sci U S A. 1975 Nov;72(11):4435-9.

29. Sun H, Taneja R. Analysis of transformation and tumorigenicity using mouse embryonic fibroblast cells. Methods Mol Biol. 2007;383:303-10.

30. Tian Q, Frierson HF Jr, Krystal GW, Moskaluk CA. Activating c-kit gene mutations in human germ cell tumors. Am J Pathol. 1999 Jun;154(6):1643-7.

31. Turner AM, Zsebo KM, Martin F, Jacobsen FW, Bennett LG, Broudy VC. Nonhematopoietic tumor cell lines express stem cell factor and display c-kit receptors. Blood 1992;**80**:374–81.

32. Webster JD, Yuzbasiyan-Gurkan V, Kaneene JB, Miller R, Resau JH, Kiupel M. The role of c-KIT in tumorigenesis: evaluation in canine cutaneous mast cell tumors. Neoplasia. 2006 Feb;8(2):104-11.

33. Willmore-Payne C, Holden JA, Tripp S, Layfield LJ. Human malignant melanoma: detection of BRAF- and c-kit-activating mutations by high-resolution amplicon melting analysis. Hum Pathol. 2005 May;36(5):486-93.

34. Winnard PT Jr, Pathak AP, Dhara S, Cho SY, Raman V, Pomper MG. Molecular imaging of metastatic potential. J Nucl Med. 2008 Jun;49 Suppl 2:96S-112S.

35. Zongaro S, de Stanchina E, Colombo T, D'Incalci M, Giulotto E, Mondello C. Stepwise neoplastic transformation of a telomerase immortalized fibroblast cell line. Cancer Res. 2005 Dec 15;65(24):11411-8.

CHAPTER 4

KARYOTYPING AND CHROMOSOMAL INSTABILITY INVESTIGATION IN CAF-KIT MUTANT CELL LINES

ABSTRACT

Chromosome instability (CIN) is a common property of cancer cells and has been proposed to drive tumorigenesis and contribute to tumor progression. In previous studies, we identified a series of mutant isoforms of c-KIT in MCTs and reported their significant association with poor prognosis. We have developed cell lines derived from normal canine fibroblasts that ectopically express one of each of three different mutant c-KIT isoforms. Functional study has demonstrated the oncogenic capacity of mutant c-KIT isoforms in the immortalization and malignant transformation in canine primary fibroblasts. In the present study, we aim to investigate the aneuploidy status contributed by ectopic expression of mutant c-KIT. The karyotypes of each set of transfected cells were evaluated. Cells were synchronized, and metaphase preparations were analyzed to determine karyotypes. Twenty metaphase spreads per cell line were examined. All mutant c-KIT harboring cells displayed aneuploidy and chromosomal instability by gaining number of chromosomes. In addition, each CAF-KIT mutant cell line revealed their distinct modal numbers. The modal chromosome numbers for CAF-KIT-Del2, CAF-KIT-Del3, CAF-KIT-Del9, and CAF-KIT-Dup2 are 121, 100, 114, and 119, respectively. Quantitative real-time PCR using canine chromosome specific primers to detect copy numbers of each chromosome also confirmed the aneuploidy status of these cell lines. These data further provide insight into the mechanism of c-KIT driven tumorigenesis.

INTRODUCTION

Genome instability is a broad term used to describe the failure of a cell to accurately pass on a copy of its genome to its daughter cells. There are several mechanisms by which this can occur, and these have been grouped into three broad categories including microsatellite instability, nucleotide excision repair-related instability, and chromosomal instability (Coschi and Dick, 2012). Chromosome instability (CIN) can be further dissected into two types, whole chromosome instability (W-CIN) and segmental chromosome instability (S-CIN) (Geigl et al., 2008). The direct consequence of CIN is an imbalance in the number of chromosomes per cell (aneuploidy) and an enhanced rate of loss of heterozygosity (Nowak et al., 2002). The concept that aneuploidy is a characteristic of malignant cells has long been known (Michor, 2005). Theodor Boveri proposed aneuploidy as a cause of cancerous transformation in the early Nineteen Century. However, the discovery of oncogenes and tumor suppressors in the late 1970s and 1980s introduced alternative potential initiators of transformation and resulted in reduced interest in the aneuploidy hypothesis (Weaver and Cleveland, 2007). Others have argued that aneuploidy is only a benign side effect of transformation (Hede, 2005). Still others have suggested that aneuploidy promotes tumor progression but not initiation (Johansson et al., 1996). A major question in cancer genetics is whether or not CIN, or any genetic instability, is an early occurrence in the tumor cells and, therefore, a driving force of tumorigenesis. Some attempts to provide an explanation for the role of aneuploidy in tumorigenesis have shown that aneuploidy was found to act either oncogenically or as a tumor suppressor depending on the cell type and the presence or absence of additional genetic damage (Weaver et al., 2007).

However, it was not until 1997, when Lengauer and Vogelstein directly demonstrated evidence of persistent chromosome missegregation in cancer cell lines, that work exploring the

role of CIN in tumorigenesis began. Genome aberrations are the hallmark of tumorigenesis (Hanahan and Weinberg, 2011). During cell division and proliferation, mitotic checkpoints control the integrity of chromosome structure (Brunet and Vernos, 2001). These checkpoints monitor chromosome alignment during metaphase and prevent premature progression through mitosis. Specifically, they can stop mitotic cells from entering anaphase and prohibit chromosomes from moving towards the spindle poles. Proper chromosome segregation is mediated by the centrosome cycle, the mitotic spindle assembly, and mitotic kinase activation (Li and Li, 2006; Malumbres and Barbacid, 2007; Jallepalli and Lengauer, 2001). Errors that occurr at mitosis can result in mitotic catastrophes, characterized by spindle collapse, multipolar spindles, or cytokinesis failure. Cells that have been encountered with mitotic catastrophes can end up either entering apoptosis or exiting from mitosis with multinucleation or chromosome aberrations. Consequently, the consequential chromosome instability is comprised of gains or losses of whole chromosome(s) (aneuploidy), translocations, amplifications/deletions, or breaks (Draviam et al., 2004; Weaver and Cleveland, 2005).

In the previous chapters, it was shown that canine primary fibroblasts-transfected with mutant c-KIT had immortalized and neoplastically transformed. Since aneuploidy or chromosome imbalance is the most massive genetic abnormalities of cancer cells. In this study, we assayed the number of chromosomes per cell and the chromosomal aberrations to determine whether aneuploidy occurred in these CAF-KIT mutant cell lines.

MATERIALS AND METHODS

Cytogenetic study

Metaphase preparation and cytogenetic analysis were performed via the double synchronization method. CAF-KIT mutant cell lines were plated into 10 cm cell culture plates until 50-70% confluency was reached. In day 1, 0.5 µg/ml methotrexate was added in the complete medium and incubated overnight at 37 °C with 5% CO_2 incubator. In the morning of day 2, cells were washed three times with DPBS and fed with fresh medium containing 10 ug/ml thymidine (Sigma) for 5 hours. In the evening of day 2, cells were washed three times and fed with fresh complete medium for overnight incubation. In the morning of day 3, colcemid (Karyomax, Invitrogen) was added to a final concentration of 0.1 ug/mL for 2 hours before harvesting. Cells were trypsinized and harvested to produce G-banded metaphase preparations. After harvesting, the cells were exposed to hypotonic solution (75 mM KCl) for 20 min at 37 °C and fixed with acetic acid/methanol (1:3). Chromosome spreading was made by dropping the cell suspension onto glass slides under humid conditions followed by drying on 65°C. Slides were incubated at 90°C-94°C for 45 minutes of aging and then stained by Leishman's staining as follows: 2.5% trypsin/PBS for 20 seconds, rinsing slides twice in PBS, Leishman's staining solution for 2 minutes, washing with distilled water and air drying. Slides were mounted with Cytoseal 60 mounting medium (Fisher Scientific). Karyotype analysis was performed by a computerized acquisition and analysis system (Cytovision, Applied Spectral Imaging). Number of chromosomes per cell from twenty metaphases of each tumor cell line was counted for chromosomal numerical abnormalities. To avoid misinterpretation due to technical error, normal canine fibroblasts were used as control.

PCR for chromosome instability analysis

Genomic DNA from CAF-KIT-Del2, CAF-KIT-Del3, CAF-KIT-Del9, CAF-KIT-Dup2, primary canine fibroblasts, and dog spleen was extracted. These cells ($2x10^6$ cells) were trypsinized and centrifuged at 1200 rpm for 10 minutes. Cells were resuspended and washed twice with DPBS. Cell pellets from each CAF-KIT mutant cell lines were lysed in 400 ul of lysis buffer, and 5 ul of 20 mg/ml proteinase K solution was added. The mixture was incubated in 42°C water bath for overnight. The next day, proteinase K was inactivated by incubating the mixture in the 95°C heat block. After centrifugation at 10,000 rpm for 10 minutes, supernatant was collected and used as a template for PCR. Before each experiment, DNA concentrations were measured using a NanoDrop ND-1000 Spectrophotometer (Biorad). Canine chromosome-specific primers, including chromosome 1-38, X and Y were designed by the Primer3 software. Presence of each chromosome was analyzed by PCR amplification in all samples. PCR was performed using GoTaq® DNA Polymerase (Promega) and 30 ng of genomic DNA. Reaction conditions were 95° for 2 min, followed by 40 cycles of 95° for 1 minute, 56-63° for 1 minute, 72° for 1 minute, with a final extension at 72° for 5 minutes. Dog spleen DNA served as a positive control. All primer sequences are shown in Table 5.

Quantitative real-time PCR

The samples were further evaluated using quantitative real-time PCR. Five nanograms of genomic DNA were PCR-amplified using the SYBR® Green PCR Master Mix (Applied Biosystems) on a StepOnePlus™ Real-Time PCR Systems (Applied Biosystems). The reaction was set up using 5 ng of DNA per reaction. Each sample was analyzed in quadruplicate. Conditions for amplification were as follows: 1 cycle at 95°C for 10 min, 40 cycles at 95°C for

30 s/62°C for 1 min/72°C for 30 s and 1 cycle at 95°C for 1 min/62°C for 30 s/95°C for 30 s. The final cycle was for producing a dissociation curve.

Chromosome X-specific primers were used as endogenous controls to establish the reference range of relative expression. As reference for the number, genomic DNA from 12 male (XY) dogs that contained one copy and 12 female (XX) dogs that contained 2 copies were used. The CT and relative quantification (RQ) were calculated by using the $2^{-\Delta\Delta CT}$ method. For analysis, the PCR reactions were calibrated to female dog spleen genomic DNA, setting two copies as the calibrators, having an RQ values of 1.

Table 5: Chromosome-specific primers of each canine chromosome and their PCR conditions

CF No	Forward primer	Reverse Primer	Size	Ann. Temp
1	AGCTCCCAGATTCGTCAGAA	GCTAGTGGGGGAACTTAGGC	143	63
2	TTTTGTCCTTGATGCCACTTC	TTCCAGTTACGACCTTTGTGG	80	56
3	ATTTTGAGGGGAAATGGACTG	CCTTTGACAGATGCAGCCTTA	127	58
4	GGGGTAAAAGCTGCATTGTAA	AGCGTGGATGTGCTTTAATGT	84	58
5	CAAGTCAGGGTGGCTATTGAG	GGAAGCTGTCTTTGCAGTCAC	140	63
6	CTGTACCAGAGCCCCCTTTAG	GGGAGGTTCACAGACTTACAGG	117	56
7	GAACATGGGTCAGCAAACTGT	ATGAGCATGATGGTGTTCCA	89	60
8	CCCCACTTCCTCTGGTCAGT	GCTCCAATCACCACCATTCT	141	60
9	CCTTACAAGAAGGAGGCAGGA	ACCAGGTCCAGAGGACAGAGT	132	56
10	AGAAGCACCATGTTTGTGAGC	GCACTTCAGGCTATCATCGTC	128	63
11	CTGCACACCTACCCCAGAAT	CACGCACGTGCTTAAACATT	123	60
12	TGCTACGCCATACACAGTCA	AGGGCACACACCACATTCTC	111	56
13	CACCGTGTTGTCCTAATCACC	ACCAGAAGGATCCAAAACCAT	107	60
14	CTCATCCATGCACGTCCTTT	TTAGGGAACAGGAAGCCTGA	146	60
15	TTCAACCTTTTGCACACTCTG	CTGCAACAGGGGGTAACATA	121	60
16	CTCCCTGAGGTTCAGCTTGT	TGCTGTTCCAGAGGCAAGTA	130	58
17	CTGTTGAAAGGAGGACACACC	CATCACCTACCCTTCCCTAGC	130	56
18	TTCCAGAGTTGGGAAACGTAA	GGATGTACAGACCACGGAACA	147	58
19	CTGACCCCCTGTCCCTAGTT	GATCAGGAGGCAGATCAGGA	111	58
20	CGCCCGATTTTCTTTGTTAG	GGCAAAGGAGGACACAGGT	143	63
21	GAAAAAGGCTGTTGCCATCT	AGACCTGCTGAGCTGACGA	143	60
22	CTGTCAGGCTTCAACCTCCT	ATTCCCTGCACTGTGGTTTC	121	60
23	ACTGATGGTTTTTCCTTGAGC	GAGCCTGACAGTGAGTGGAAC	98	60
24	TCACCTGGCTCCTCTCCTAGT	CGTGCAGGATTCCCTCTTTAC	108	58
25	CCAGGAATTCAGACCAACCT	TTCCAAGTGGGGAAAGTGAG	100	60
26	CTTTGGGTTTGCATGGTGTA	TCTCCCACTTGGTGTTCCTC	140	58
27	GCAAGAGTGCCTTGACGATAC	GGGCCTGCACAAATCAATA	108	58
28	CAGCACCCTTGGGAGAATAA	GCAGGACCCCAAATTAGATTC	101	58
29	GCCTGCTTCACAAAATGACA	GCTGCCCCAAAAAGTGTATTA	132	58
30	CCGTCCTTAACCACATGATTTC	ACCTGTGGTCACTTGGAATGT	123	58
31	TGGAAACCAGCCATCTACCT	GGTCAAGATTCCCTCAGATCC	116	58
32	TGCCAGATTCCTCAACTTCC	CTGCACACAAGAGGTGATAAGC	139	58
33	AGATGGGGTGATTTGTTAGGC	ATCCTTGTGGAAGCATCTTGA	124	58
34	ATCGACCTGGAAATTGAGGA	GGAGGAGATGCCCTCAGATA	91	56
35	GCACAGACAGGCATACAGTCA	GGACCACTGTTTGCTTCCTAC	123	60
36	CAGGTTCCCTCTCCACCTTT	TTTCAGGCAAGCCTCTCATT	149	60
37	AGTCCCAGGCAGGAGAGAAT	TGATCCCCGATTGTGTTGTA	148	60
38	GATGTGAAAGCCAAGGAGGT	ACTCTCCTGCCCTGGTGAAG	147	63
X	AACCAATGGACTGCAAGCAT	CGTGAGGACAAAGGGGAATA	125	63
Y	ATGAGCTTGGAAACTTGCT	TCAACGTGCTCTCTCCTCAA	100	56

RESULTS

To confirm the direct role of ectopic expression of mutant c-KIT in canine primary fibroblasts (CAF-KIT mutant cell lines) in the induction of chromosomal instability, we tested whether CAF-KIT-Del2, CAF-KIT-Del3, CAF-KIT-Del9, and CAF-KIT-Dup2 could cause chromosome aberrations.

Dog chromosomes were arranged by their size from big to small. A normal dog chromosome is acrocentric and very small in size, which makes them very difficult to differentiate using G-banding.

The result showed that no normal 78,XY or 78,XX cells were observed in CAF-KIT-Del2, CAF-KIT-Del3, CAF-KIT-Del9, and CAF-KIT-Dup2. The composite karyotype of each cell line is presented in table 2. The CAF-KIT-Del2 cell line was derived from a female dog and defined as a hyperdiploid cell line with a modal number of 121 chromosomes. The chromosome number ranged from 79 to 124 in 20 metaphases analyzed and none of them presented a normal karyotype. The CAF-KIT-Del3 also showed a hyperdiploid chromosome ranging from 76 to 109 with a modal number of 100 chromosomes. Karyotyping results of CAF-KIT-Del9 and CAF-KIT-Dup2 also revealed their hyperdiploid with modal numbers of 114 and 119 chromosomes respectively. Chromosome numbers ranged from 50 to 119 chromosomes in CAF-KIT-Del9 and 111-121 chromosomes in CAF-KIT-Dup2. To summarize, ectopic expression of c-KIT mutant isoforms including Del2, Del3, Del9, and Dup2 is sufficient to induce aneuploidy in canine primary fibroblasts.

To verify the aneuploidy detected by counting chromosomes, the appropriate experimental conditions for PCR of each chromosome were established. These PCR products were specific for each chromosome according to the BLAST alignment. In addition, agarose gel

visualization also confirmed a single band of the expected size, which amplified from each primer set. Validation studies were successful in all cell lines tested. Results showed that 90-150 bp of PCR products from all chromosome amplification (Chromosome 1-38) were detected in CAF-KIT-Del2, CAF-KIT-Del3, CAF-KIT-Del9, and CAF-KIT-Dup2, as shown in Figure 7A, 7B, 7C, and 7D respectively. Chromosomes X and Y were also amplified to determine genders of cell-derived animals. Consistent with the karyotype, results from PCR showed that C2 mast cell line, spleen, CAF-KIT-Del2, CAF-KIT-Del9, and CAF-KIT-Dup2 cells were derived from a female dog, whereas CAF-KIT-Del3 cells were derived from a male dog.

Moreover, copy number of each cell was analyzed by using quantitative real-time PCR amplified with canine chromosome specific primers. The reference ranges for one and two copies of the *c-KIT* gene were established by sex chromosome copy number analyses of normal male and female control in different experiments. On the basis of mean ratio ± 1.5 of standard deviation value, the reference intervals were set as 0.8–1.4 for karyotypes with one X-chromosome (n = 12) and 1.6–2.3 for karyotypes with two X-chromosomes (n = 12). The two reference ranges were not overlapping with each other, thus the copy number of each chromosome in each cell line are accurate to within this degree of variability. Consistent with the .6karyotype results, gain of chromosome of all CAF-KIT mutant cells and C2 mast cell line was detected by quantitative real-time PCR (as shown in Figure 3). Number of chromosomes was ranged from as low as 0.57 in chromosome 28 in CAF-KIT-Del3 to as high as 18.61 in chromosome 23 in CAF-KIT-Dup2.

Figure 15: Karyogram of canine primary fibroblast. Chromosomes were arranged and assigned their chromosome numbers by size from largest to smallest. Pairing of each chromosome was based on their G-banding. Cytogenetic analysis of normal canine primary fibroblasts revealed normal number of chromosome (78, XX) (100x).

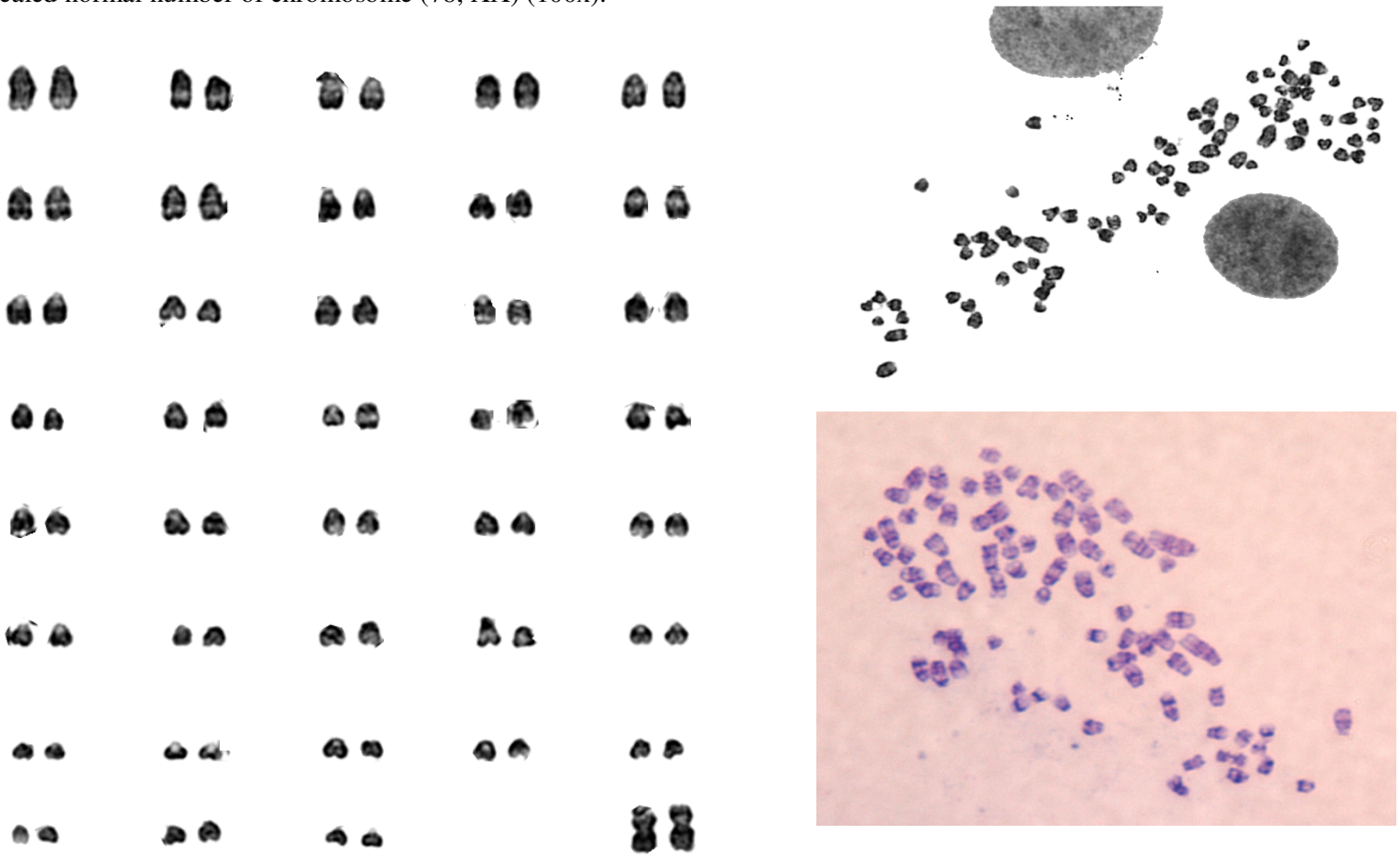

Figure 16: A representative metaphase spread from CAF-KIT-Del2 showing aneuploidy by gain of chromosome (n=119).

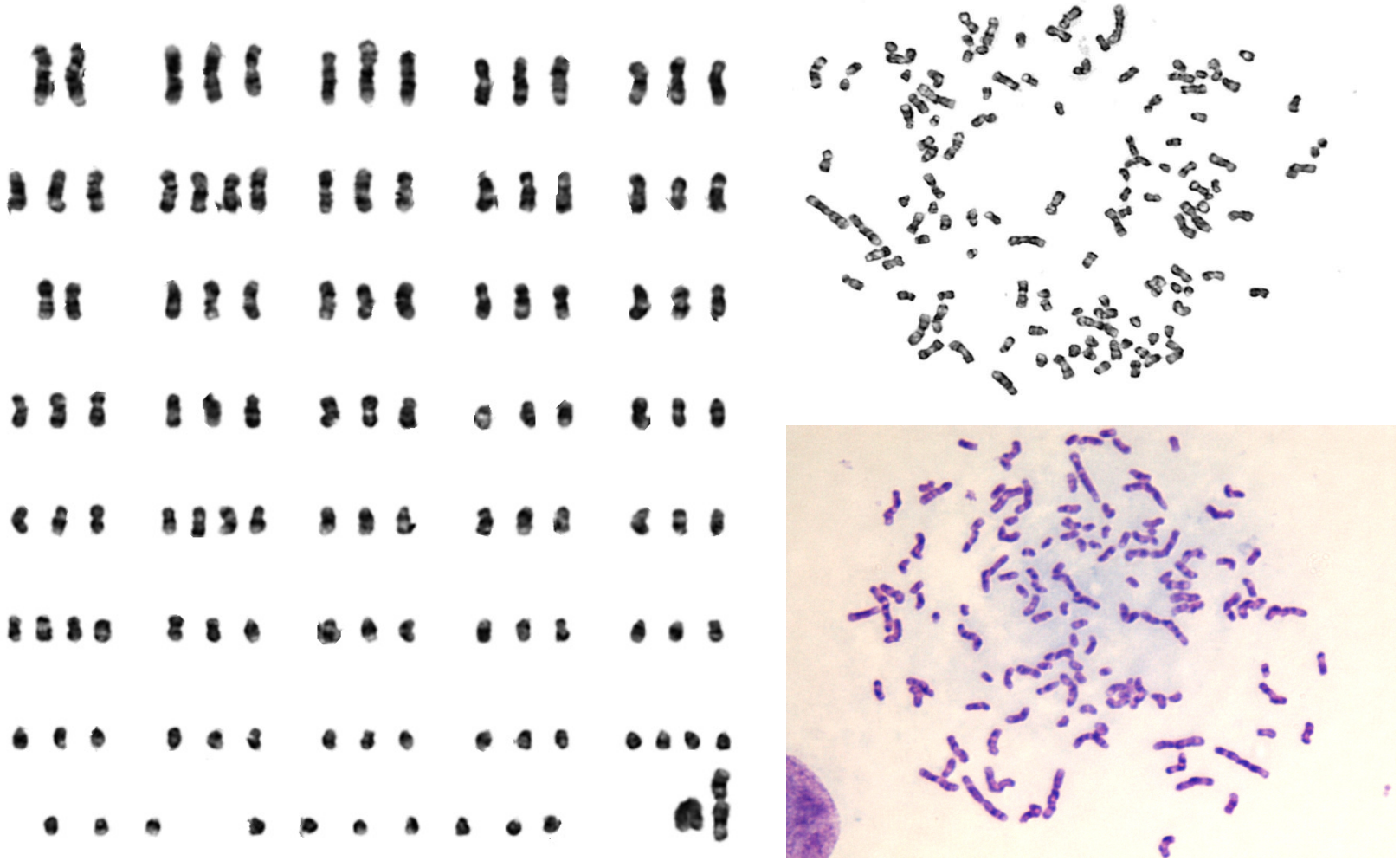

Figure 17: Photomicrographs showing CAF-KIT-Del3 karyotyping analysis (n=104).

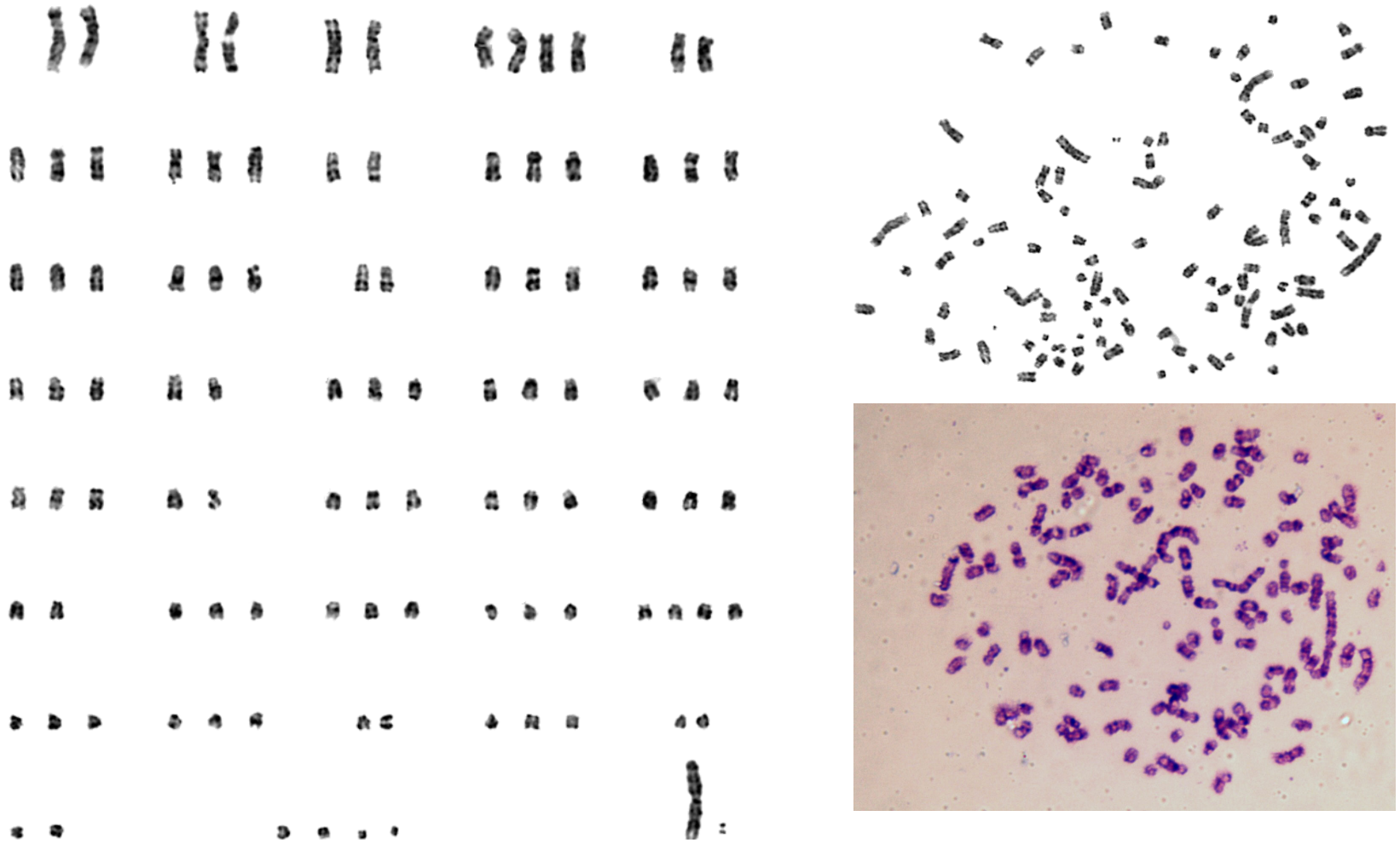

Figure 18: Images depicting the karyotype of CAF-KIT-Del9 (N=111).

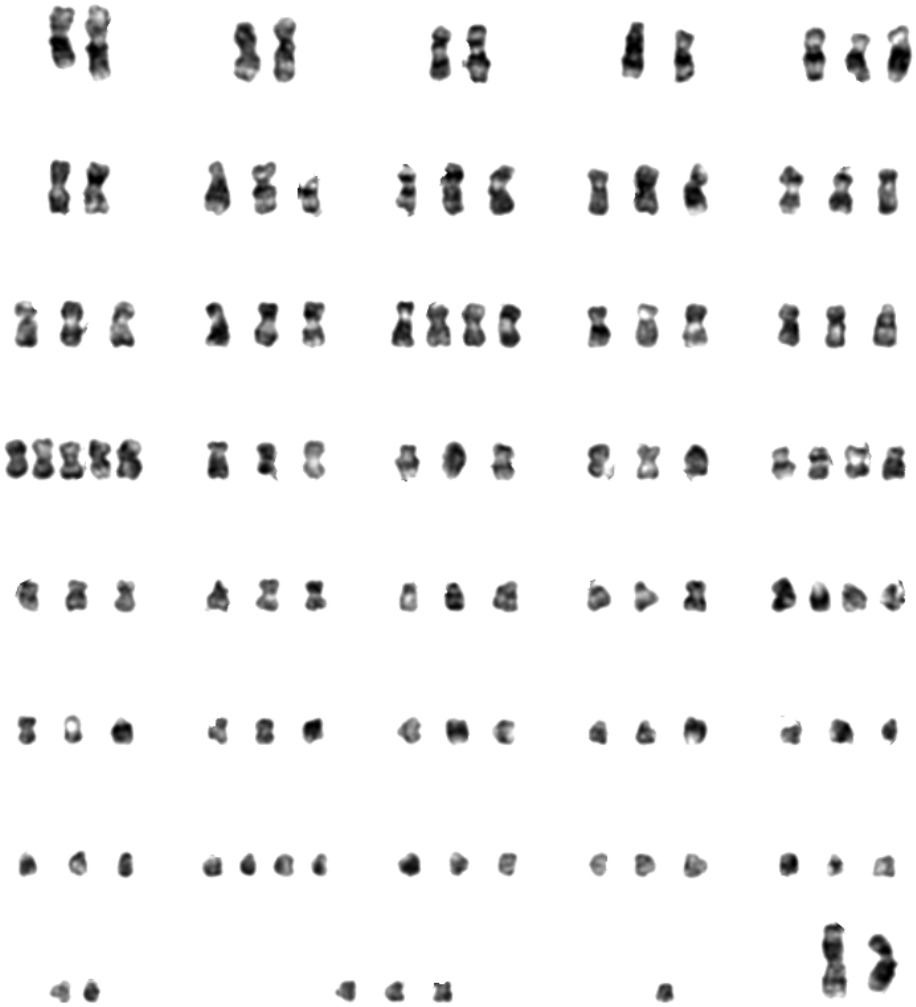

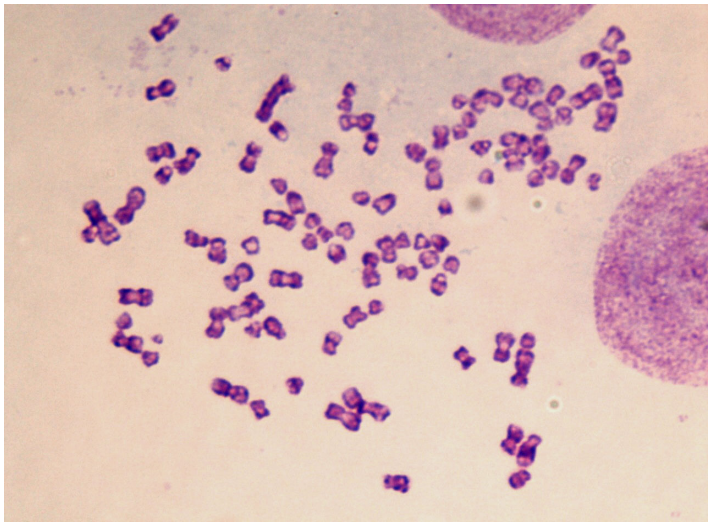

Figure 19: Karyotypic analyses of CAF-KIT-Dup2 showing an aneuploid karyotype (n=118).

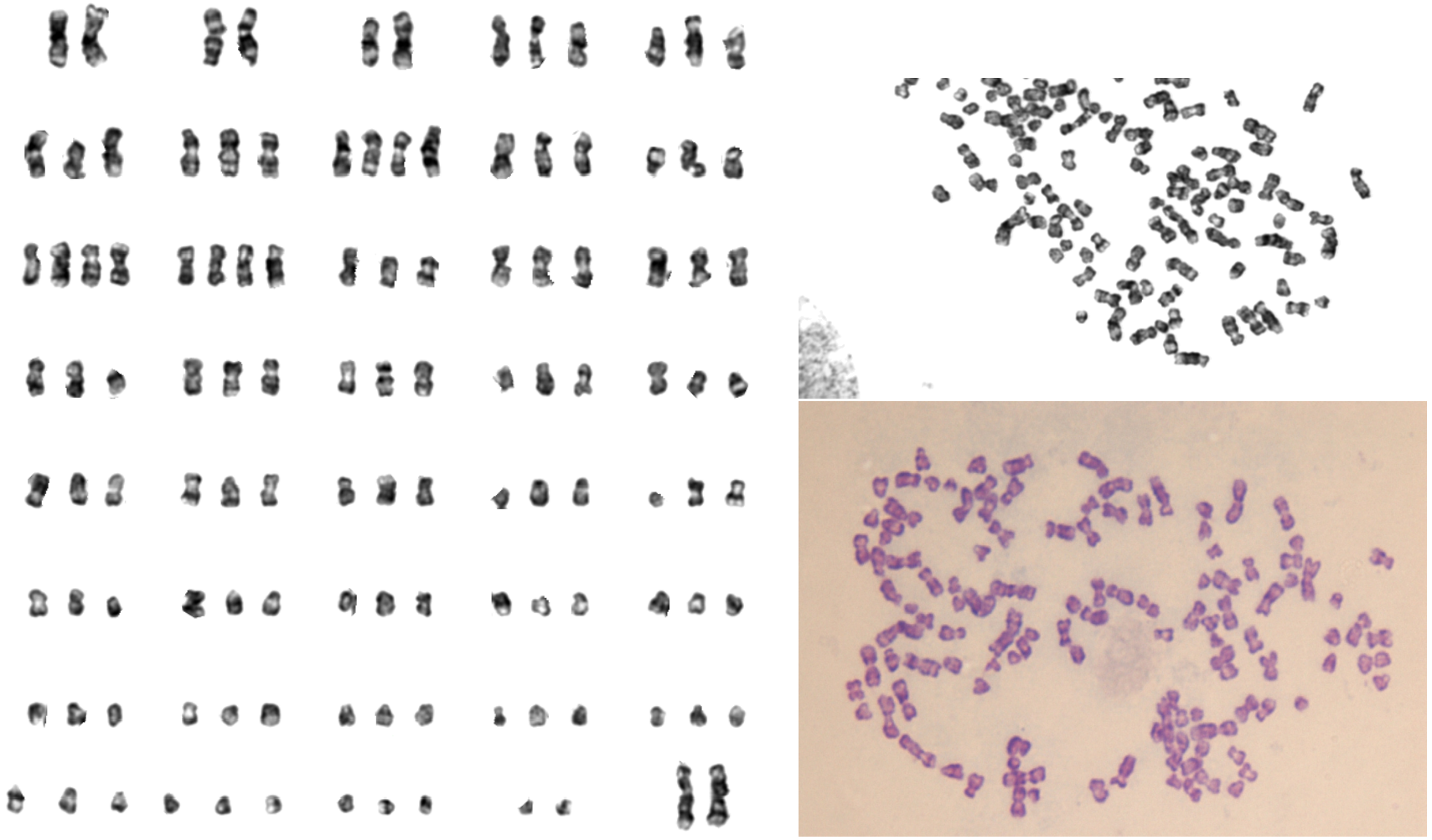

Figure 20: A depiction of karyotypes of the C2 MCT mast cell line showing their aneuploidy (n=101).

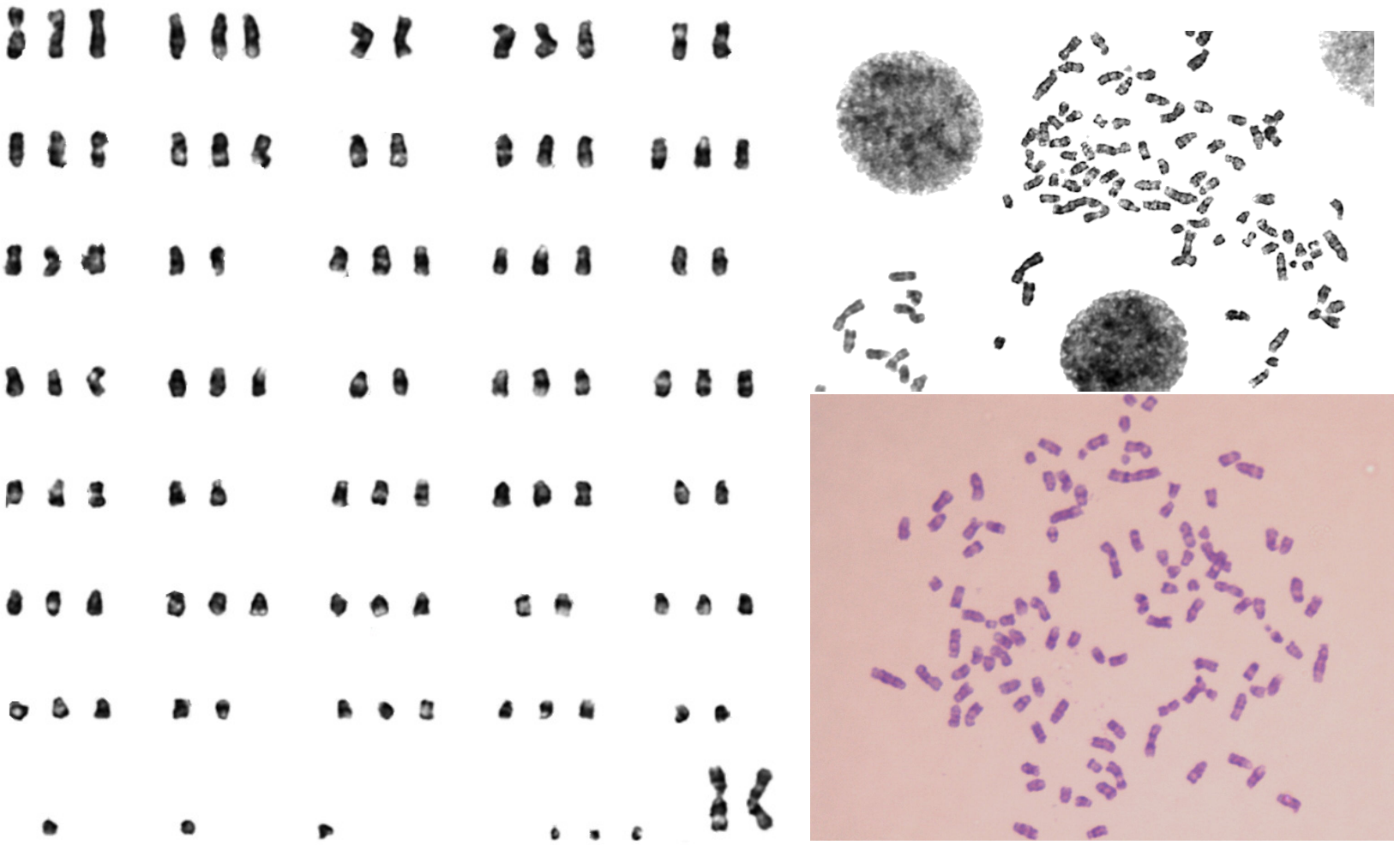

Figure 21: Representative 2.0% agarose gel picture of chromosome-specific amplicons. PCR amplification of each chromosome using canine chromosome specific forward and reverse primers gives rise of 90-150 bp PCR products. Lane 1-8, X and Y corresponding PCR product from chromosome 1-38, x, and Y. Abbreviation used: L, 100 bp ladders. A, CAF-KIT-Del2; B, CAF-KIT-Del3; C, CAF-KIT-Del9; D, CAF-KIT-Dup2.

A

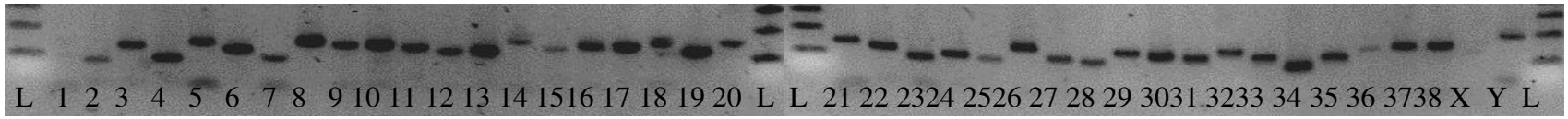

B

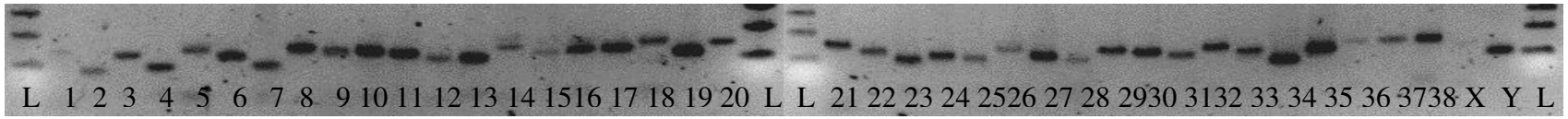

C

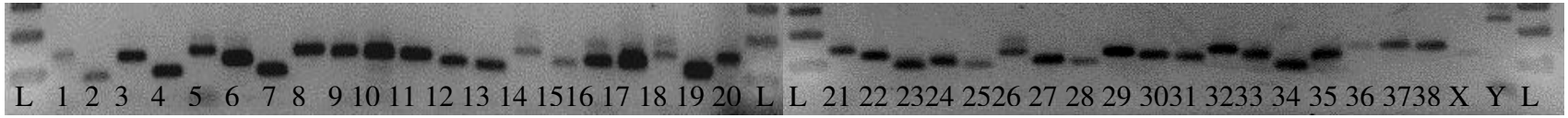

D

Table 6: Number of chromosomes per cell of each cell line counted in 20 metaphases.

	CAF-KIT-Del2	**CAF-KIT-Del3**	**CAF-KIT-Del9**	**CAF-KIT-Dup2**	**C2MCT**	**NI-1**
Metaphase 1	121	108	113	120	102	72
Metaphase 2	118	104	112	118	98	64
Metaphase 3	124	91	95	118	90	74
Metaphase 4	122	80	109	119	94	70
Metaphase 5	119	100	102	116	92	71
Metaphase 6	121	107	104	114	95	68
Metaphase 7	123	105	114	114	104	67
Metaphase 8	119	96	77	119	99	67
Metaphase 9	121	108	112	115	99	57
Metaphase 10	122	109	115	119	100	72
Metaphase 11	117	76	106	114	101	68
Metaphase 12	121	94	114	118	71	70
Metaphase 13	119	93	118	116	100	70
Metaphase 14	119	97	109	119	90	69
Metaphase 15	116	95	119	117	96	70
Metaphase 16	79	88	50	111	100	71
Metaphase 17	118	90	114	113	102	71
Metaphase 18	117	100	115	116	99	69
Metaphase 19	117	98	115	112	97	69
Metaphase 20	116	100	114	121	100	70
Mode	**121**	**100**	**114**	**119**	**100**	**70**

Table 7: Number of chromosomes of each cell line measured by quantitative real-time PCR.

CF	CAF-KIT-Del2 copy number	CAF-KIT-Del 3 copy number	CAF-KIT-Del9 copy number	CAF-KIT-Dup2 copy number	C2 MCT copy number
CF1	2.27	1.93	1.99	2.61	3.59
CF2	3.08	4.24	2.28	2.31	2.72
CF3	1.89	1.76	1.91	2.36	2.40
CF4	1.95	1.33	1.55	2.09	2.03
CF5	2.68	2.13	2.76	2.61	3.76
CF6	1.88	1.67	1.81	2.06	1.95
CF7	1.85	0.98	1.64	2.21	2.98
CF8	3.35	1.95	3.02	4.60	2.61
CF9	1.87	1.74	1.77	1.91	2.94
CF10	2.34	1.17	2.40	1.82	1.27
CF11	2.03	1.25	2.18	2.49	2.00
CF12	2.11	1.93	1.67	1.68	3.05
CF13	3.64	1.60	2.52	3.66	2.93
CF14	1.84	1.64	1.63	1.77	2.95
CF15	2.37	2.16	2.47	3.05	2.05
CF16	5.59	1.34	4.42	5.94	3.27
CF17	3.15	1.64	3.12	3.38	3.45
CF18	2.28	1.56	1.90	1.92	2.26
CF19	1.75	1.71	1.54	1.64	2.62
CF20	1.89	1.23	2.15	1.96	4.74
CF21	3.31	2.13	3.79	3.67	3.74
CF22	1.37	0.77	1.15	1.40	1.46
CF23	12.75	0.95	12.73	18.61	1.71
CF24	2.20	1.30	2.25	2.85	2.70
CF25	1.97	1.67	1.83	2.28	2.66
CF26	2.84	1.86	2.91	3.25	3.43
CF27	1.44	1.75	1.16	1.51	3.65
CF28	2.22	0.54	1.90	2.19	1.71
CF29	0.90	0.93	0.81	0.98	2.44
CF30	4.07	1.43	3.68	4.43	4.70
CF31	3.61	1.90	3.08	4.06	8.28
CF32	5.61	1.30	5.35	5.52	1.44
CF33	1.82	1.04	1.65	1.62	2.76
CF34	1.11	2.11	0.88	0.82	4.29
CF35	2.50	2.40	1.67	2.06	1.83
CF36	0.61	1.09	1.17	0.57	2.63
CF37	2.86	1.71	2.27	3.19	7.78
CF38	0.93	1.64	0.82	1.13	1.56

DISCUSSION

In the previous study, it was shown that mutant c-KIT transfected canine fibroblasts were readily immortalized in culture and that immortalized CAF-KIT mutant cell lines showed tumorigenic transformation properties *in vitro*. In this study, results show that ectopic expression of mutant c-KIT leads to increased genetic instability in canine primary culture. In addition, metaphase analyses demonstrate that all neoplastic CAF-KIT mutant cell lines have a high incidence of gross chromosomal instabilities displaying aneuploidy with gains of chromosomes.

Aneuploidy is a prominent phenotype of cancer. It refers to deviations from the normal number of chromosomes in a cell as a result of whole-chromosome loss or gain (Fang and Zhang, 2011). Numerical chromosome changes are very common in solid and hematological tumors (Lengauer et al., 1997; Weaver and Cleveland, 2006). It has been suggested that chromosomal instability (CIN) plays an important role in malignant transformation (Deusberg et al., 2004). Under normal circumstances, aneuploidy may act as a barrier to suppress tumorigenesis by reducing the growth of preneoplastic cells (Holland and Cleveland 2009).

Genomic instability in early cancer stages has been shown to be caused by stress on the DNA replication, induced by oncogene expression (Bartkova et al., 2006; Di Micco et al., 2006). More recently, oncogene-induced DNA replication stress is suggested as a model. According to this model, the mechanism by which oncogenes induce genomic instability in early stages of cancer development is by causing replication stress leading to DNA double-strand breaks (Halazonetis et al., 2008; Bester et al., 2011). In addition, these induced DNA lesions are accumulated in mitotic cells, and oncogene activation primarily accelerates S-phase entry, thereby the resulting DNA lesions are primarily associated with DNA replication stress in the S phase (Bartkova et al., 2005; Ichijima et al., 2010). Double-strand breaks (DSBs) are the most

dangerous damage to the integrity of the genome. They can be repaired either by nonhomologous end joining or by homology-dependent repair mechanisms such as homologous recombination, break-induced replication, single-strand annealing, and synthesis-dependent strand annealing (Pâques Haber, 1999; McGlynn and Lloyd, 2002; Collura et al., 2005). Unrepaired DNA double-strand breaks or eroded telomeres can also lead to chromosomal instability by serving as substrates for chromosomal fusions and translocations (Morgan et a., 1998). These events can lead to tumorigenesis if, for example, the deleted chromosomal region encodes a tumor suppressor or if an amplified region encodes a protein with oncogenic potential. In the cases of chromosomal translocations, this can sometimes lead to a gene fusion that dysregulates or alters the functions of a proto-oncogene (Richardson and Jasin, 2000; Khanna and Jackson, 2001).

Our results show that the ectopic expression of c-KIT mutation leads to aneuploidy in CAF-KIT mutant cell lines, however, the specific mechanism of c-KIT that mediates aneuploidy has been impeded by the limited understanding of the direct evidence regulating the generation of aneuploidy. Indeed, the ectopically expressed mutant c-KIT contributes to the immortalization and neoplastic transformation of canine primary fibroblasts. As a consequence, DNA double strand breaks happen from the oncogene-induced replication stress which can confer sister chromatid bridging at fragile sites, elevated multinucleation, and aberrant mitosis and cytokinesis (Chan et al., 2009; Zhang et al., 2011).

In conclusion, these results strongly suggest that the ectopic expression of mutant c-KIT in canine primary fibroblasts causes aneuploidy. However, whether this chromosomal instability precedes tumorigenesis or is a by-product of transformation is not clear. It will be important in the future to further investigate the sequential steps of c-KIT mutation during the

immortalization and the malignant transformation in addition to the role of chromosomal instability in this process.

REFERENCES

REFERENCES

1. Bartkova J, Horejsí Z, Koed K, Krämer A, Tort F, Zieger K, Guldberg P, Sehested M, Nesland JM, Lukas C, Ørntoft T, Lukas J, Bartek J. DNA damage response as a candidate anti-cancer barrier in early human tumorigenesis. Nature. 2005 Apr 14;434(7035):864-70.

2. Bartkova J, Rezaei N, Liontos M, Karakaidos P, Kletsas D, Issaeva N, Vassiliou LV, Kolettas E, Niforou K, Zoumpourlis VC, Takaoka M, Nakagawa H, Tort F, Fugger K, Johansson F, Sehested M, Andersen CL, Dyrskjot L, Ørntoft T, Lukas J, Kittas C, Helleday T, Halazonetis TD, Bartek J, Gorgoulis VG. Oncogene-induced senescence is part of the tumorigenesis barrier imposed by DNA damage checkpoints. Nature. 2006 Nov 30;444(7119):633-7.

3. Bester AC, Roniger M, Oren YS, Im MM, Sarni D, Chaoat M, Bensimon A, Zamir G, Shewach DS, Kerem B. Nucleotide deficiency promotes genomic instability in early stages of cancer development. Cell. 2011 Apr 29;145(3):435-46.

4. Brunet S, Vernos I. Chromosome motors on the move. From motion to spindle checkpoint activity. EMBO Rep. 2001 Aug;2(8):669-73.

5. Chan KL, Palmai-Pallag T, Ying S, Hickson ID (2009) Replication stress induces sister-chromatid bridging at fragile site loci in mitosis. Nat Cell Biol 11:753–760.

6. Collura A, Blaisonneau J, Baldacci G, Francesconi S. The fission yeast Crb2/Chk1 pathway coordinates the DNA damage and spindle checkpoint in response to replication stress induced by topoisomerase I inhibitor. Mol Cell Biol. 2005 Sep;25(17):7889-99.

7. Coschi CH, Dick FA. Chromosome instability and deregulated proliferation: an unavoidable duo. Cell Mol Life Sci. 2012 Jun;69(12):2009-24.

8. De Keersmaecker K, Real PJ, Gatta GD, Palomero T, Sulis ML, Tosello V, Van Vlierberghe P, Barnes K, Castillo M, Sole X, Hadler M, Lenz J, Aplan PD, Kelliher M, Kee BL, Pandolfi PP, Kappes D, Gounari F, Petrie H, Van der Meulen J, Speleman F, Paietta E, Racevskis J, Wiernik PH, Rowe JM, Soulier J, Avran D, Cavé H, Dastugue N, Raimondi S, Meijerink JP, Cordon-Cardo C, Califano A, Ferrando AA. The TLX1 oncogene drives aneuploidy in T cell transformation. Nat Med. 2010 Nov;16(11):1321-7.

9. Di Micco R, Fumagalli M, Cicalese A, Piccinin S, Gasparini P, Luise C, Schurra C, Garre' M, Nuciforo PG, Bensimon A, Maestro R, Pelicci PG, d'Adda di Fagagna F. Oncogene-induced senescence is a DNA damage response triggered by DNA hyper-replication. Nature. 2006 Nov 30;444(7119):638-42.

10. Draviam VM, Xie S, Sorger PK. Chromosome segregation and genomic stability. Curr Opin Genet Dev. 2004 Apr;14(2):120-5.

11. Duesberg P, Fabarius A, Hehlmann R. Aneuploidy, the primary cause of the multilateral genomic instability of neoplastic and preneoplastic cells. IUBMB Life 2004;56: 65–81.

12. Fang X, Zhang P. Aneuploidy and tumorigenesis. Semin Cell Dev Biol. 2011 Aug;22(6):595-601.

13. Geigl JB, Obenauf AC, Schwarzbraun T, Speicher MR. Defining 'chromosomal instability'. Trends Genet. 2008 Feb;24(2):64-9.

14. Halazonetis TD, Gorgoulis VG, Bartek J. An oncogene-induced DNA damage model for cancer development. Science. 2008 Mar 7;319(5868):1352-5.

15. Hanahan D, Weinberg RA. Hallmarks of cancer: the next generation. Cell. 2011 Mar 4;144(5):646-74.

16. Hede K. Which came first? Studies clarify role of aneuploidy in cancer. J Natl Cancer Inst 2005; 97: 87–9.

17. Holland AJ, Cleveland DW. Boveri revisited: chromosomal instability, aneuploidy and tumorigenesis. Nat Rev Mol Cell Biol. 2009 Jul;10(7):478-87.

18. Jallepalli PV, Lengauer C. Chromosome segregation and cancer: cutting through the mystery. Nat Rev Cancer. 2001 Nov;1(2):109-17.

19. Johansson B, Mertens F, Mitelman F. Primary vs. secondary neoplasia-associated chromosomal abnormalities-balanced rearrangements vs. genomic imbalances? Genes Chromosomes Cancer 1996; 16: 155–63.

20. Keen-Kim, D., Nooraie, F. & Rao, P. N. Cytogenetic biomarkers for human cancer. Front. Biosci. (2008)13, 5928–5949.

21. Khanna KK, Jackson SP. DNA double-strand breaks: signaling, repair and the cancer connection. Nat Genet. 2001 Mar;27(3):247-54.

22. Lengauer C, Kinzler KW, Vogelstein B. Genetic instability in colorectal cancers. Nature. 1997;386(6625):623–627.

23. Li JJ, Li SA. Mitotic kinases: the key to duplication, segregation, and cytokinesis errors, chromosomal instability, and oncogenesis. Pharmacol Ther. 2006 Sep;111(3):974-84.

24. Malumbres M, Barbacid M. Cell cycle kinases in cancer. Curr Opin Genet Dev. 2007 Feb;17(1):60-5.

25. Manchado E, Guillamot M, Malumbres M. Killing cells by targeting mitosis. Cell Death Differ. 2012 Mar;19(3):369-77.

26. McGlynn P, Lloyd RG. Recombinational repair and restart of damaged replication forks. Nat Rev Mol Cell Biol. 2002 Nov;3(11):859-70.
27. Michor F. Chromosomal instability and human cancer. Philos Trans R Soc Lond B Biol Sci. 2005 Mar 29;360(1455):631-5.

28. Morgan WF, Corcoran J, Hartmann A, Kaplan MI, Limoli CL, Ponnaiya B. DNA double-strand breaks, chromosomal rearrangements, and genomic instability. Mutat Res. 1998 Aug 3;404(1-2):125-8.

29. Nikitin PA, Luftig MA. The DNA damage response in viral-induced cellular transformation. Br J Cancer. 2012 Jan 31;106(3):429-35.

30. Nowak MA, Komarova NL, Sengupta A, Jallepalli PV, Shih IeM, Vogelstein B, Lengauer C. The role of chromosomal instability in tumor initiation. Proc Natl Acad Sci U S A. 2002 Dec 10;99(25):16226-31.

31. Pâques F, Haber JE. Multiple pathways of recombination induced by double-strand breaks in Saccharomyces cerevisiae. Microbiol Mol Biol Rev. 1999 Jun;63(2):349-404.

32. Richardson, C. & Jasin, M. Frequent chromosomal translocations induced by DNA double-strand breaks. Nature 2000; 405: 697–700.

33. Weaver BA, Cleveland DW. Aneuploidy: instigator and inhibitor of tumorigenesis. Cancer Res. 2007 Nov 1;67(21):10103-5.

34. Weaver BA, Cleveland DW. Decoding the links between mitosis, cancer, and chemotherapy: The mitotic checkpoint, adaptation, and cell death. Cancer Cell. 2005 Jul;8(1):7-12.

35. Weaver BA, Cleveland DW. Does aneuploidy cause cancer? Curr Opin Cell Biol 2006; 18: 658–667.

36. Weaver BA, Silk AD, Montagna C, Verdier-Pinard P, Cleveland DW. Aneuploidy acts both oncogenically and as a tumor suppressor. Cancer Cell 2007; 11: 25–36.

37. Zhang Z, Arora S, Zhou Y, Cherry A, Wang TS. Replication-compromised cells require the mitotic checkpoint to prevent tetraploidization. Chromosoma. 2011 Feb;120(1):73-82.

CHAPTER 5

IN VIVO STUDY ON TUMORFORMATION EFFICIENCY OF CAF-KIT MUTANT CELL LINES

ABSTRACT

The proto-oncogene c-KIT is a tyrosine kinase receptor that plays important roles in many pathways. Mutations of the *c-KIT* gene have been reported in many types of tumors, but it is not clear if the mutant c-KIT isoforms observed can drive tumorigenesis. In dogs, c-KIT mutations correlate with tumor grade and poor survival. Various types of mutations have been reported, and many are predicted to lead autophosphorylation of the c-KIT receptor. In the previous study, four of six c-KIT mutant isoforms encountered in human GISTs, canine GIST, and canine mast cell tumors demonstrated their capacity to induce immortalization, malignant transformation, and chromosomal instability in canine primary fibroblasts. In this current study, the tumorigenicity of these CAF-KIT mutant cell lines was examined *in vivo*. As expected, transplantation of CAF-KIT mutant cell lines in immunodeficient mice resulted in soft tissue sarcoma formation *in vivo* in each and every case. Moreover, tumor metastasis also occurred in two out of four CAF-KIT mutant cell lines xenograft. These findings show for the first time that mutant c-KIT expression can drive tumorigenesis in otherwise normal fibroblasts. These findings provide significance for our understanding of c-KIT mutation-mediated tumorigenesis as well as testing grounds for novel and improved treatments for c-KIT driven cancers.

.

INTRODUCTION

The c-KIT receptor tyrosine kinase is constitutively activated by activating mutations. The *KIT* gene is a proto-oncogene that was originally discovered as the cellular homolog (*c-KIT*) of the feline sarcoma virus oncogene v-kit (Besmer et al., 1986). The deregulation of c-Kit involved in tumorigenesis have been described in certain tumors, including myeloid leukemia, cutaneous melanomas, germ cell tumors, mast cell tumors, gastrointestinal stromal tumors (GISTs), small cell lung cancers (SCLCs), breast cancers, and neuroblastomas (Matsuda et al., 1993; 8–12; Ko et al., 2003; Krystal et al., 1996; Faderl et al., 1999; Heinrich et al., 2002; Lefevre et al., 2004; Tian et al., 1999;Cohen et al., 1994; Zemke et al., 2002; Gregory-Bryson et al., 2010; Longley et al., 1999).

To date, c-KIT activating mutations have been identified in the exon 9 extracellular domain, the exon 11 juxtamembrane domain, and the exon 17 kinase domain (Bodemer et al., 2010; Furitsu et al., 1993; Lux et al., 2000; Tsujimura et al., 1999). Several *in vitro* systems have been used to investigate these mutations. It has been shown that activating mutations in the juxtamenbrnane domain (V559G) and the kinase domain (D814V) of c-KIT cause the constitutive activation in a ligand-independent manner and neoplastic transformation in multiple hematopoietic cells and cell lines. The consistent results were reported *in vivo* that cells expressing these activating mutations resulted in production of large tumors at the injection sites and/or the development of acute leukemia in transplanted mice (Kitayama et al, 1995; Kitayama et al., 1996).

For the relationship studies between cell growth behaviors *in vitro* and *in vivo*, investigations have concluded that only anchorage requirements *in vitro* correlate with tumorigenicity (DiMayorca et al., 1973; Freedman et al., 1974; Stiles at al., 1976). Ultimately,

however, the validity of any such in vitro system can only be justified by demonstrating a direct correspondence with the behavior of the same cells *in vivo* (Chan and Little, 1979). In other words, what are regarded as normal cells must not be tumorigenic in an appropriate host animal, whilst cells that are judged to be transformed in vitro must be (Shields, 1976). Until *in vitro* transformation can be compared to *in vivo* tumorigenesis in terms of molecular mechanism, *in vivo* testing will remain as the most vital operational criterion (Chan and Little, 1979).

The objective of this study is to ensure the role of c-KIT mutation on tumorigenesis *in vivo*. We evaluated the impact of a series of c-KIT mutations observed in canine MCTs on tumor formation and metastatic potential in immunodeficent mice. In this study, transformed CAF-KIT-mutants were injected via subcutaneous injection to study tumor formation. Xenografted tumor formation and metastatic tumors were investigated by macroscopic and microscopic examination. The expression of c-KIT in the tumors was quantified. Matrigel invasion assay and cytogenetic analysis of the re-cultured tumor cells were also explored.

MATERIALS AND METHODS

Xenograft study

Animal procedures were performed in accordance with approved protocols and followed recommendations from the Institutional Animal Care and Use Committee (IACUC) at Michigan State University. For the injection preparation, cells were trypsinized and washed with PBS twice. Cell viability was also measured by the Trypan blue exclusion method. Two different doses of cells (3 mice for each dose) including low dose ($1x10^5$ cells) and high dose ($1x10^6$ cells) were resuspended in the 1:1 mixture of cell culture media and Matrigel™ (BD Biosciences, USA) in a total volume of 200 ul. 5-week-old female NOD scid gamma mice (The Jackson lab, ME) were anesthetized via isoflurane inhalation and then inoculated subcutaneously on both rear flanks. Mice injected with normal CAF, CAF-KIT-wt, and CAF-GFP were served as a control groups. Tumor-bearing mice were sacrificed when the tumors had grown to a noticeable size above the skin surface (approximately 1-2 cm in diameter). At necropsy, the size of a tumor appearing on the skin was measured in three dimensions with a caliper. The organs were examined for metastatic evidence. At the end of the experiment (240 days after the injection), all surviving mice were sacrificed, and organs were also examined.

Histological examination and immunohistochemistry

Tumors were fixed in 10% neutral buffered formaldehyde, paraffin-embedded, and processed by routine methods to get 5-µm histological sections that were used for H&E staining and immunohistochemical studies for c-KIT expression. Microscopic lesions of formed tumors were evaluated by veterinary pathologist. Sections at 5 µm were deparaffinized in of xylene and rehydrated in a graded series of ethanol to distilled water. Antigen retrieval was done in antigen retrieval solution in a steamer (Black & Decker) for 20 minutes and endogenous peroxidases

treatment was performed with 3% hydrogen peroxide for 5 minutes followed by rinsing for 5 minutes in distilled water. Protein-blocking agent (Dako) was used to prevent non specific antibody binding. Then, sections were placed in autostainer and incubated with rabbit anti-human c-kit antibody (Dako) at a dilution of 1:300 for 30 minutes. Subsequently, sections were incubated with biotinylated secondary antibody (LSAB, Dakocytomation) for 30 min, washed in PBS, and incubated with streptavidin-peroxidase conjugate (LSAB, Dakocytomation) for 30 min. Finally, the reaction was developed using 3,3′-diaminobenzidine substrate (Dako). Slides were counterstained in hematoxylin and dehydrated, and cover slips added. Control slides were run simultaneously. Confirmed canine MCTs cases were used as a positive control, whereas slides stained without primary antibody were served as a negative control.

Re-cultured tumor cell lines

Two grams of tumors was collected during the necropsy. After rinsing with DPBS supplemented with 100 U/ml penicillin, 100 mg/ml streptomicin and 1 ug/ml amphotericin B, tumors were minced and digested with collagenase type IA (1 mg/ml) in Hank's Balanced Salt Solution (HBSS, Invitrogen) at 37°C for 2 hours. Cells then were washed three times with DPBS and filtered through a 70 µm nylon mesh cell strainer (BD biosciences) and plated in 10 cm cell culture plate with complete medium. After 24 hour incubation, medium and unattached cells were removed, and attached cells were washed and expanded in complete medium. After reaching their confluence, cells were subcultured and frozen down for further study.

Expression of c-KIT in re-cultured tumor

Total RNA from re-cultured tumor cells was isolated with Acid-Phenol:Chloroform (Ambion) and the mirVana™ miRNA Isolation Kit (Ambion) according to the instructions of the manufacturer. Three micrograms of total RNA was treated with TURBO DNA-free™ (Ambion)

to remove contaminating DNA. First-strand cDNA synthesis was performed using SuperScript III Reverse Transcriptase (Invitrogen) with random primers (Promega). The cDNA was then column-purified by using QIAquick PCR Purification Kit (QIAGEN), and eluted with distilled nuclease-free water at concentration 50 ng/µl. PCR was performed in the reaction as follows: initial denaturation at 94°C for 4 min; 40 cycles at 94°C for 1 minute, 58°C for 1 minute, 72°C for 1 minute; and a final extension at 72°C for 5 minutes. The primer sequences were as follows: c-KIT forward primer: VYG2085 5'-GCG TTT CTT ACG TTG TGC CA -3' ; c-KIT reverse primer: VYG2086 5'- GCC AAC TCA TCA TCT TCC AT -3' ; Beta-2-microglobulin (β2MG) forward primer: VYG1487 5'- AGA AGG TAG TGA AGC AGG CAT C -3' ; β2MG reverse primer: VYG1488 5'- GTG GAA GAG TGG GTG TCA TTG -3'. The expected sizes of products were 109 bp for c-KIT and 106 bp for β2MG. The PCR products were separated on a 2% agarose gel, stained in ethidium bromide, and visualized on a UV.

Quantitative real-time PCR using SYBR Green (Applid Biosystems) for amplification of c-KIT was also performed using a StepOnePlus™ Real-Time PCR Systems (Applied Biosystems). All analyses were done in quadruplicate, and the mean was used for further calculations. The baseline was set automatically, and the threshold Ct was defined as the number of cycles in which the fluorescence exceeded the automatically set threshold. After the reaction, c-KIT mRNA expression was normalized by the expression of β2MG. The mRNA relative quantitation was done using the ΔCt method. The difference (ΔCt) between the average of c-KIT and the housekeeping gene (β2MG) was calculated. Fold changes in c-KIT expression of each CAF-KIT cell line as compared to primary canine fibroblasts were calculated using the delta-delta Ct (ΔΔCt) method using β2MG as the normalization control.

Matrigel Invasion assay of re-cultured tumor cells

Cell invasiveness of re-cultured cells from tumors was evaluated using Matrigel-coated semipermeable-modified Boyden inserts. BioCoat Growth Factor-Reduced Matrigel invasion chambers (24-well cell culture inserts containing an 8.0-µm polyethylene terephthalate (PET) membrane with a uniform layer of Matrigel matrix; BD) were used to assess cell invasion following the manufacturer's instructions. After determination of cell count and viability in a hemocytometer by the trypan blue exclusion test, cells resuspended in DMEM with L-glutamine, penicillin/streptomicin were added to the upper compartment of the chamber (2.5 × 105 cells/chamber). DMEM supplemented with 10% FBS was placed in the bottom well, with 10% FBS providing the chemo-attractants. Incubation was carried out for 20 hours at 37 °C in humidified air with 5% CO_2. The cells on the insert were removed by wiping gently with a cotton swab. Cells on the reverse side of the insert were fixed and stained with DiffQuick according to the manufacturer's instructions and mounted on glass slides. Total number of cells that crossed the membrane was counted under a light microscope and the average value was calculated. Experiments were performed three chambers/cell line.

Chromosomal instability study

Double synchronization method was applied for metaphase preparation. Cells were plated into 10 cm cell culture plate until 50-70% confluency of each cell lines was reached. On day 1, 0.5 µg/ml methotrexate was added in the complete medium and incubated overnight at 37 °C with 5% CO_2 incubator. In the morning of day 2, cells were washed three times with DPBS and fed with fresh medium containing 10 ug/ml thymidine (Sigma) for 5 hours. In the evening of day 2, cells were washed three times and fed with fresh complete medium for overnight incubation. In the morning of day 3, colcemid (Karyomax, Invitrogen) was added to a final concentration of 0.1 µg/mL for 2 hours before harvesting. Cells were trypsinized and harvested to produce G-

banded metaphase preparations. After harvesting, the cells were exposed to hypotonic solution (75 mM KCl) for 20 min at 37 °C and fixed with acetic acid/methanol (1:3). Chromosome spreads were made by dropping the cell suspension onto glass slides under humid conditions followed by drying on 65°C. Slides were incubated at 90°C-94°C for 45 minutes and then stained by the method of Leishman as follows: 2.5% trypsin/PBS for 20 seconds, slides were rinsed twice in PBS, Leishman's staining solution for 2 minutes, washed with distilled water and air dried. Slides were mounted with Cytoseal 60 mounting medium (Fisher Scientific). Karyotype analysis was performed by a computerized acquisition and analysis system (Cytovision, Applied Spectral Imaging). The number of chromosomes per cell from twelve metaphases of each tumor cell lines was analyzed for chromosomal numerical abnormalities.

RESULTS

To assess the *in vivo* tumorigenic ability of mutant c-KIT cell lines, NOD-SCID-Gamma (NSG) mice were subcutaneously injected with CAF-KIT-Del2 (n=6), CAF-KIT-Del3 (n=6), CAF-KIT-Del9 (n=6), and CAF-KIT-Dup2 (n=6), whereas untransfected primary canine fibroblasts (n=6), empty vector-transfected cells (n=1 at low dose only due to the limited senescent cells), and CAF-KIT-wild-type (n=1 at low dose only due to the limited senescent cells) were used as controls. Tumor formation was monitored in all tested animals for a total of 8 months. The xenograft was prepared in two doses at 1 x 10^5 cells/injection (low dose) and 1 x 106 cells/injection (high dose), and six injections per dose of all cell lines were conducted. Cells were mixed with matrigel and injected subcutaneously in flanks of female NSG mice. Consistent with the results of the in vitro studies, we found that tumors were formed in all xenografted mice transplanted with CAF-KIT-Del2 (3/3), CAF-KIT-Del3 (3/3), CAF-KIT-Del9 (3/3), and CAF-KIT-Dup2 (3/3) in both low and high doses of injection. Animals injected with primary canine fibroblast, CAF-GFP, and CAF-KIT-wild-type were tumor free even after 8 months, while all mice injected with CAF-KIT-Del2, CAF-KIT-Del9, and CAF-KIT-Dup2 cells with both low dose and high dose rapidly developed tumors at the injection site (Table 8). Tumors became detectable in 8 weeks post-injection and grew steadily to a final tumor size of 1.5 cm diameter at 9-10 weeks after injection. Intriguingly, the 6 mice injected with CAF-KIT-Del3 cells showed very slow tumor development after a nearly 4-month latency in reaching a final tumor size. There was no difference in tumor formation time between low and high dose. More interestingly, primary tumor-derived CAF-KIT-Del2 and CAF-KIT-Dup2 cells showed the ability to form disseminated tumors (Figure 2B-C and Figure 5T-U). Additionally, in CAF-KIT-Del2 (1/6), tumor spread sites included the omentum, intestines, pancreas, and the spleen. Furthermore, the

disseminated tumors in CAF-KIT-Dup2 (3/6) invaded intraperitoneal and retroperitoneal organs including the omentum, spleen, liver, pancreas, ovary, intestine and kidneys. Tumor volume was calculated (Euhus et al., 1986). Thus, these transformed cells are highly proliferative and possess invasive activity.

Histological analysis of the tumors confirmed them to be poorly differentiated, highly malignant soft tissue sarcomas, and also confirmed cell infiltration into the abdominal organs. The most common form of tumor phenotype histologically was soft tissue sarcoma, subtype osteosarcoma, characterized by bony matrix deposition and mineralization within the tumor, which was founded in CAF-KIT-Del2 (Figure 22D), CAF-KIT-Del9 (Figure 24P), and CAF-KIT-Dup2 (Figure 25V, 5X)-xenografted mice. Some tumors in CAF-KIT-Del3 (Figure 23J) showed the well differentiated fibrosarcoma subtype, characterized by densely packed, hyperchromatic spindle cells arranged in the interwoven pattern. Tumor cells showed a high nuclear:cytoplasmic ratio with prominent large nuclei, frequent mitotic figures, and areas of necrosis. Dissemination in the peritoneal cavity and the histological appearance of CAF-KIT-Del2 and CAF-KIT-Dup2 tumors were similar to those formed at the injection site.

Table 8: Summary of *in vivo* tumorigenicity results.

Cell type	Tumor formation	Days	Tumor volume (mm^3)	Morphologic diagnosis	Metastasis
Del2 low dose	6/6	72-76	750 – 1687.5	Soft tissue sarcoma	1/6 (abdominal cavity, pancreas, spleen, intestinal fat)
Del2 high dose	6/6*	81-87	125 - 1,000	Soft tissue sarcoma	No
Del3 low dose	6/6	117-166	62.5 – 2,250	Soft tissue sarcoma	No
Del3 high dose	6/6	117-126	62.5 – 2,250	Soft tissue sarcoma	No
Del9 low dose	6/6	77-93	187.5 - 750	Soft tissue sarcoma	No
Del9 high dose	6/6	73-83	62.5 - 750	Soft tissue sarcoma	No
Dup2 low dose	6/6	77-83	500 – 2,250	Soft tissue sarcoma	2/6 (abdominal cavity, ovary, liver, spleen, intestinal fat)
Dup2 high dose	6/6	73-83	187.5 - 1678.5	Soft tissue sarcoma	1/6 (abdominal cavity, liver, spleen, intestinal fat)
CAF low dose	0/6	249	No tumor formation		
CAF high dose	0/6	243	No tumor formation		
GFP low dose	0/1	249	No tumor formation		
wt-KIT low dose	0/1	249	No tumor formation		

Figure 22: Gross and histopathological features of CAF-KIT-Del2 derived xenografts formed in immunodeficient mice (Panel A-C). Representative paraffin embedded, hematoxylin and eosin-stained sections of a poorly differentiated soft tissue sarcoma (F, 40x), subtype osteosarcoma (E, 40x). Metastatic tumor nearby pancreas shown (D, 10x).

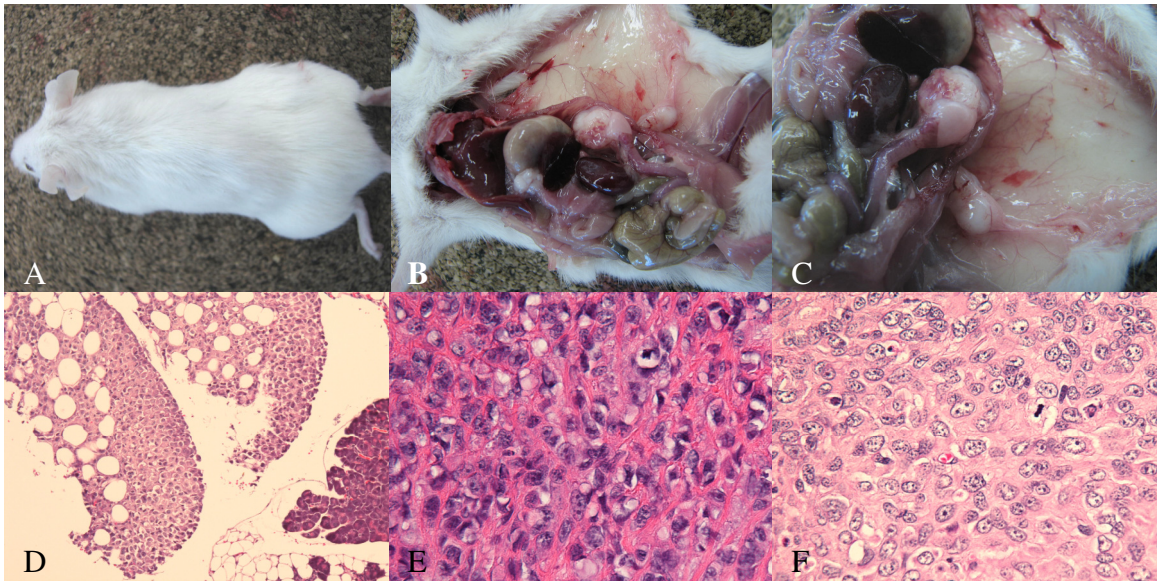

Figure 23: Gross and histopathological findings of the CAF-KIT-Del3 xenografts formed in immunodeficient mice (Panel G-I). Hematoxylin and eosin photomicrographs of subcutaneous xenograft show a poorly differentiated soft tissue sarcoma in 10x magnification (J) and 40x magnification (K-L).

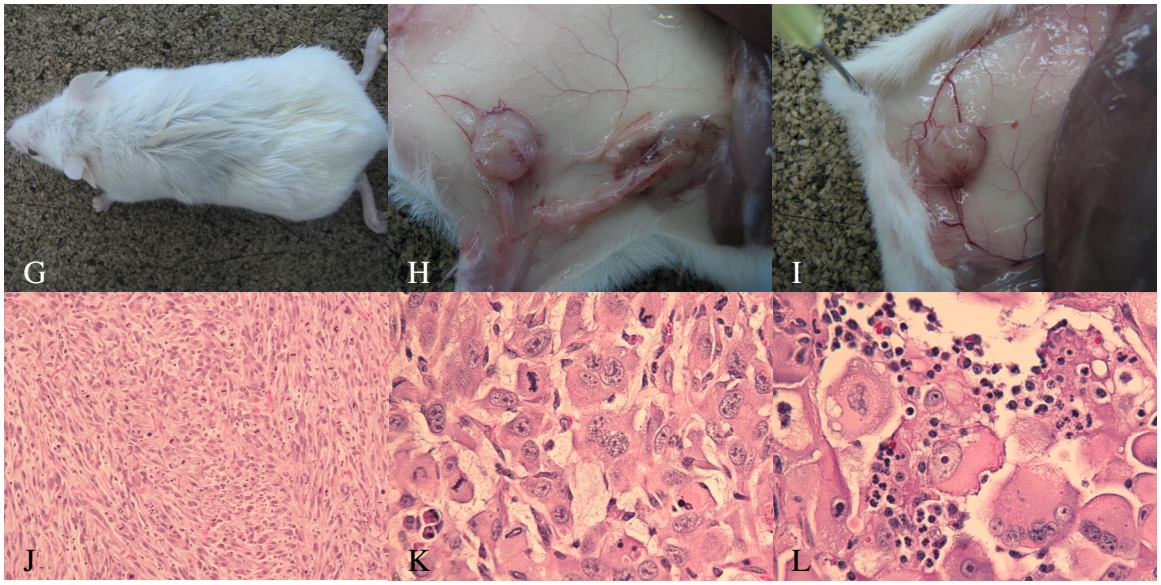

Figure 24: Gross and histopathological appearance of CAF-KIT-Del9 xenografts formed in immunodeficient mice (M-O). Representative histology of paraffin embedded, hematoxylin and eosin-stained sections of a poorly differentiated soft tissue sarcoma, subtype osteosarcoma (Q, 10x). Note the frequent mitotic figure founded in the 40 x magnification sections (R-S).

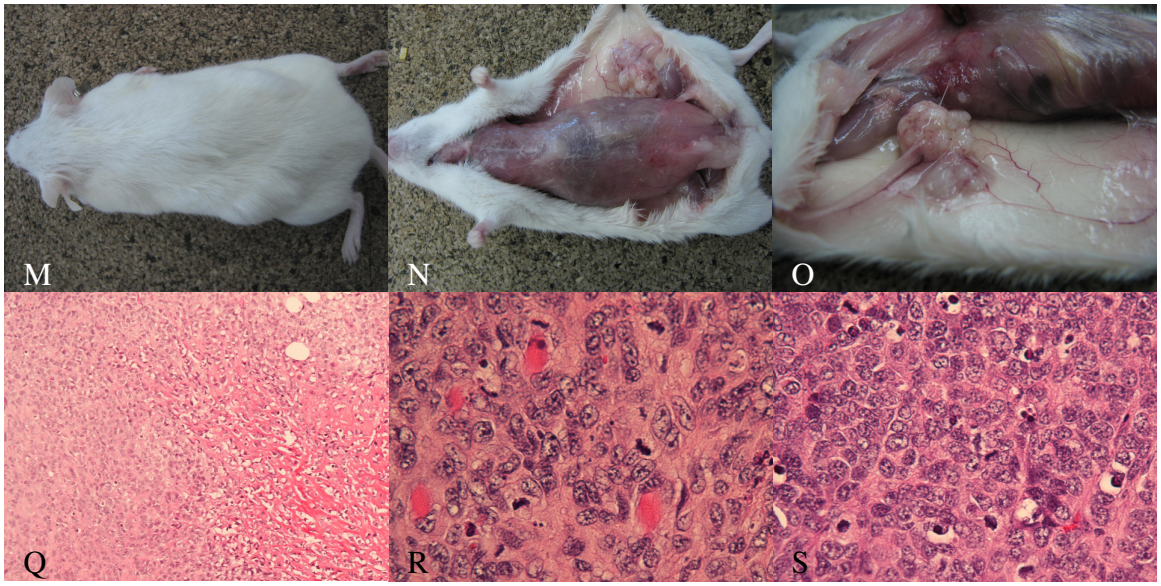

Figure 25: Gross and histopathological examinations from CAF-KIT-Dup2-xenografted immunodeficient mice. Animal shows noticeable tumor and jaundice symptom (F-T). Metastatic tumors are observable in abdominal cavity and organs (T-U). Figure V (10x) and W-X (40x) depict a poorly differentiated soft tissue sarcoma, subtype osteosarcoma).

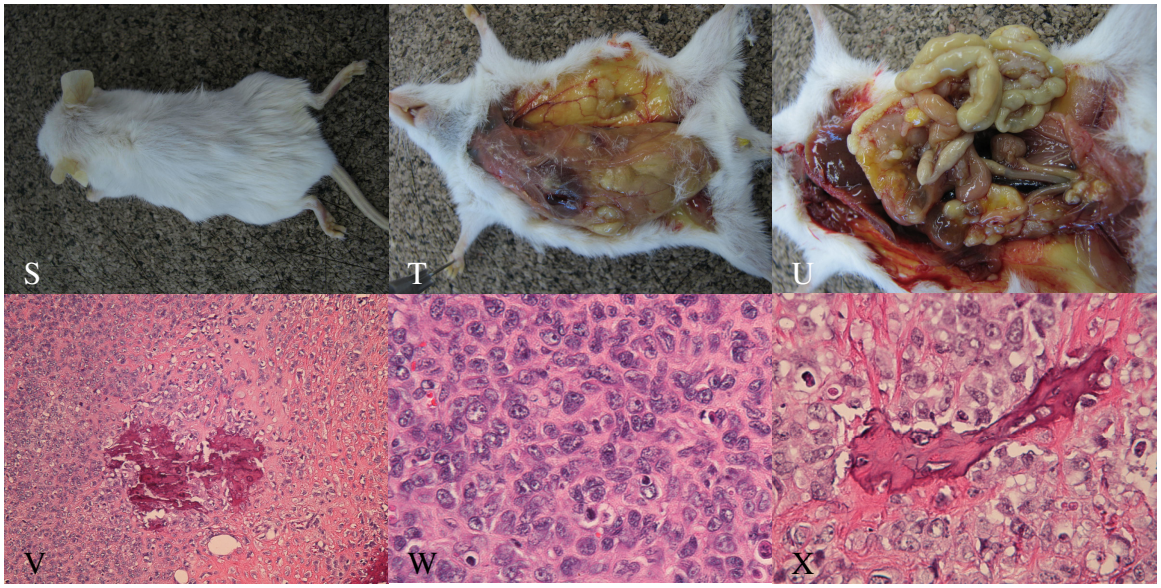

Re-cultured cell lines from randomly selected tumors were generated from the xenografts in order to analyze them in more detail and to determine whether their c-KIT expression, invasiveness and ploidy had been altered *in vivo*.

Quantitative real-time reverse transcriptase PCR results using total RNA extracted from tumors formed from all cell lines and normal fibroblast control show that expression of c-KIT in tumor cells formed from each cell line was elevated, compared with normal canine primary fibroblast. The relative expression level of c-KIT mRNA is shown in Table 9.

Table 9: Quantitative real-time RT-PCR on c-KIT mRNA expression, compared to C2 mast cell line. Data shown in fold change calibrated to canine primary fibroblast.

Primary fibroblast as a calibrator	**RQ average**	**RQ min**	**RQ max**
Fibroblast	1	0.4	2.2
Mouse Del2	5.2	3.3	8.0
Mouse Del3	2.1	N/A	N/A
Mouse Del9	40.4	26.7	61.0
Mouse Dup2	3.4	1.5	7.6
C2 MCT	36,990.7	26,253.9	52,118.4

Matrigel invasion assay also found that the invasiveness of all CAF-KIT-mutant cell lines was retained. Consistent with all CAF-KIT mutant cell lines before xenograft, tumor cells derived from CAF-KIT-Del2, CAF-KIT-Del9, and CAF-KIT-Dup2 show their high invasiveness behavior (Figure 26A, 26C, and 26D, respectively). More than 1,000 cells were able to penetrate through matrigel-mimicking basement membrane invasion. Interestingly, CAF-KIT-Del3-xenografted cells (Figure 26B) also reveal their low degree invasiveness, consistent with their behavior prior xenograft.

Figure 26: Matrigel invasion assay of re-established xenograft tumor cells. A, CAF-KIT-Del2 xenografted cells; B, CAF-KIT-Del3 xenografted cells; C, CAF-KIT-Del9 xenografted cells; D, CAF-KIT-Dup2 xenografted cells.

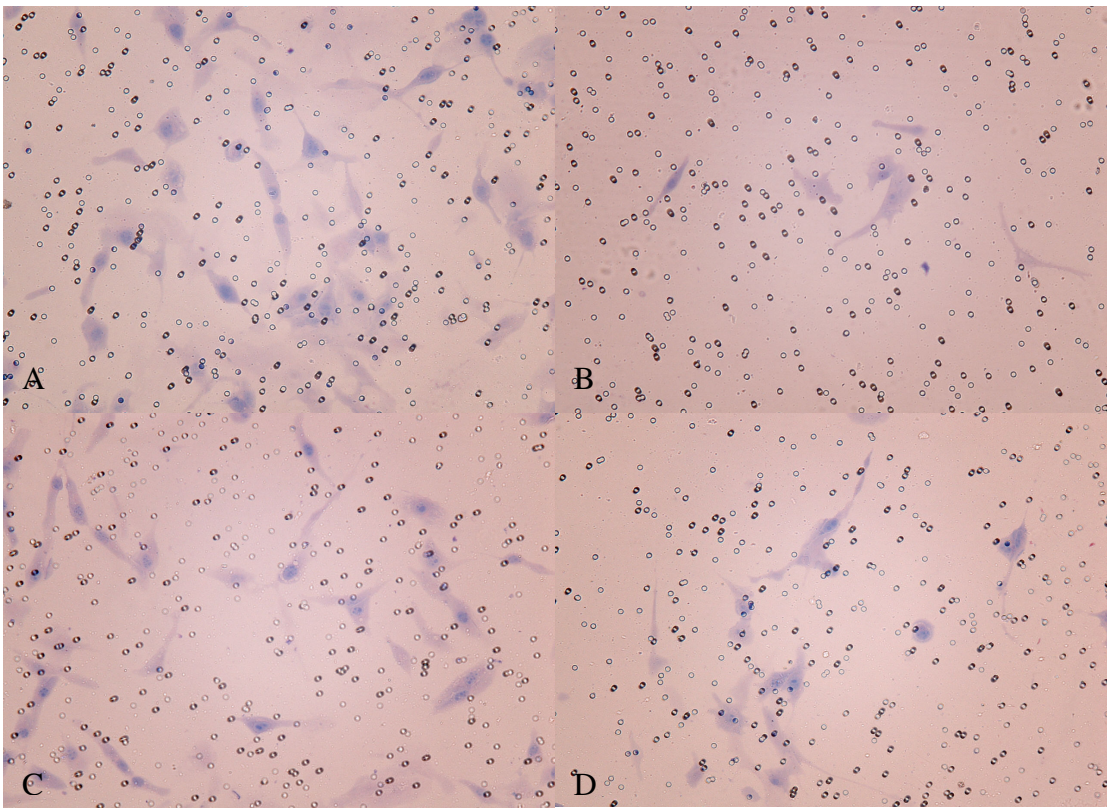

Metaphase spreads made from all of the re-established CAF-KIT mutant tumor cell lines demonstrate aneuploidy (Figure 27). Aneuploidy is also verified by karyotyping 12 metaphases from each of the tumor cell lines. The number of chromosomes in CAF-KIT-Del2 tumor cell line ranged from 106 to 122 chromosomes with a modal number of 116 chromosomes (Table 10). Tumor cells derived from CAF-KIT-Del9 and CAF-KIT-Dup2 also show their aneuploidy karyotypes, which ranged from 94-122 with a modal number of 110 and 106-116 with a modal number of 113, respectively. Interestingly, tumor cells derived from CAF-KIT-Del3 xenograft appear to harbor normal chromosome numbers. Chromosome loss and gain were also observed.

Figure 27: Karyotypes of tumor cells arise from the re-establised tumor cells of all CAF-KIT mutant cell lines showing aneuploidy. A, CAF-KIT-Del2 xenografted cells; B, CAF-KIT-Del3 xenografted cells; C, CAF-KIT-Del9 xenografted cells; D, CAF-KIT-Dup2 xenografted cells.

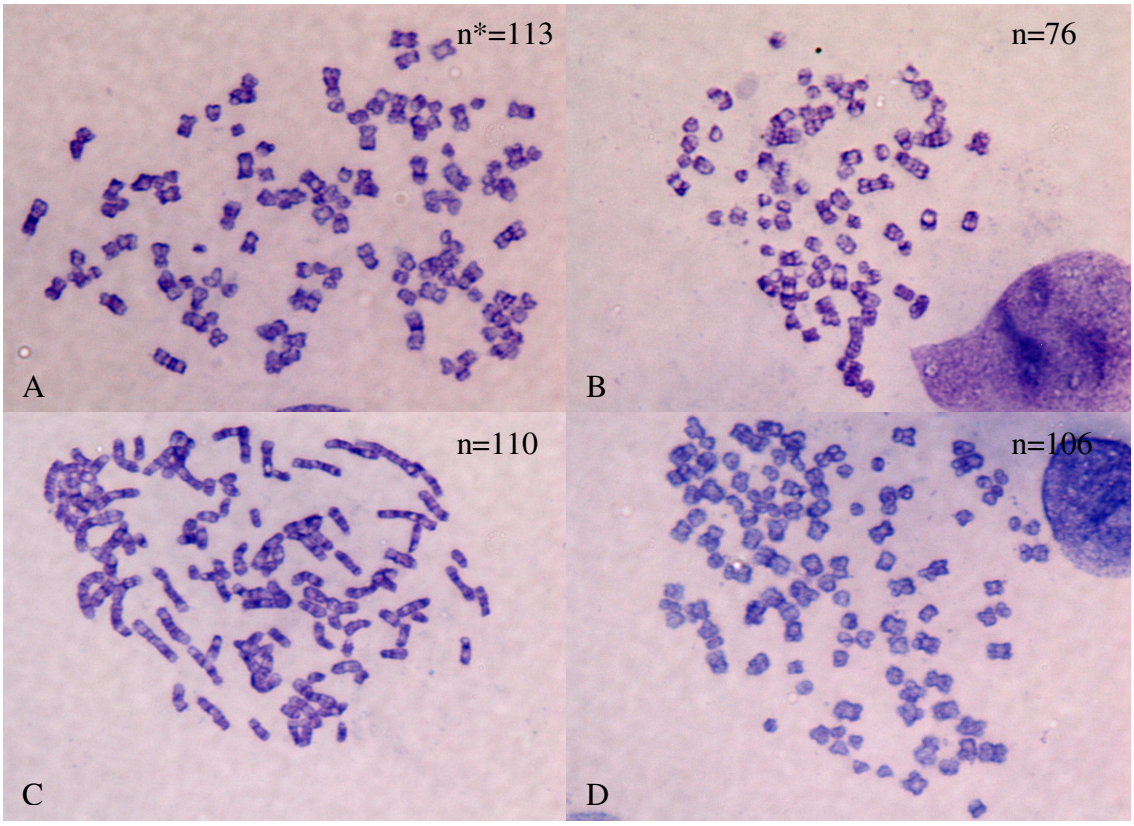

* The "n" represents number of chromosomes.

Table 10: Representative number of chromosomes-per-cell and a modal number of each re-established tumor cells.

	Mouse Del2	Mouse Del3	Mouse Del9	Mouse Dup2
Metaphase 1	117	82	116	108
Metaphase 2	106	78	114	115
Metaphase 3	111	75	110	108
Metaphase 4	112	94	111	113
Metaphase 5	107	84	122	114
Metaphase 6	120	78	104	114
Metaphase 7	122	86	105	115
Metaphase 8	116	82	94	116
Metaphase 9	116	78	110	106
Metaphase 10	118	144	98	111
Metaphase 11	112	76	112	113
Metaphase 12	116	78	109	113
Modal	116	78	110	113

Taken together, these data confirm that all CAF-KIT mutant tumor cell lines had maintained their properties in c-KIT expression, invasiveness, and ploidy after grafting cells in mice.

DISCUSSION

In human GISTs, canine GISTs, and canine mast cell tumors, c-KIT mutations have been mainly identified in the exon 11 juxtamembrane domain. It was initially reported by Reith et al., 1990 and subsequently reviewed by Blechman et al., 1993 that activation of the c-KIT receptor associated with gain-of-function mutations of c-KIT results in uncontrolled autophosphorylation of the c-KIT receptor with ligand-independent, constitutive signaling and, ultimately, autonomous proliferation of cells (Lev et al., 1994).

To address the role of these c-KIT mutants in the tumor formation *in vivo*, the oncogenic property of these mutant c-KIT transfected fibroblasts activated by juxtamembrane domain mutants was investigated. In the previous studies, it is clearly shown that the exon 11 c-KIT mutations ectopically expressed in canine primary fibroblasts can induce immortalization, malignant transformation, and chromosomal instability in vitro. When these cells were injected subcutaneously into NOD/SCID/gamma immunodeficient mice, soft tissue sarcomas arose in all mice (100%) of all CAF-KIT mutant cell lines. In addition, mice injected with CAF-KIT-Del2 and CAF-KIT-Dup2 developed metastatic disease. These results are in line with the *in vitro* observations that show CAF-KIT-Del2 and CAF-KIT-Dup2 are anchorage-independent, capable of growing in low density and low serum, fast migrated quickly, and are highly invasive. It is worth mentioning that cell type also represents an important factor influencing c-KIT mutation induced-transformation and the development of soft tissue sarcoma *in vivo*. The introduction of c-KIT mutant isoforms into skin-derived normal fibroblasts could contribute to the reprogramming of fibroblasts into tumorigenically mesenchymal cells, which can derive to various cell types. A series of soft tissue sarcoma subtypes formed in vivo are osteosarcoma and fibrosarcoma.

To provide more detail in the tumorigenicity of CAF-KIT mutant cell lines, cells from the resultant tumors were recultured to determine whether the changes in their cellular behavior were observed in the parental CAF-KIT mutant cell lines or in their recultured cells isolated from tumors. Parental CAF-KIT-Dup2 cell lines and recultured CAF-KIT-Del3 and CAF-KIT-Dup2 tumor cells were found to exhibit similar biological properties in vitro, including equivalent invasiveness and chromosomal instability status. In contrast, recultured CAF-KIT-Del2 and CAF-KIT-Del9 tumor cells showed a dramatic increase in their invasiveness properties *in vitro*. Consistent with *in vivo* studies, CAF-KIT-Del2 also produced more tumor metastases. Even though recultured CAF-KIT-Del9 also showed elevated invasiveness, parental CAF-KIT-Del9 cell lines were unable to grow in low serum, which possibly reflects their lack of ability to grow in low nutrient areas such as metastatic sites. Interestingly, recultured tumor cells from CAF-KIT-Del3 mice showed lesser degrees of aneuploidy. A plausible explanation can be offered. These changes may come from the influence of host stromal factors. It is likely that the alteration in the cellular and molecular properties is emerging from each cell passage in *in vivo* due to an adaptation in the new microenvironment. Another possibility is that the heterogeneity of tumor cells in the *in vivo* environment selects the rare subpopulation that begins to dominate the xenograft tumor. Potentially consistent with this latter model, several other cancer cell lines are also contained in this rare subpopulation called “side-populations (SP)”. The results also show that the SPs are largely responsible for malignancy *in vivo* (Kondo et al., 2004; Hirschmann-Jax et al., 2004; Jessani et al., 205)

Taken together, the current studies demonstrate that c-KIT mutations ectopically expressed in canine primary fibroblasts contribute to the highly tumorigenic and metastatic phenotype in immunodeficient mice.

REFERENCES

REFERENCES

1. Blechman JM, Lev S, Givol D, Yarden Y. Structure-function analyses of the kit receptor for the steel factor. Stem Cells. 1993 Jul;11 Suppl 2:12-21.

2. Bodemer C, Hermine O, Palmérini F, Yang Y, Grandpeix-Guyodo C, Leventhal PS, Hadj-Rabia S, Nasca L, Georgin-Lavialle S, Cohen-Akenine A, Launay JM, Barete S, Feger F, Arock M, Catteau B, Sans B, Stalder JF, Skowron F, Thomas L, Lorette G, Plantin P, Bordigoni P, Lortholary O, de Prost Y, Moussy A, Sobol H, Dubreuil P. Pediatric mastocytosis is a clonal disease associated with D816V and other activating c-KIT mutations. J Invest Dermatol. 2010 Mar;130(3):804-15.

3. Chan GL, Little JB. Correlation of in vitro transformation with in vivo tumorigenicity in 10T1/2 mouse cells exposed to UV light. Br J Cancer. 1979 May;39(5):590-3.

4. Cohen PS, Chan JP, Lipkunskaya M, Biedler JL, Seeger RC. Expression of stem cell factor and c-kit in human neuroblastoma. The Children's Cancer Group. Blood. 1994 Nov 15;84(10):3465-72.

5. DiMayorca, G., Greenblatt, M., Trauthen, T., Soller, A., and Giordano, R. Malignant Transformation of BHK2 Clone 13 Cells in vitro by Nitrosamines-A Conditional State. Proc. NatI. Acad. Sci. U. S., 70: 46-49, 1973.

6. Euhus DM, Hudd C, LaRegina MC, Johnson FE. Tumor measurement in the nude mouse.J Surg Oncol 1986, 31:229-234.

7. Faderl S, Talpaz M, Estrov Z, O'Brien S, Kurzrock R, Kantarjian HM. The biology of chronic myeloid leukemia. N Engl J Med. 1999 Jul 15;341(3):164-72.

8. Freedman, V. H., and Shin, S. Cellular Tumorigenicity in Nude Mice: Correlation with Cell Growth in Semi-Solid Medium. Cell 1974, 3: 355-359.

9. Furitsu, T., Tsujimura, T., Tono, T., Ikeda, H., Kitayama, H., Koshimizu, U., Sugahara, H., Butterfield, J. H., Ashman, L. K., Kanayama, Y., et al. (1993) Identification of mutations in the coding sequence of the proto-oncogene c-kit in a human mast cell leukemia cell line causing ligand-independent activation of c-kit product. J. Clin. Invest. 92, 1736–1744.

10. Gregory-Bryson E, Bartlett E, Kiupel M, Hayes S, Yuzbasiyan-Gurkan V. Canine and human gastrointestinal stromal tumors display similar mutations in c-KIT exon 11. BMC Cancer. 2010 Oct 15;10:559.

11. Heinrich MC, Rubin BP, Longley BJ, Fletcher JA. Biology and genetic aspects of gastrointestinal stromal tumors: KIT activation and cytogenetic alterations. Hum Pathol. 2002 May;33(5):484-95.

12. Hirschmann-Jax C, Foster AE, Wulf GG, Nuchtern JG, Jax TW, Gobel U, Goodell MA, Brenner MK. A distinct "side population" of cells with high drug efflux capacity in human tumor cells. Proc Natl Acad Sci U S A. 2004 Sep 28;101(39):14228-33.
13. Jessani N, Niessen S, Mueller BM, Cravatt BF. Breast cancer cell lines grown in vivo: what goes in isn't always the same as what comes out. Cell Cycle. 2005 Feb;4(2):253-5.

14. Kitayama H, Kanakura Y, Furitsu T, Tsujimura T, Oritani K, Ikeda H, Sugahara H, Mitsui H, Kanayama Y, Kitamura Y, et al. Constitutively activating mutations of c-kit receptor tyrosine kinase confer factor-independent growth and tumorigenicity of factor-dependent hematopoietic cell lines. Blood. 1995 Feb 1;85(3):790-8.

15. Kitayama H, Tsujimura T, Matsumura I, Oritani K, Ikeda H, Ishikawa J, Okabe M, Suzuki M, Yamamura K, Matsuzawa Y, Kitamura Y, Kanakura Y. Neoplastic transformation of normal hematopoietic cells by constitutively activating mutations of c-kit receptor tyrosine kinase. Blood. 1996 Aug 1;88(3):995-1004.

16. Ko CD, Kim JS, Ko BG, Son BH, Kang HJ, Yoon HS, Cho EY, Gong G, Ahn SH. The meaning of the c-kit proto-oncogene product in malignant transformation in human mammary epithelium. Clin Exp Metastasis. 2003;20(7):593-7.

17. Kondo T, Setoguchi T, Taga T. Persistence of a small subpopulation of cancer stem-like cells in the C6 glioma cell line. Proc Natl Acad Sci U S A. 2004 Jan 20;101(3):781-6.

18. Krystal GW, Hines SJ, Organ CP. Autocrine growth of small cell lung cancer mediated by coexpression of c-kit and stem cell factor. Cancer Res. 1996 Jan 15;56(2):370-6.

19. Lefevre G, Glotin AL, Calipel A, Mouriaux F, Tran T, Kherrouche Z, Maurage CA, Auclair C, Mascarelli F. Roles of stem cell factor/c-Kit and effects of Glivec/STI571 in human uveal melanoma cell tumorigenesis. J Biol Chem. 2004 Jul 23;279(30):31769-79.

20. Lev S, Blechman JM, Givol D, Yarden Y. Steel factor and c-kit protooncogene: genetic lessons in signal transduction. Crit Rev Oncog. 1994;5(2-3):141-68.

21. Liang R, Wallace AR, Schadendorf D, Rubin BP. The phosphatidyl inositol 3-kinase pathway is central to the pathogenesis of Kit-activated melanoma. Pigment Cell Melanoma Res. 2011 Aug;24(4):714-23.

22. Longley BJ Jr, Metcalfe DD, Tharp M, Wang X, Tyrrell L, Lu SZ, Heitjan D, Ma Y. Activating and dominant inactivating c-KIT catalytic domain mutations in distinct clinical forms of human mastocytosis. Proc Natl Acad Sci U S A. 1999 Feb 16;96(4):1609-14.

23. Lux ML, Rubin BP, Biase TL, Chen CJ, Maclure T, Demetri G, Xiao S, Singer S, Fletcher CD, Fletcher JA. KIT extracellular and kinase domain mutations in gastrointestinal stromal tumors. Am J Pathol. 2000 Mar;156(3):791-5.

24. Matsuda R, Takahashi T, Nakamura S, Sekido Y, Nishida K, Seto M, Seito T, Sugiura T, Ariyoshi Y, Takahashi T, et al. Expression of the c-kit protein in human solid tumors and in corresponding fetal and adult normal tissues. Am J Pathol. 1993 Jan;142(1):339-46.

25. Reith AD, Rottapel R, Giddens E, Brady C, Forrester L, Bernstein A. W mutant mice with mild or severe developmental defects contain distinct point mutations in the kinase domain of the c-kit receptor. Genes Dev. 1990 Mar;4(3):390-400.

26. Shields R. (1976) Transformation and tumorigenicity. Nature, 262, 348.

27. Stiles CD, Desmond W, Chuman LM, Sato G, Saier MH Jr. Relationship of cell growth behavior in vitro to tumorigenicity in athymic nude mice. Cancer Res. 1976 Sep;36(9 pt.1):3300-5.

28. Tian Q, Frierson HF Jr, Krystal GW, Moskaluk CA. Activating c-kit gene mutations in human germ cell tumors. Am J Pathol. 1999 Jun;154(6):1643-7.

29. Zemke D, Yamini B, Yuzbasiyan-Gurkan V. Mutations in the juxtamembrane domain of c-KIT are associated with higher grade mast cell tumors in dogs. Vet Pathol. 2002 Sep;39(5):529-35.

CHAPTER 6

C-KIT MUTATIONS-DRIVEN CELLULAR TRNASFORMATION IN A HUMAN MODEL

ABSTRACT

c-KIT is a type III membrane receptor tyrosine kinase which is expressed on a variety of cells including hematopoietic progenitor cells, interstitial cells of Cajal and mast cells. Activating c-KIT mutations are found in a variety of cancers, including human mastocytosis, gastrointestinal tumors (GISTs) in humans and dogs, and mast cell tumors in both dogs and cats, and activating mutations generally correlate with poor prognosis. However, the significance of the mutation in driving the tumorigenic process has not been completely clarified. In the canine primary fibroblast context, ectopic expression of c-KIT mutant isoforms caused the malignant transformation and soft tissue sarcoma in immunodeficient mice. In this study, the retroviral vectors carrying c-KIT mutations observed in human GISTs, canine GISTs, and canine mast cell tumors were transduced into human primary fibroblasts. Functional consequences derived from ectopic expression were examined. Results showed that mutations identified in GISTs can lead to extended lifespan and immortalization, whereas cells transduced with duplication mutations reported uniquely in canine mast cell tumors resulted in premature senescence. However, none of these mutations is sufficient for neoplastic transformation. The findings suggest that additional genetic alteration(s) may be required for c-KIT driven tumorigenesis.

INTRODUCTION

Normal human cells have a limited lifespan in vitro (Wagner et al., 2008). After a certain number of cell divisions, cells enter senescence, which is morphologically characterized by enlarged and irregular cell shapes and ultimately a halt in proliferation, termed the Hayflick limit (Hayflick, 1965). There are several protective processes that prevent neoplastic transformation (Hahn and Weinberg, 2002). One important process preventing tumorigenic transformation is replicative senescence (Campisi, 2003). Even though human cells that have occasionally bypassed senescence exhibit an extended lifespan in culture, they remain non-tumorigenic *in vivo* (Hahn, 2002; Rubin, 2002). Moreover, these cells may eventually cease proliferation, due to the activation of a second proliferative barrier called 'crisis' (Mason et al., 2006).

Tumorigenesis is a multistep process in which a series of genetic and epigenetic events leads to the emergence of cells that have escaped normal growth control mechanisms (Vogelstein and Kinzler, 2004). To override the protective mechanism, multiple further genetic alterations are required in human cells in order to initiate immortalization and neoplastic transformation. Immortalization (senescence bypass) is a critical rate-limiting step in the malignant transformation of mammalian somatic cells. Human cells must escape at least two distinct senescence barriers to permit unfettered clonal evolution during cancer development: (1) stress- or oncogene-induced premature senescence (SIPS/OIS), mediated via the p16-Rb and/or ARF-p53-p21 tumour-suppressive pathways (Larrson, 2011), and (2) replicative senescence triggered by telomere shortening (Yasaei et al., 2012). Consequently, overexpression of the catalytic subunit of human telomerase, hTERT, can cooperate with SV40 T antigens and oncogenic Ras to cause neoplastic transformation of normal human cells (Hahn et al., 1999, Elenbaas et al., 2001). On the other hand, telomerase-independent mechanisms also exist. For

instance, the combined expression of three oncogenes, adenovirus E1A, H-RasV12, and Mdm2, is sufficient to convert a normal human cell into a cancer cell in the absence of telomerase (Seger et al., 2002).

In the previous chapter, a single mutant oncogene, c-KIT, was introduced into canine primary fibroblasts, followed by the *in vitro* neoplastic transformation studies and the *in vivo* tumorigenic property analysis. The results showed that canine primary fibroblasts can be tumorigenically transformed by a single mutant c-KIT oncogene resulting in a loss of contact inhibition, anchorage-independent growth, immortalization, and tumor formation in immunodeficient mice.

Gain-of-function mutations in c-KIT receptor in humans are associated with gastrointestinal stromal tumors, systemic mastocytosis, melanoma, and acute myelogenous leukemia (Hirota et al., 1998; Longley et al., 2001; Nagata et al., 1995; Willmore-Payne et al., 2005). Stable transfection of the mutant c-kit complementary DNAs induced malignant transformation of Ba/F3 murine lymphoid cells, suggesting that the mutations contribute to tumor development (Hirota et al., 1998).

Studies of human primary fibroblasts have played an important role in the elucidation of the molecular mechanisms underlying cellular immortalization, transformation, and tumorigenesis in human cancer. In this chapter, methods for analysis of cellular immortalization, as well as transformation of human primary fibroblast cells using a series of mutant c-KIToncogenic retroviruses are provided. This is followed by protocols for karyotype analysis, cell invasiveness, and tumor formation of mutant c-KIT transduced fibroblasts in immunodeficient mice.

MATERIALS AND METHODS

Cell culture

Human normal primary dermal fibroblasts were purchased from the American Type Culture Collection (ATCC, catalog number: PCS-201-010) and cultured under recommended conditions in DMEM medium supplemented with 10% fetal bovine serum, L-glutamine, non-essential amino acid, sodium pyruvate, and penicilin/streptomycin (refered to as complete medium) at 37ºC and 5% CO2. These cells were obtained from neonatal foreskin and are negative for pathogens including Hepatitis B, Hepatitis-C, HIV-1. The complete medium was changed twice a week.

Production of retroviral vectors containing the c-KIT gene

Full-length human c-KIT cDNA in pBlueScript-human KIT (Origene) was purchased and transformed into the TOP10 *Escherichia* coli strain (Invitrogen). Plasmid DNA was isolated and purified from 5 ml of an overnight culture using the Miniprep DNA Purification System (Qiagen), and used as template for PCR amplification. Full-length human wild type (wt) c-KIT cDNA was amplified by PCR using iProof™ High-Fidelity DNA Polymerase (Biorad). The following primers were used: the human wt KIT forward 5′- CTG GCC GCC TGG GCC CAT GAG AGG CGC TCG CGG CGC CT and reverse 5′- CTT TGG ATC CTC AGA CAT CGT CGT GCA CAA GCA GA, the human wt KIT-YFP forward 5′- AGC TTT GAT ATC AAA TGA GAG GCG CTC GCG G and reverse 5′- CCA TCG ATT CAG ACA TCG TCG TGC ACA AGC. The PCR amplification consisted of 1 cycle at 98°C for 30 seconds, 35 cycles at 98°C for 10 seconds, 72°C for 30 seconds, and 72°C for 45 seconds; and 1 cycle at 72°C for 10 minutes for a final extension. The PCR products were separated by electrophoresis using a 0.8% (w/v) agarose gel, stained in ethidium bromide (Sigma-Aldrich) and visualized on a UV

transluminator. Then PCR fragments were digested with SfiI and BamHI or EcoRV and ClaI, purified by QIAquick PCR Purification Kits (Qiagen) according to the manufacturer's protocol. The retroviral vector, pHIT derived from Moloney murine leukemia virus (MMLV) was kindly provided by Dr. Steven Suhr, Michigan State University (Suhr et al., 2001). This replication-defective pHIT vector contains a Tet-off system, a hygromycin resistance gene, and an internal ribosome entry site (IRES). The expression of the transgene was driven by tet-O-CMV promoter in the absent of doxycyclin. The plasmid pHIT-YFP was modified by incorporation of Yellow Fluorescence Protin (YFP) in the plasmid provided by Dr. Manish Neupane (Harvard University). To generate pHIT-wild type KIT, the purified PCR products were ligated to pHIT-YFP plasmids digested by Sfi and BamHI restriction enzymes.

The wild type c-KIT and YFP expressing vector (pHIT- wt KIT-YFP) was also constructed by ligation of full length human c-KIT with pHIT-YFP vector digested by PmeI and ClaI restriction enzymes. The pHIT-wt KIT and pHIT-wt KIT-YFP plasmid vectors were transformed into the competent *E. coli* DH5α bacteria. After ampicillin selection, plasmid DNA was isolated with the IsoPure™ Plasmid Maxi II Prep Kit according to the manufacturers' protocol (Denville Scientific, Inc.). The constructs were then verified by restriction enzyme digestion and sequencing.

Figure 28: Diagram of the pHIT tetracycline (tet)-regulatable retroviral vector used to generate cells expressing human c-KIT. The viral LTR transcribes a bicistronic mRNA that, in the presence of an IRES (internal ribosomal entry site) element is translated into two proteins: tTA (tet repressor-VP16 fusion gene) and hygromycin resistance protein (Hygro). In the absence of tetracycline (-tet), tTA binds to the tetO sequence and activates a tetracycline operator sequence (tetO) fused to the human cytomegalovirus (CMV) minimal promoter, thus resulting in expression of c-KIT. In the presence of tet (+tet), tTA cannot bind to the tetO sequences, and expression of c-KIT mRNA ceases.

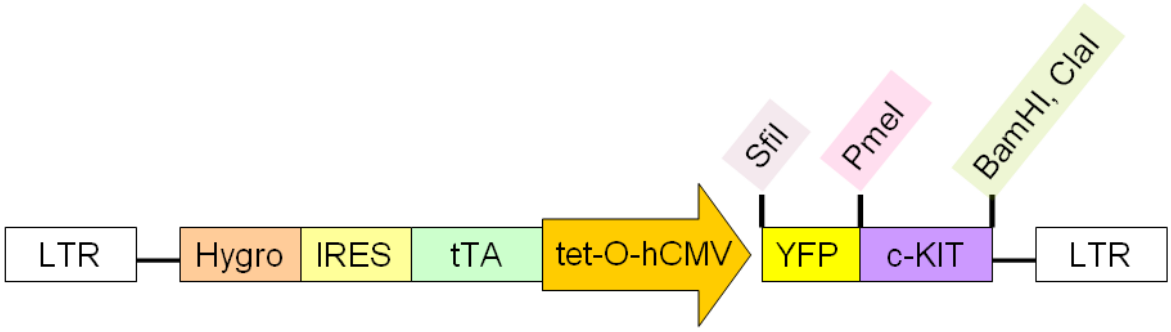

Production of pHIT-mutant KIT plasmids

Six different c-KIT mutant isoforms, including three distinct deletion and three distinct internal tandem duplication mutations within exon 11 (Zemke et al., 2002), were studied. The pHIT-wt KIT and pHIT-wt KIT-YFP plasmids were used as templates for mutagenesis. The deletion mutants were constructed using the QuikChange Site-Directed Mutagenesis (Stratagene) according to the manufacturer's instructions, whereas duplication mutants were constructed by the PCR-based megaprimer method. Megaprimer amplification was performed in two steps. The first step was to generate the duplication megaprimer (171 base pairs DNA fragments) amplified with the following primers: VYG1296 5'-CCA TGT ATG AAG TAC AGT GGA AG-3' and VYG1564 5'-CAA AGC TCA GCC TGT TTC TGG-3'. The PCR products were purified using

a QIAquick PCR Purification kit (Qiagen), and used as primer for the second step. Then, megaprimer PCR was performed with 200 ng of the purified PCR products from the first step and iProof™ High Fidelity DNA Polymerase kit (Biorad). Thermal cycle conditions were: 1 cycle of 98 °C for 30 seconds, 40 cycles of 98 °C for 10 seconds, 72 °C for 30 seconds, 72 °C for 3.5 minutes, followed by 72 °C for 10 min. Following the mutagenesis, the plasmid DNA was transformed into XL10-Gold® ultracompetent cells (Agilent Technologies) following the manufacturer's instructions. Maxi scale preparation of the plasmids were extracted by the IsoPure™ Plasmid Maxi II Prep Kit (Denville Scientifi,c Inc.) and named as pHIT-Del2, pHIT-Del3, pHIT-Del9, pHIT-Dup1, pHIT-Dup2, pHIT-Dup5, pHIT-Del2-YFP, pHIT-Del3-YFP, pHIT-Del9-YFP, pHIT-Dup1-YFP, pHIT-Dup2-YFP, and pHIT-Dup5-YFP. The constructs were then verified by restriction enzyme digestion.

Figure 29: Scheme of c-KIT mutations used in this study. Three different deletion mutations were located at codon 560-562 (Deletion 2), codon 559-561 (Deletion 3), and codon 560-561 (Deletion 9), resulting in the deletion of 2 amino acids. Three different duplication mutations were characterized by 15-16 amino acids-repeating codon, involved at codon 575-591. All mutations are in-frame mutation.

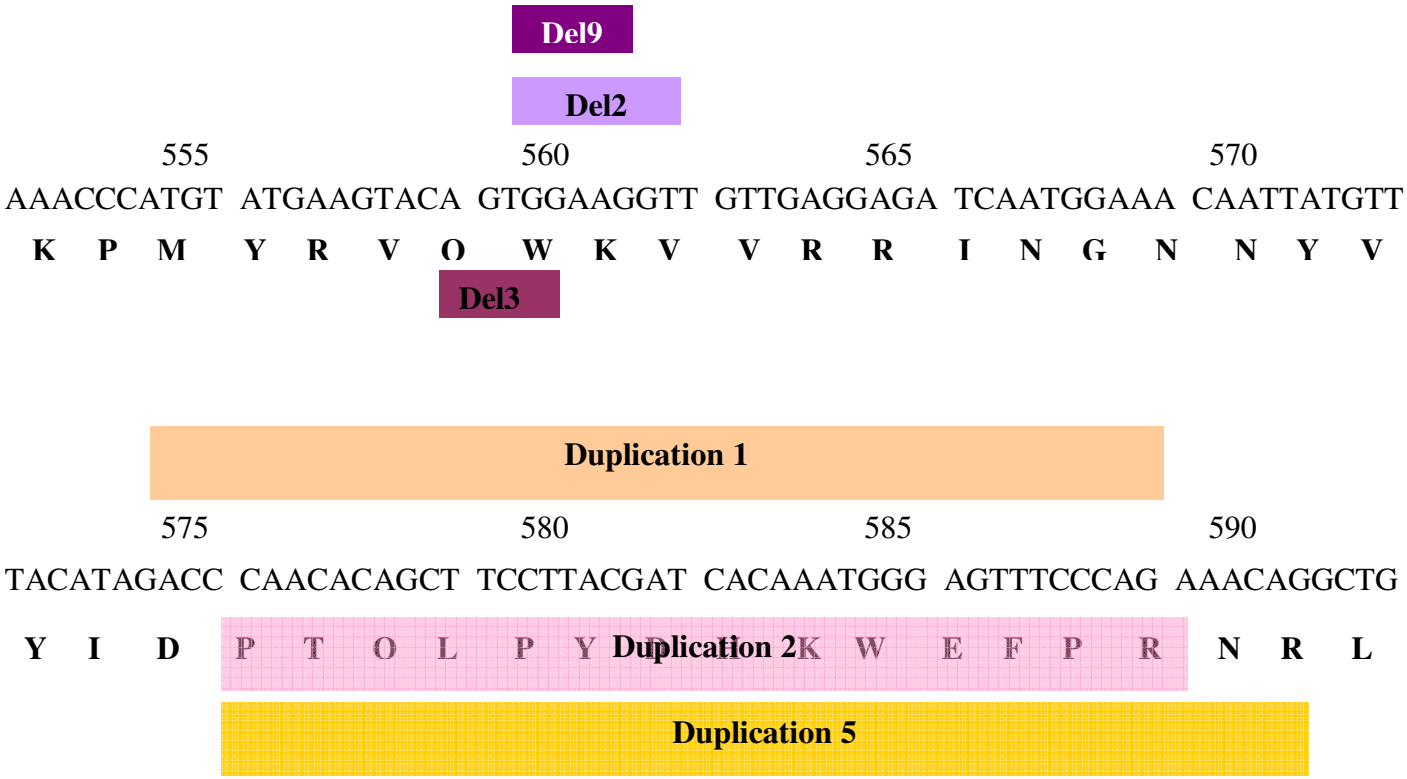

Production of retrovirus

For retrovirus production, $1.5x10^6$ cells of HEK293FT cell line were plated in 10 cm dishes. Cells were cultured in DMEM (Invitrogen) supplemented with 10% FBS and incubated overnight at 37 °C with 5% CO_2. The next morning, cells were grown to 50-70% confluence. A combination of 12 micrograms (μg) of constructed pHIT containing transgene (either pHIT-wt KIT, pHIT-wt KIT-YFP, pHIT-Del2, pHIT-Del3, pHIT-Del9, pHIT-Dup1, pHIT-Dup2, pHIT-Dup5, pHIT-Del2-YFP, pHIT-Del3-YFP, pHIT-Del9-YFP, pHIT-Dup1-YFP, pHIT-Dup2-YFP, or pHIT-Dup5-YFP), 6 μg of the VSV-G plasmid, and 6 μg of the gag-pol plasmid (kindly provided by Dr. Steven Suhr, Michigan State University) was prepared in 150 μl distilled water. Then 25 μl of 2M calcium chloride and 125 μl of 2x HEPES ((4-(2-hydroxyethyl)-1-piperazineethanesulfonic acid) Buffered Saline (HEBS) were added slowly to obtain the transfection mixture. Transfection was by calcium-chloride precipitation (Chen and Okayama, 1987). Transfection mixture was adding drop wise to the plate of HEK293FT cells. Medium was changed with fresh complete medium after overnight incubation. Starting at 40 hours after changing medium, virus supernatant was harvested every ten hours at 40, 50, 60, and 70 hours. Medium was collected, centrifuged at 2000 rpm for 5 minutes, and passed through a 0.45-μm filter (Nalgene), and the viral supernatant was frozen at −80 °C. Virus from pHIT and pHIT-YFP was also produced and served as the control.

Viral transduction with viral supernatant

Human normal dermal fibroblasts were plated in 60 mm cell culture plate and grown until reaching 40-50% confluence (day 0). The next morning (day 1), 5 ml of viral supernatant with 8 μg/ml polybrene (Santa Cruz Biotechnology) was added into the plate and incubated at 37ºC in 5% CO_2 incubator. In the evening, cells received the second round of transduction by removing

the virus containing medium and adding 5 ml of fresh viral supernatant with 8 μg/ml polybrene. The third and forth round of transduction were done in the morning and evening of day 2, respectively. In the morning of day 3, cells were fed with fresh complete medium. Each viral supernatant was transduced with human normal fibroblasts. In the morning of day 4, transduced cells were passaged at 1:10, and 100 μg/ml of hygromycin (Sigma) was added into the culture media for 10 days for the stable transduction. Colonies of hygromycin-resistant cells were separately isolated by using Cloning Cylinders (Corning), and expanded in the hygromycin containing complete medium.

RNA Isolation and transgene mRNA detection

Total RNA from expanded hygromycin-resistant cells was isolated with Acid-Phenol:Chloroform (Ambion) and the mirVana™ miRNA Isolation Kit (Ambion) according to the instructions of the manufacturer. Three micrograms of total RNA was treated with TURBO DNA-free™ (Ambion) to remove contaminating DNA. First-strand cDNA synthesis was performed using SuperScript III Reverse Transcriptase (Invitrogen) with random hexamers (Promega). cDNA was then column-purified by using a QIAquick PCR Purification Kit (QIAGEN), and eluted with distilled nuclease-free water at the concentration of 50 ng/μl. PCR was performed as follows: initial denaturation at 94°C for 4 min, 40 cycles at 94°C for 1 minute, and 58°C for 1 minute, 72°C for 1 minute, and a final extension at 72°C for 5 minutes. The primer sequences were as follows: c-KIT forward primer: 5'-ACC ACC ATT CTG TGC GGA TC-3' ; c-KIT reverse primer: 5'-CCT ACA GGT GGG GTC TTT CAT TC-3' ; Beta-2-microglobulin (β2MG) forward primer: 5'-CCA GCA GAG AAT GGA AAG-3'; βMG reverse primer: 5'-CCA GTC CTT GCT GAA AGA CA-3'. The expected sizes of products were 152 bp

for c-KIT and 141 bp for β2MG. The PCR products were separated on a 2% agarose gel, stained in ethidium bromide, and visualized on a UV transilluminator.

Quantitative real-time PCR using SYBR Green (Applid Biosystems) for amplification of c-KIT was also performed using a StepOnePlus™ Real-Time PCR Systems instrument (Applied Biosystems). Conditions for amplification were as follows: 1 cycle at 95°C for 10 min, 40 cycles at 95°C for 30 seconds, 62°C for 1 minute, 72°C for 30 seconds, 1 cycle at 95°C for 1 minute, then 62°C for 30 seconds and 95°C for 30 seconds. All analyses were done in quadruplicate, and the mean was used for further calculations. The baseline was set automatically by the StepOnePlus software, and the threshold Ct (threshold cycle)was defined as the number of cycles in which the fluorescence exceeded the automatically set threshold. After the reaction, c-KIT mRNA expression was normalized by the expression of β2MG. The mRNA relative quantitation was done using the ΔCt method. The difference (ΔCt) between the average of c-KIT and the housekeeping gene (β2MG) was calculated. Fold changes in c-KIT expression of each CAF-KIT cell line as compared to primary canine fibroblasts were calculated using the delta-delta Ct (ΔΔCt) method using β2MG as the normalization control.

Immunohistochemistry

Transduced cells were trypsinized by 0.025% trypsin-EDTA (Invitrogen) and centrifuged at 1200 rpm for 10 minutes. The cell pellet was fixed in 10% neutral buffered formaldehyde, and paraffin-embedded. Sections of formalin-fixed paraffin embedded (FFPE) material from cell pellet at 5 μm were deparaffinized in xylene and rehydrated in a graded series of ethanol to distilled water. Antigen retrieval step was done in antigen retrieval solution in a steamer (Black & Decker) for 20 minutes, and endogenous peroxidases treatment was performed with 3% hydrogen peroxide for 5 minutes followed by rinsing for 5 minutes in distilled water. Protein-

blocking agent (Dako) was used for non-specific binding prevention. Then, sections were placed in autostainer and incubated with rabbit anti-human c-kit antibody (Dako) at dilutions of 1:300 for 30 minutes. Subsequently, sections were incubated with biotinylated secondary antibody (LSAB, Dakocytomation) for 30 min, washed in PBS, and incubated with streptavidin-peroxidase conjugate (LSAB, Dakocytomation) for 30 min. Finally, the reaction was developed using 3,3′-diaminobenzidine substrate (Dako). Slides were counterstained in hematoxylin and dehydrated, and cover slips added. Control slides were run simultaneously. Confirmed canine MCTs cases were used as a positive control whereas slides stained without primary antibody served as negative control.

Matrigel invasion assay

Cell invasiveness of transduced cells from tumors was evaluated using Matrigel-coated semipermeable-modified Boyden inserts. BioCoat Growth Factor-Reduced Matrigel invasion chambers (24-well cell culture inserts containing an 8.0-µm PET membrane with a uniform layer of Matrigel matrix; BD) were used to assess cell invasion following the manufacturer's instructions. After determination of cell count and viability in a hemocytometer by the trypan blue exclusion test, cells resuspended in DMEM with L-glutamine, penicillin/streptomicin were added to the upper compartment of the chamber (2.5 × 105 cells/chamber). DMEM supplemented with 10% FBS was placed in the bottom well, with 10% FBS providing the chemo-attractants. Incubation was carried out for 20 hours at 37 °C in humidified air with 5% CO_2. The cells on the insert were removed by wiping gently with a cotton swab. Cells on the reverse side of the front of the insert were fixed and stained with DiffQuick according to the manufacturer's instructions and mounted on glass slides. The total number of cells that crossed

the membrane were counted under a light microscope and the average value was calculated. Experiments were performed with three chambers per cell line.

Chromosomal instability study

Double synchronization method was applied for metaphase preparation. Transduced cells were plated into 10 cm cell culture plate until 50-70% confluency of each cell line was reached. In day 1, 0.5 µg/ml methotrexate was added in the complete medium and incubated overnight at 37 °C in a 5% CO_2 incubator. Next morning, cells were washed three times with DPBS and fed with fresh medium containing 10 µg/ml thymidine (Sigma) for 5 hours. In the evening of day 1, cells were washed three times and fed with fresh complete medium for overnight. On the morning of day 2, colcemid (Karyomax, Invitrogen) was added to a final concentration of 0.04 mg/mL for 2 hours before harvesting. Cells were trypsinized and harvested to produce metaphase preparations. After harvesting, the cells were exposed to hypotonic solution (75 mM potassium chloride) and fixed with acetic acid/methanol (1:3). The slides of each tumor cell line were prepared and stained using Leishman's staining. Karyotype analysis was performed by a computerized acquisition and analysis system (Cytovision, Applied Spectral Imaging). The numbers of chromosomes per cell from ten metaphases of all cell lines were analyzed for chromosomal numerical abnormalities.

Western blot analysis

Cell lysates were prepared by extracting proteins with RIPA buffer (Thermo Scientific) supplemented with Protease Inhibitor Cocktail (Sigma) following the manufacturer's instructions. Lysates were then centrifuged at 14,000 rpm for 15 minutes, and the supernatant was collected. Protein quantification was accomplished by the Bradford assay (Biorad). Four dilutions of bovine serum albumin were used to establish the standard curve. Briefly, total

volume of 800 µl of each standard and diluted cell lysate was used and mixed with 200 µl of Bradford dye reagent. Each mixture was incubated at room temperature for 5 minutes, and the absorbance at 595 nm was measured. Western blotting was performed by loading 3 µg of protein on an 8% sodium dodecyl sulfate polyacrylamide gel and separating proteins by electrophoresis, then transferred to Immobilon®-FL PVDF membranes (Millipore).

The membranes were put in a blocking solution with 1:1 dilution of Odyssey Blocking Buffer (Odyssey) and PBS for 1 hour at room temperature, then probed with rabbit anti-human c-KIT antibody (Dako) at dilutions of 1:300 in 0.1% Tween-20 in Odyssey blocking buffer at 4°C for overnight. In the next morning, human β-actin mouse monoclonal antibody (Cell signaling) was added at dilution of 1:1000, and the membrane was then incubated for another 2 hours at room temperature. After primary antibody incubation, membrane was washed four times for 5 minutes each in 0.1% Tween-20 in phosphate buffer solution (PBST). The membrane was further incubated with IRDye 800CW goat anti-mouse and IRDye 680 goat-anti-rabbit secondary antibodies (Li-Cor) at 1:10,000 dilutions in 0.01% SDS/Odyssey blocking buffer for 1 hour at room temperature. Washes were repeated after secondary labeling by washing three times for 5 minutes each in PBST, and then placed in PBS. The signals were detected using the Odyssey Infrared Imaging System (Li-Cor). The images were analyzed using the Odyssey Application Software, version 3.0 (Li-Cor) to obtain the integrated intensities.

RESULTS

In previous experiments in canine primary fibroblast (CAF), transfection of mutant oncogenic c-KIT (Del2, Del3, Del9, and Dup2) into canine primary fibroblast cells resulted in immortalization, oncogenic transformation *in vitro,* and tumor formation in immunodeficient mice *in vivo*. Thus, mutant c-KIT isoforms were serially transduced into human primary fibroblasts. Cultured human primary fibroblasts were grown to form a flat monolayer that persists without cell overgrowth for more than a month. Cells showed their normal typical fibroblast phenotypes.

To express mutant c-KIT isoforms in controllable and stable manner, tet-off system retroviral vectors were used because of their stable integration into the genomes of infected cells. The retrovirus used in this study contained a cytomegalovirus immediate-early (CMV) promoter followed by the encephalomyocarditis virus internal ribosomal entry site (IRES) driving expression of mutant c-KIT isoforms with- or without-YFP.

To test for oncogenic activity of mutant c-KIT, human primary fibroblasts were exposed with the infectious pHIT virus particles encoding a constitutive form of different mutant c-KIT isoforms or with a retrovirus carrying the empty expression vector (pHIT or pHIT-YFP) at a multiplicity of infection of four for 3 consecutive days. After 10 days of hygromycin antibiotic selection at 100 ng/ml, efficient transduction with YFP-expressing retrovirus was observed by fluorescence microscopy analysis.

Within 2 weeks after retrovirus transduction and antibiotic selection, the transformed foci characterized by large foci, which contained densely packed spindle-shaped cells were observed. Each transformation focus was isolated, expanded independently, and frozen down for further studies. In human fibroblast transduced by wild type c-KIT in pHIT-YFP vector, two

transformation foci were isolated. Also, there were four transformation foci observed and isolated from pHIT-Del2 transduced cells. One cell focus was isolated from pHIT-Del9-YFP transduced fibroblasts. Four and five clones of pHIT-Dup2 and pHIT-Dup5 transduced fibroblasts respectively were isolated.

To summarize the lifespan of these transduced cells, human fibroblasts carrying deletion 2 showed their prolonged life span without any sign of senescence. Since human fibroblasts were obtained from neonatal foreskin with a record of more than 10 population doublings, cells maintained their active morphology without any signs of senescence after 2 months in culture. In addition, empty vector (pHIT or pHIT-YFP)-transduced cells were also normal lifespan, same as in human fibroblasts. Interestingly, in this study we found an extended lifespan in Del9-YFP harboring cells. These cells had a longer lifespan and grew slower after four months in culture. However, cells carrying wild type and duplication 2 showed signs of senescence after three months in culture characterized by enlarged, flatted cellular morphology and slow growth rate. In contrast, Del2 transduced cells grew continuously for over 5 months in culture, indicating that the cells were immortal.

To investigate the integration of mutant c-KIT retroviral vectors into the genome of transduced fibroblasts and select cell for further study, each transformation clone was examined for human c-KIT transgene RNA expression by RT-PCR using primer flanking retrovirus plasmid backbone and c-KIT insert. Positive clones showing the expression of transgene were selected for *in vitro* stu

Figure 30: Representative images of control group. Untransduced human fibroblasts (A-C), fibroblast transduced with pHIT empty vector (D-F), pHIT-YFP empty vector (G-H), wt-YFP cells (J-L) at 4x magnification (A,D,G,J), 10x magnification (B,E,H,K), and 40x magnification (C,E,I,L). Cells were grown as monolayer and retained their normal fibroblast morphology characterized by spindle, elongated shape.

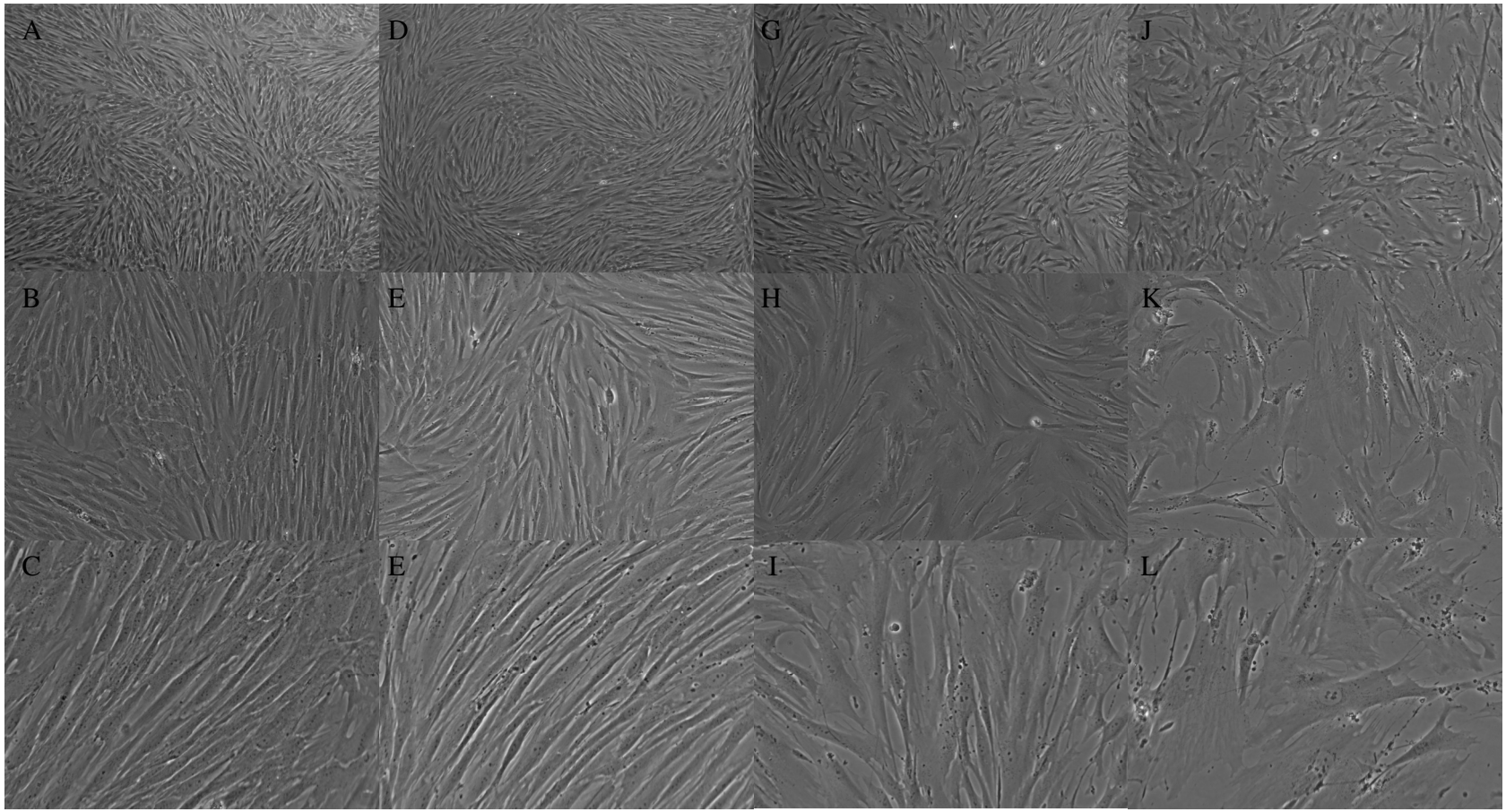

Figure 31: Morphology of mutant c-KIT transduced human fibroblasts at low (4x; Panel A,D,G,J), 10x (Panel B,E,H,K), and 40x (Panel C,E,I,L) magnification. Human fibroblasts carrying deletion 2 (A-C), deletion 9 (D-E), and duplication 2 (Dup2 C.3, G-I; Dup2 C.5, J-L) showed normal spindle, elongated morphology.

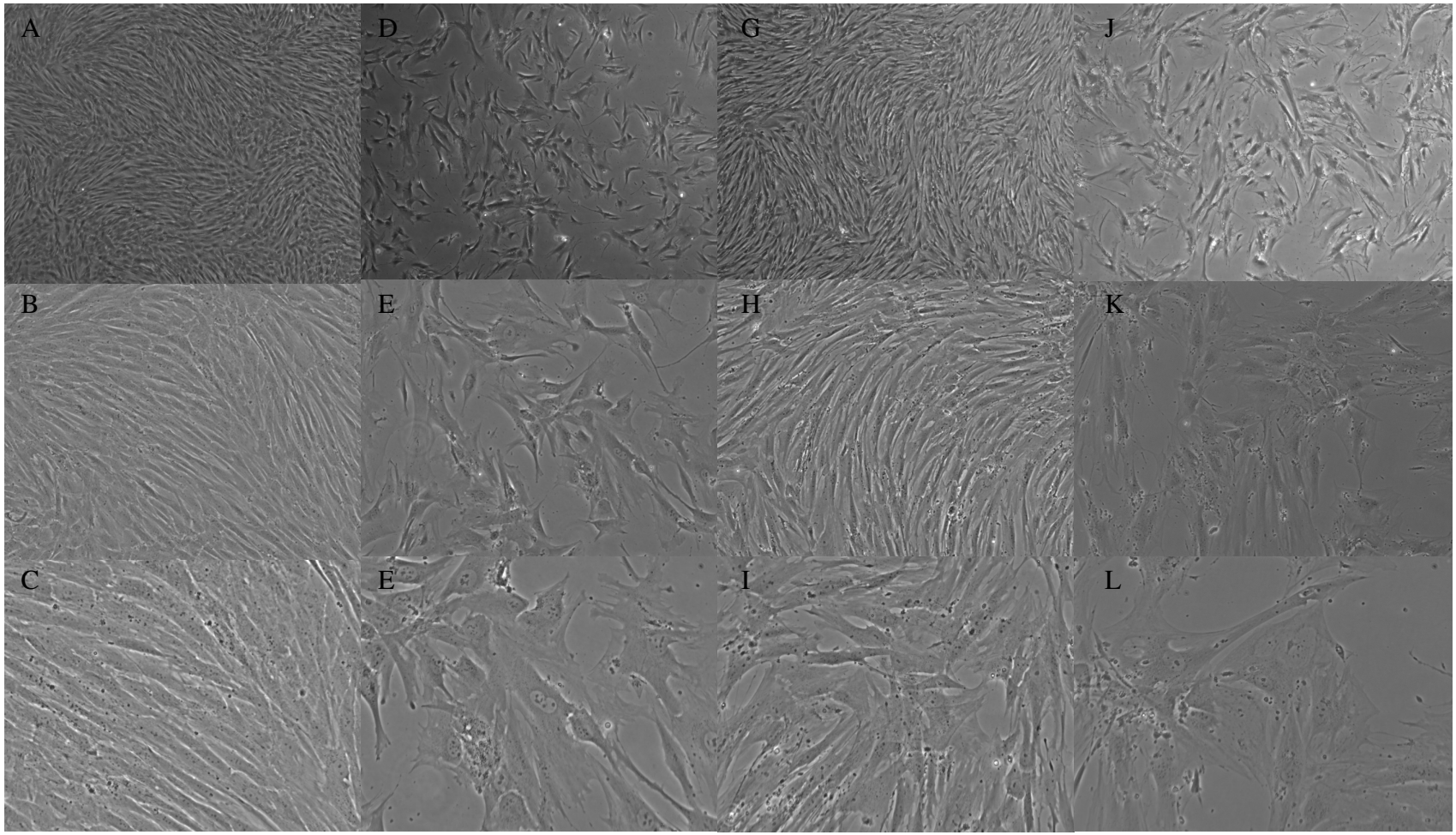

For the in vitro study, one clone of each construct that expressed c-KIT was submitted for total RNA extraction for quantitative real-time RT-PCR for c-KIT mRNA expression level measurement, immunohistochemistry and western blot analysis for c-KIT protein expression, karyotyping for aneuplody analysis, and matrigel invasion assay for their invasiveness properties. The wt-YFP (expressing wild type c-KIT in pHIT-YFP vector), Del2 C.2 (expressing deletion 2 mutation in pHIT vector), Del9-YFP (expressing deletion 9 mutation in pHIT-YFP vector), Dup2 C.3 and Dup2 C.5 (expressing duplication 2 mutation in pHIT vector) were finally selected for in vitro study. Untransduced human fibroblasts and fibroblasts transduced with empty vector (either pHIT or pHIT-YFP) were also included in the *in vitro* study as control groups.

Figure 32: Detection of transgenes in human primary fibroblasts. After selection, total RNA was extracted from transduced cells and subjected to RT-PCR. Target size at 176 bp was detected in wt-YFP (lane 4), Del2 C.2 (lane 5), Del9-YFP (lane 6), Dup2 C.3 (lane 7) Dup2 C.5 (lane 8), neither in untransduced fibroblasts (lane1), fibroblasts transduced by pHIT (lane 2), nor pHIT-YFP vector (lane 3). Plasmids containing human c-KIT gene (lane 9) and water (lane 10) served as positive and negative controls. L represents 100 bp ladder.

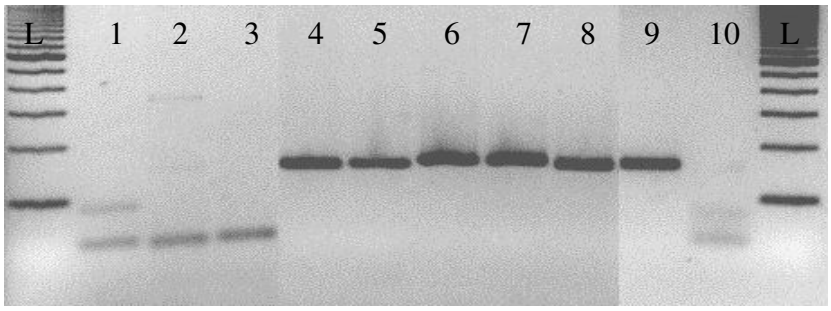

Total RNA extraction and quantitative real-time RT-PCR on c-KIT mRNA expression was performed. As compared to normal human primary fibroblasts which express endogenous c-KIT, all cells except wt-YFP showed their elevated c-KIT mRNA expression (Table 1) ranging from the fold change of 1.4 in empty vector pHIT-transduced cells to the fold change of 218.4 in Del9-YFP cells.

Table 11: Quantitative real-time RT-PCR result on c-KIT mRNA expression. Data shown in fold change as compared to normal human fibroblasts.

	RQ without Doxy	RQ with Doxy
Human fibroblast	1	1
HIT	2.2	1.5
HIT-YFP	1.4	0.8
wt-YFP	0.5	0.6
Del2 C.2	11.2	64.9
Del9-YFP	218.4	104.6
Dup2 C.3	2.3	1.1
Dup2 C.5	44.9	7.9
Dog spleen	1.2	1.4
C2MCT	646.8	549.9
NI-1	131.3	167.3

Expression of c-KIT protein was analyzed by immunohistochemistry and western blotting. The result showed an overexpression of c-KIT protein in all mutant c-KIT transduced cells including Del2 C.2, Del9-YFP, Dup2 C.3 and Dup2 C.5 (Figure 33). Five percent of untransduced human primary fibroblasts were positive to c-KIT IHC showing their endogenous c-KIT protein expression within the cells (Figure 33A). Also, in the control group, very few (5-10%) of empty vector pHIT and pHIT-YFP- transduced cells (Figure 33B and 33C) were positive to c-KIT protein. In wt-YFP cells, there is slightly positive for c-KIT expression founded in the cytoplasm (Figure 33D). Interestingly, all c-KIT mutant transduced cells show a remarkably strong positive signal of c-KIT protein expression (40-70% of cells: Figure 33E, Del2 C.2; Figure 33F, Del9-YFP; Figure 33E, Dup2 C.3). Moreover, Dup2 C.5 cells (Figure 33H) show a very strong positive expression of c-KIT protein (90-95% of cells) in the cytoplasm.

Figure 33: Immunohistochemical analysis of c-KIT expression. Sections of formalin fixed, paraffing-embeded cell pellet were subjected to immunohistochemical staining with antibody to human c-KIT. Pictures with a 10x magnification are shown and positive signals are brown in color from DAB chromogen (Dako). Cell pellets from untransduced human fibroblasts (Panel A), fibroblasts with empty vector (Panel B, C), and wild type c-KIT (Panel D) infection show slightly positive expression of c-KIT protein. Del2 C.2 (Panel E), Del9-YFP (Panel F), Dup2 C.3 (Panel G), and Dup2 C.5 (Panel H) show higher expression levels of c-KIT.

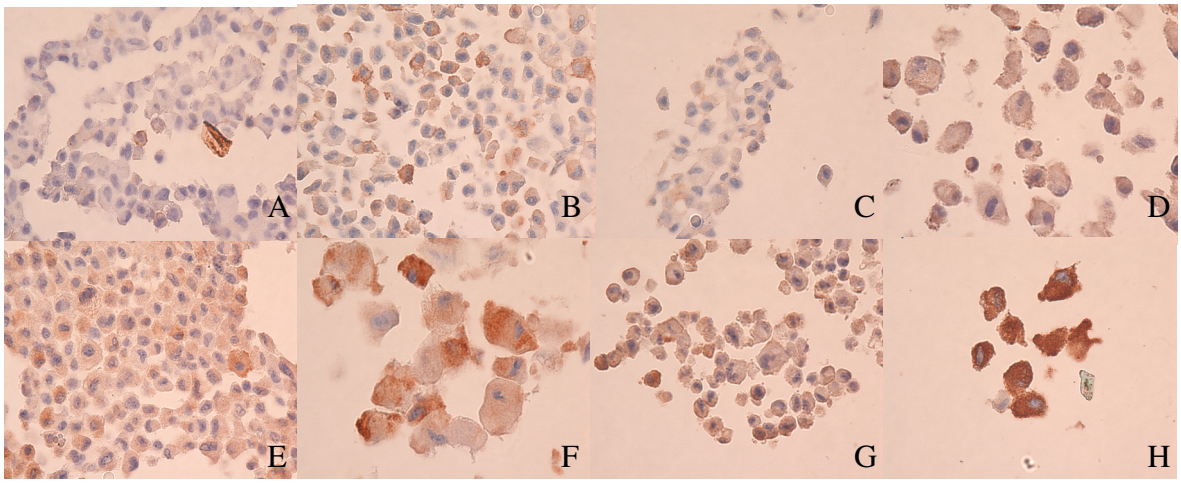

Expression of c-KIT protein was also confirmed by western blot (Figure 34). Whole cell lysates were assessed for c-KIT proteins. Blots were reprobed with an antibody against beta actin (β-actin) to ensure equal loading of proteins. Consistent with quantitative real-time RT-PCR and IHC results, western blot analysis confirms increased expression of c-KIT protein in transduced human fibroblasts carrying deletion 2, deletion 9, and duplication 2 of c-KIT mutation.

Figure 34: Expression of human c-KIT protein detected by western blot analysis with human c-KIT (red channel, target size of 145 kilo Daltons) and β-actin (loading control, green channel, target size of 45 kilo Daltons) antibodies. Lane 1, lysate from human primary fibroblasts; lane 2, lysate from pHIT empty vector transduced cells; lane 3, lysate from pHIT-YFP empty vector transduced cells; lane 4, lysate from wt-YFP cells; lane 5, lysate from Del2 C.2 cells; lane 6, lysate from Del9-YFP cells; lane 7, lysate from Dup2 C.3; lane 8, lysate from Dup2 C.5; lane 9, lysate from C2 mast cell line; M, prestained BenchMark protein markers (Iinvitrogen).

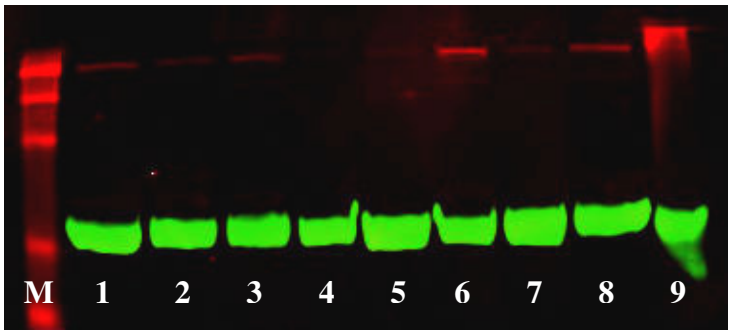

Matrigel invasion assay was used to analyze the invasiveness of these transduced fibroblasts. Human primary fibroblasts expressing wild type, deletion 2, and duplication 2 show increased migration, as compared to untransduced cells. Interestingly, Del9-YFP cells and empty vector transduced cells reveal their loss of invasiveness.

Figure 35: Representative images (10x magnification) from invasion assays of untransduced human fibroblasts (Panel A), fibroblast transduced by empty vector pHIT (Panel B), empty vector pHIT-YFP (Panel C), wild-type (wt-YFP, Panel D), Del2 C.2 (Panel E), Del9-YFP (Panel F), Dup2 C.3 (Panel G) and Dup2 C.5 (Panel H). Pictures show the stained mesh after completion of the invasion assays of a representative experiment from three independent experiments. Invading cells were visualized by blue stain.

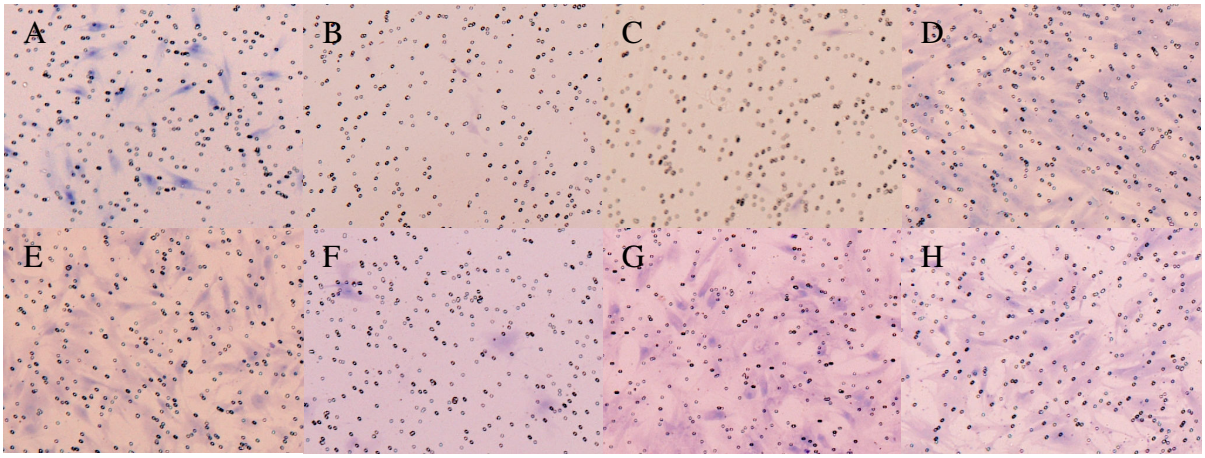

Karyotype results selected from untransduced human fibroblasts and Dup2 C.3 cells showing normal karyotypes. Also, all transduced cells retained their normal chromosome number of 46.

Figure 36: Representative cytogenetic analysis images (100x magnification) of normal untransduced human fibroblasts (left panel) and Dup2 C.3 cells (right panel). Normal karyotypes (n=46) were detected in both representative cells. Other transduced cells also contain normal karyotypes (data not shown).

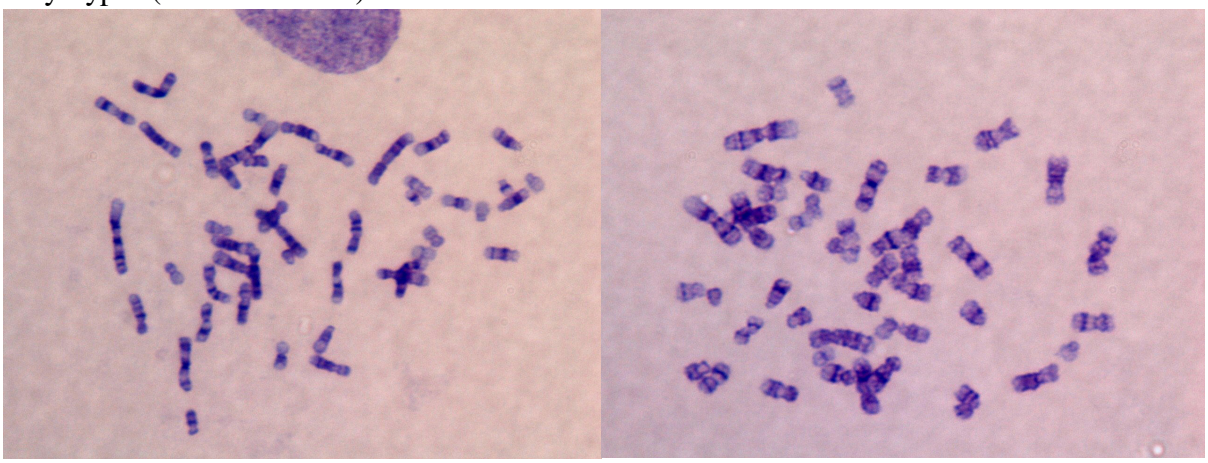

DISCUSSION

The novelty here was to assess the role for c-KIT mutations as an activated proto-oncogene capable of mediating tumorigenesis in more primitive *in vitro* systems such as human primary fibroblasts. In this study, mutant c-KIT isoforms identified in human GISTs (Rubin et al., 2001; Taniguchi et al., 1999), canine GISTs (Gregory-Bryson et al., 2010, and canine mast cell tumors (Zemke et al., 2002) were successfully constructed in retroviral vector and transduced in human primary fibroblasts. In this report, we described the extension of lifespan and immortalization of cultured human primary fibroblasts induced by mutant c-KIT isoforms, resulting in their long-term propagation in culture, and suggested potential mechanisms for its oncogene effect. The extension of lifespan occurred when normal human fibroblasts were transduced with pHIT-Del9-YFP plasmids. Moreover, an immortal cell line was established when human fibroblasts were transduced with pHIT-Del2 plasmids. However, three of six normal human primary fibroblasts transduced with mutant c-KIT alone and wild type c-KIT failed to overcome senescence. After transduction and hygromycin selection, the elevated expression levels of c-KIT transgene were detected by RT–PCR and quantitative real-time RT-PCR. The expression level of c-KIT protein detected by immunohistochemistry staining and western blot analysis was greater in the four immortal cell lines than in the control cells. However, a small percentage of expression of c-KIT cells (five percent) was detected in normal primary fibroblasts. This finding suggests the source of fibroblasts which derived from neonatal foreskin and remained their progenitor characteristics.

c-KIT is a cell surface type III tyrosine kinase (TK) receptor implicated in cell transformation through overexpression or oncogenic mutation. Two categories of c-KIT mutants displaying mutations either in the juxtamembrane intracellular domain (regulatory mutants) or in

the catalytic domain (catalytic mutants) have been described (Bougherara et al., 2009). Activating mutations in c-KIT have been identified in patients with gastrointestinal stromal tumors, cutaneous melanoma, mastocytosis, and acute myeloid leukemia. Reported mutations were commonly found in three regions in the KIT gene including the extracellular membrane domain at exon 8, exon 11 at the juxtamembrane domain, and exon 17 found at the tyrosine kinase domain (Heinrich et al., 2002; Longley et al., 1999; Gari et al., 1999; Beghini et al., 2004; Tang et al., 2004; Beadling et al., 2008; Lorenzo et al., 2006). The impact of c-KIT mutations in tumorigenesis has been studied mainly in immortalized cells transduced with the mutant c-KIT-expressing vector. However, the consequences of activated oncogene expression are varied and cell type-dependent, which illustrate the importance of the appropriate cellular context. Thus, it appears that the cellular context, namely the presence or absence of additional mutations such as immortalized cell, cell lines, or primary cells, can determine the consequences of oncogene activation (Hibi et al., 1993; Dorrell et al., 2004; Dean et al., 2010; Guerra et al., 2003).

In the previous study, the same results were obtained from canine primary fibroblasts. The tumorigenesis caused by a series of c-KIT mutations was investigated in the context of canine primary fibroblasts. Results show that four out of six mutations can induce immortalization and tumorigenic transformation *in vitro*. These mutant c-KIT-transfected cells were capable of tumor formation in immunodeficient mice. In addition, two of four c-KIT mutant isoforms can cause metastatic tumor formation *in vivo*.

The mechanism of immortalization of human fibroblasts by the transduced mutant c-KIT transgenes is unclear. Human fibroblasts rarely, if ever, undergo spontaneous transformation to an immortalized cell type (Luo et al., 2004). Although the mechanism for the ectopic expression

of mutant c-KIT has not been clarified, these findings suggest that ectopic expression of mutant c-KIT may have an important role in the immortalization of human primary fibroblasts.

It is worthnoting that Del9-YFP-, Dup2 C.3-, and Dup2 C.5- harboring cells showing short lifespans had the highest c-KIT expression. These findings offer a perspective on oncogene induced premature senescence. This phenomenon was first described in 1997 (Serrano et al., 1997) when results showed growth arresting in the G1 phase of the cell cycle induced by the overexpression of oncogene ras. This senescence functions as the barrier to oncogenesis and prematurely activates in response to an oncogenic stimulus (Bartkova et al., 2006).

Unlike the previous results obtained from canine primary fibroblasts, the introduction of a single hit of mutant c-KIT into human primary fibroblasts was demonstrated to have immortalization capacity but not transformation activity. This result was consistent with the results of other studies reviewed by McCormick and Maher (2011). Malignant transformation of normal human primary fibroblasts would require multiple "hits" rather than a single hit from ectopic expression of the oncogene. Ectopic expression of the oncogene can transform established, but not primary, mammalian cells. This implies that mutant c-KIT expression may possess the ability to enhance the tumorigenic potential of already immortalized cells. Thus, immortality is an essential requirement for malignant transformation that cooperates with other oncogenic changes to program the neoplastic state (Kavsan et al., 2011).

To investigate the consequences of each mutant c-KIT isoform activity, the invasiveness properties were measured. As compared to human primary fibroblasts, cells transduced with empty vectors show a loss of invasiveness, whereas cells transduced with mutant c-KIT isoforms reveal increased invasiveness properties. However, Del9 transduced cells did lose their invasiveness. These results suggested the distinct phenotype of cells may result from difference

mutant c-KIT isoforms. Furthermore, this phenomenon results in a cell population that shows no gross chromosomal changes.

In summary, this study describes mutant c-KIT functions in modulating senescence and contributing to immortalization, but not tumorigenic transformation. The immortalized mutant c-KIT harboring cells are stable and have an unlimited life span, but the current results leave doubt that these cells are going through a malignant transformation process. However, if theses cells stay in the immortalized state, it may be possible that additional genetic alterations would be required to drive the malignant transformation process. Extensions to the present study will be useful to elucidate the unexplored roles of c-KIT mutations in tumors and the new therapeutic strategies for c-KIT signaling driven cancers.

REFRENCES

REFERENCES

1. Bartkova J, Rezaei N, Liontos M, Karakaidos P, Kletsas D, Issaeva N, Vassiliou LV, Kolettas E, Niforou K, Zoumpourlis VC, Takaoka M, Nakagawa H, Tort F, Fugger K, Johansson F, Sehested M, Andersen CL, Dyrskjot L, Ørntoft T, Lukas J, Kittas C, Helleday T, Halazonetis TD, Bartek J, Gorgoulis VG. Oncogene-induced senescence is part of the tumorigenesis barrier imposed by DNA damage checkpoints. Nature. 2006 Nov 30;444(7119):633-7.

2. Beadling C, Jacobson-Dunlop E, Hodi FS, Le C, Warrick A, Patterson J, Town A, Harlow A, Cruz F 3rd, Azar S, Rubin BP, Muller S, West R, Heinrich MC, Corless CL. KIT gene mutations and copy number in melanoma subtypes. Clin Cancer Res. 2008 Nov 1;14(21):6821-8.

3. Beghini A, Ripamonti CB, Cairoli R, Cazzaniga G, Colapietro P, Elice F, Nadali G, Grillo G, Haas OA, Biondi A, Morra E, Larizza L. KIT activating mutations: incidence in adult and pediatric acute myeloid leukemia, and identification of an internal tandem duplication. Haematologica. 2004 Aug;89(8):920-5.

4. Bougherara H, Subra F, Crépin R, Tauc P, Auclair C, Poul MA. The aberrant localization of oncogenic kit tyrosine kinase receptor mutants is reversed on specific inhibitory treatment. Mol Cancer Res. 2009 Sep;7(9):1525-33.

5. Campisi,J. (2003) Cancer and ageing: rival demons? Nat. Rev. Cancer, 3, 339–349.

6. Chen C, Okayama H (1987) High-efficiency transformation of mammalian cells by plasmid DNA. Mol Cell Biol 7: 2745–2752.

7. Dean JL, McClendon AK, Stengel KR, Knudsen ES. Modeling the effect of the RB tumor suppressor on disease progression: dependence on oncogene network and cellular context. Oncogene. 2010 Jan 7;29(1):68-80.

8. Dorrell C, Takenaka K, Minden MD, Hawley RG, Dick JE. Hematopoietic cell fate and the initiation of leukemic properties in primitive primary human cells are influenced by Ras activity and farnesyltransferase inhibition. Mol Cell Biol. 2004 Aug;24(16):6993-7002.

9. Elenbaas,B., Spirio,L., Koerner,F., Fleming,M.D., Zimonjic,D.B., Donaher,J.L., Popescu,N.C., Hahn,W.C. and Weinberg,R.A. (2001) Human breast cancer cells generated by oncogenic transformation of primary mammary epithelial cells. Genes Dev., 15, 50–65.

10. Gari M, Goodeve A, Wilson G, Winship P, Langabeer S, Linch D, Vandenberghe E, Peake I, Reilly J. c-kit proto-oncogene exon 8 in-frame deletion plus insertion mutations in acute myeloid leukaemia. Br J Haematol. 1999 Jun;105(4):894-900.

11. Guerra C, Mijimolle N, Dhawahir A, Dubus P, Barradas M, Serrano M, Campuzano V, Barbacid M. Tumor induction by an endogenous K-ras oncogene is highly dependent on cellular context. Cancer Cell. 2003 Aug;4(2):111-20.

12. Hahn,W.C. (2002) Immortalization and transformation of human cells. Mol. Cells, 13, 351–361.

13. Hahn,W.C. and Weinberg,R.A. (2002) Rules for making human tumor cells. N. Engl. J. Med., 347, 1593–1603.

14. Hahn,W.C., Counter,C.M., Lundberg,A.S., Beijersbergen,R.L., Brooks,M.W. and Weinberg,R.A. (1999) Creation of human tumour cells with defined genetic elements. Nature, 400, 464–468.

15. Hayflick L (1965). The limited in vitro lifetime of human diploid cell strains. Exp Cell Res 37: 614–636.

16. Heinrich MC, Rubin BP, Longley BJ, Fletcher JA. Biology and genetic aspects of gastrointestinal stromal tumors: KIT activation and cytogenetic alterations. Hum Pathol. 2002 May;33(5):484-95.

17. Hibi S, Löhler J, Friel J, Stocking C, Ostertag W. Induction of monocytic differentiation and tumorigenicity by v-Ha-ras in differentiation arrested hematopoietic cells. Blood. 1993 Apr 1;81(7):1841-8.

18. Hirota S, Isozaki K, Moriyama Y, Hashimoto K, Nishida T, Ishiguro S, Kawano K, Hanada M, Kurata A, Takeda M, Muhammad Tunio G, Matsuzawa Y, Kanakura Y, Shinomura Y, Kitamura Y. Gain-of-function mutations of c-kit in human gastrointestinal stromal tumors. Science. 1998 Jan 23;279(5350):577-80.

19. Kavsan VM, Iershov AV, Balynska OV. Immortalized cells and one oncogene in malignant transformation: old insights on new explanation. BMC Cell Biol. 2011 May 23;12:23.

20. Larsson LG. Oncogene- and tumor suppressor gene-mediated suppression of cellular senescence. Semin Cancer Biol. 2011 Dec;21(6):367-76.

21. Longley BJ Jr, Metcalfe DD, Tharp M, Wang X, Tyrrell L, Lu SZ, Heitjan D, Ma Y. Activating and dominant inactivating c-KIT catalytic domain mutations in distinct clinical forms of human mastocytosis. Proc Natl Acad Sci U S A. 1999 Feb 16;96(4):1609-14.

22. Longley BJ, Reguera MJ, Ma Y. Classes of c-KIT activating mutations: proposed mechanisms of action and implications for disease classification and therapy. Leuk Res. 2001 Jul;25(7):571-6.

23. Lorenzo F, Nishii K, Monma F, Kuwagata S, Usui E, Shiku H. Mutational analysis of the KIT gene in myelodysplastic syndrome (MDS) and MDS-derived leukemia. Leuk Res. 2006 Oct;30(10):1235-9.

24. Luo P, Tresini M, Cristofalo V, Chen X, Saulewicz A, Gray MD, Banker DE, Klingelhutz AL, Ohtsubo M, Takihara Y, Norwood TH. Immortalization in a normal foreskin fibroblast culture following transduction of cyclin A2 or cdk1 genes in retroviral vectors. Exp Cell Res. 2004 Apr 1;294(2):406-19.

25. Mason DX, Keppler D, Zhang J, Jackson TJ, Seger YR, Matsui S, Abreo F, Cowell JK, Hannon GJ, Lowe SW, Lin AW. Defined genetic events associated with the spontaneous in vitro transformation of ElA/Ras-expressing human IMR90 fibroblasts. Carcinogenesis. 2006 Feb;27(2):350-9.

26. McCormick JJ, Maher VM. Malignant transformation of human skin fibroblasts by two alternative pathways. Adv Exp Med Biol. 2011;720:191-207.

27. Nagata H, Worobec AS, Oh CK, Chowdhury BA, Tannenbaum S, Suzuki Y, Metcalfe DD. Identification of a point mutation in the catalytic domain of the protooncogene c-kit in peripheral blood mononuclear cells of patients who have mastocytosis with an associated hematologic disorder. Proc Natl Acad Sci U S A. 1995 Nov 7;92(23):10560-4.

28. Rubin BP, Singer S, Tsao C, Duensing A, Lux ML, Ruiz R, Hibbard MK, Chen CJ, Xiao S, Tuveson DA, Demetri GD, Fletcher CD, Fletcher JA. KIT activation is a ubiquitous feature of gastrointestinal stromal tumors. Cancer Res. 2001 Nov 15;61(22):8118-21.

29. Rubin H. The disparity between human cell senescence in vitro and lifelong replication in vivo. Nat Biotechnol. 2002 Jul;20(7):675-81.

30. Seger,Y.R., Garcia-Cao,M., Piccinin,S., Cunsolo,C.L., Doglioni,C., Blasco,M.A., Hannon,G.J. and Maestro,R. (2002) Transformation of normal human cells in the absence of telomerase activation. Cancer Cell, 2, 401–413.

31. Serrano M, Lin AW, McCurrach ME, Beach D, Lowe SW. Oncogenic ras provokes premature cell senescence associated with accumulation of p53 and p16INK4a. Cell. 1997 Mar 7;88(5):593-602.

32. Suhr ST, Senut MC, Whitelegge JP et al. Identities of sequestered proteins in aggregates from cells with induced polyglutamine expression. J Cell Biol 2001;153:283-294.

33. Tang X, Boxer M, Drummond A, Ogston P, Hodgins M, Burden AD. A germline mutation in KIT in familial diffuse cutaneous mastocytosis. J Med Genet. 2004 Jun;41(6):e88.

34. Taniguchi M, Nishida T, Hirota S, Isozaki K, Ito T, Nomura T, Matsuda H, Kitamura Y. Effect of c-kit mutation on prognosis of gastrointestinal stromal tumors. Cancer Res. 1999 Sep 1;59(17):4297-300.

35. Tsutsui T, Kumakura S, Yamamoto A, Kanai H, Tamura Y, Kato T, Anpo M, Tahara H, Barrett JC. Association of p16 INK4a and pRb inactivation with immortalization of human cells. Carcinogenesis 2002;23:2111–7.

36. Tsutsui T, Tanaka Y, Matsudo Y, Hasegawa K, Fujino T, Kodama S, Barrett JC. Extended lifespan and immortalization of human fibroblasts induced by X-ray irradiation. Mol Carcinog 1997;18: 7–18.

37. Vogelstein,B. and Kinzler,K.W. (2004) Cancer genes and the pathways they control. Nat. Med., 10, 789–799.

38. Wagner W, Horn P, Castoldi M, Diehlmann A, Bork S, Saffrich R, Benes V, Blake J, Pfister S, Eckstein V, Ho AD. Replicative senescence of mesenchymal stem cells: a continuous and organized process. PLoS One. 2008 May 21;3(5)

39. Willmore-Payne C, Holden JA, Tripp S, Layfield LJ. Human malignant melanoma: detection of BRAF- and c-kit-activating mutations by high-resolution amplicon melting analysis. Hum Pathol. 2005 May;36(5):486-93.

40. Yasaei H, Gilham E, Pickles JC, Roberts TP, O'Donovan M, Newbold RF. Carcinogen-specific mutational and epigenetic alterations in INK4A, INK4B and p53 tumour-suppressor genes drive induced senescence bypass in normal diploid mammalian cells. Oncogene. 2012 Mar 12. [Epub ahead of print]

CHAPTER 7

CONCLUSION, OPEN QUESTIONS, AND FUTURE DIRECTION

Since the U.S. passed the National Cancer Act of 1971, overall cancer death rates for all sites combined, and for the leading cancer sites among men and women have continuously declined from the baseline rates of 1970/71. This decline is largely the result of tobacco prevention and control efforts, screening, improvements in treatment for many cancers, and, most importantly, early detection of some cancers. Scientists are steadily able to develop more potent therapeutic approaches, improve routine screening and early detection for the prevention, and to better understand the fundamental nature of cancer. The challenge of new era cancer treatment is personalized cancer medicine. The mission of this particular therapeutics is to pinpoint the genes and molecular pathways that disrupt these diseases, to identify the biomarkers which are the unique molecular characteristics of cancer cells, and to develop more precise and less harmful treatment strategies known as targeted therapy for the individual.

Within more than 290 genes related to the cause of cancer, c-KIT is one of genes that is involved in tumorigenesis of many cancers. It was first described by Dr. Peter Besmer in 1985 as a new oncogene homologous to the viral genome of a new acute transforming feline retrovirus. Although the contributions of c-KIT and c-KIT mutations in tumorigenesis have been defined for the past three decades, we are still moving forward to understand the in depth role of c-KIT in tumors and to develop effective c-KIT targeted therapeutics. In humans, deregulation of c-KIT has been described in many cancers, including myeloid leukemia, gastrointestinal stromal tumors (GISTs), mast cell leukemia, systemic mastocytosis, germ cell tumors, malignant melanoma, and non-small cell lung cancer. In animals, especially in dogs, c-KIT also mediates similar types of tumors as found in humans. Over expression and mutation of c-KIT was also reported in canine mast cell tumors (MCTs) and canine GISTs. Using the concepts of comparative medicine and translational research, the similarities and differences in biology among animals will enhance the

understanding of mechanisms in human and animal diseases alike and translate basic science knowledge into applied clinical information. The significance of c-KIT mutations explored in animal models might elucidate the role in tumorigenesis in humans.

In this study, we explored the role of c-KIT mutation in tumorigenesis using both *in vitro* and *in vivo* systems. Mutations of c-KIT were detected in the exon 11 juxtamembrane domain in MCTs. The mutation status is significantly associated with poor prognosis and the disease recurrence rate in patients. Moreover, mutations identified in canine MCTs were also reported in canine GISTs and human GISTs. Therefore, we proposed to uncover the role of these c-KIT mutations in tumor initiation and tumorigenesis by ectopic expression of these mutant c-KIT isoforms in canine primary fibroblasts. Unlike other experiments using hematopoietic progenitor cells, canine primary fibroblasts, which do not expression c-KIT protein, were excluded from the experiment because of the influence of endogenous c-KIT expression. Questions have been raised about using fibroblasts, which are not the real target cell type harboring mutation in MCTs and GISTs. Cutaneous mast cells and interstitial cells of Cajal are the cell-of-origin of MCTs and GISTs, respectively. Ideally, these cells would be the best for *in vitro* models. However, the remaining normal alleles of c-KIT or endogenous expression may interfere the consequence mediated by the ectopically expressed mutant alleles. Therefore, canine primary fibroblasts were used to avoid additional genetic alteration by using the immortalized cell lines.

Six c-KIT mutant isoforms were constructed into the expression vectors. The expression of transgenes was driven by a cytomegalovirus promoter, which was tagged with green fluorescence protein as a reporter gene and to allow fluorescence cell sorting. Four of six c-KIT mutant isoforms cause malignant transformation in canine primary fibroblast, including three isoforms of deletion and one isoform of duplication mutation. Control cells comprised of canine

primary fibroblasts transfected by empty vector and wild type c-KIT isoforms went senescence and died after antibiotic selection. Although the expression of this transgene was low and detectable only by RT-PCR, it clearly shows their capacity to drive tumorigenic transformation via *in vitro* studies. In addition, CAF-KIT mutant cells stayed in replicative arrest for eight months before bypassing senescence and undergoing malignant transformation. The tumorigenicity of these mutant c-KIT transfected cells was confirmed by xenograft study in NOD/SCID-Gamma (NSG) mice. Although spontaneous transformation in canine primary fibroblasts has never been confirmed, it is unlikely that oncogenic transformation resulting in these malignant phenotypes is solely caused by unregulated ectopic expression of the mutant c-KIT transgenes. Although additional genetic and/or epigenetic changes are probably necessary for transformation, it would appear that the process of tumorigenic transformation is initiated by gain-of-function mutation occurring in association with, and possibly caused by, ectopic expression of mutant c-KIT. Many new techniques might help us to better understand the characteristics of these CAF-KIT mutant cell lines. Studied that included the complete exome sequencing, gene expression microarray, and microRNA microarray will provide in-depth genomic information in relationship to phenotypes.

In addition, these CAF-KIT cell lines acquired aneuploidy by gaining additional chromosomes. The expression of mutant c-KIT isoforms might only produce the pre-neoplastic aneuploidy. Then, after many proliferating generations in culture conditions, cells became tumorigenicity due to the evolution process from pre-neoplastic to neoplastic aneuploidy. It is important to question whether the chromosomal instability is a cause or a consequence of tumorigenic transformation. To answer this question, the identification of the chromosome aberration would allow us to understand the consequences mediated by the ectopic expression of

c-KIT mutation in the context of chromosomal instability. Unfortunately, the resources helping the identification of chromosomal abnormalities in canine species are limited. Even though the schematic representations of the canine ideogram have been described, the karyotype of the dog is still widely accepted as one of the most difficult to karyotype. In metaphase, the dog karyotype consists of 78 acrocentric chromosomes, which appear to be quite small, show only a gradual decrease in their size, and are difficult to identify unambiguously. Other useful tools to precisely identify each chromosome, such as whole chromosome painting or canine specific chromosome probes, are still required. Not only at the whole chromosome level but also at the level, of chromosome translocations, specific genomic region aberrations, and a combination of both types of aberrations, the detection of genes that are involved within these aberrations could eventually offer insights on the malignant transformation and tumorigenesis of these CAF-KIT cell lines.

We have performed preliminary studies to replicate those findings in human primary fibroblasts using the inducible tetracyclin-off retroviral system. In using this system, the expression of mutant c-KIT transgene was able to be “turned on” or “turned off”. Unlike the previous study, in this study we were able to detect the expression of c-KIT transgene at the protein levels. However, results show that mutant c-KIT was not sufficient to tumorigenically transform the human primary fibroblasts into the malignant phenotype. The ectopically expressed mutant c-KIT was only able to extend the lifespan or immortalize these cells. These findings were consistent with other studies showing that multiple “hits” are required for tumorigenesis. Further work in this area may help to define important differences between the human and canine cells.

Recent therapeutic breakthroughs in the treatment of c-KIT signaling driven tumors involve the tyrosine kinase inhibitors (TKIs). TKIs are promising new agents for selective, specific inhibition of malignant cell growth and metastasis formation of tyrosine kinase receptor signaling mediated tumors. It is clear that the development of newer agents will require appropriate preclinical study models to precisely predict the efficacy of the agents. To study the specific effect of the new TKI on this particular genetic alteration, cells carrying the mutation are an ideal preclinical system for drug development. Unfortunately, the proliferation of CAF-KIT mutant cell lines are c-KIT-independent, which shows no value of these cell lines for TKI study purpose.

In conclusion, our findings have shown the impact of different c-KIT mutation isoforms in tumorigenesis within the context of primary fibroblasts. Preclinical study models of cells carrying specific genetic alterations that are responsible for diseases are needed to improve the processes of clinical study. As dogs and humans share close similarity in their genome contents and living environments, comparative medicine using canine cells as study models will provide much needed information on tumorigenesis and new cancer therapies in humans.